A broad introduction to geophysical studies of subduction zones

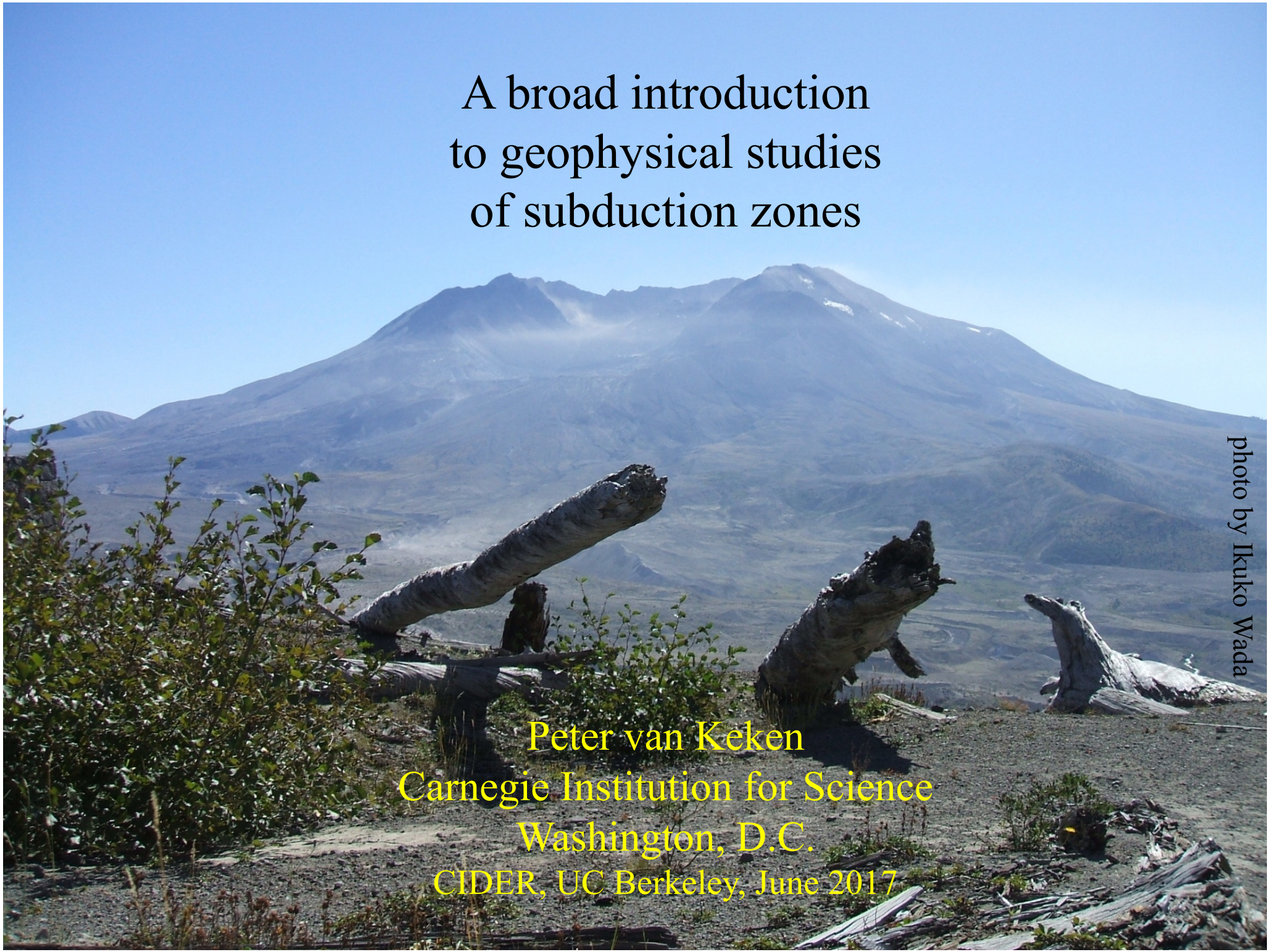

photo by Ikuko Wada

Peter van Keken
Carnegie Institution for Science
Washington, D.C.

CIDER, UC Berkeley, June 2017

A brief (and ancient) history of mantle convection

Examples of geophysical studies of:

- Incoming plate
- Seismogenic zone
- Deep (80-250 km) slab processes
- Mantle wedge and overriding plate

MARGINS

NSF

Geo PRISMS

Geodynamic Processes at Rifting and Subducting Margins

photo by Juli Morgan

Theory of continental drift (1915)

Alfred Wegener (1880-1930)

Coastline shape
Similar geology across continents
- rock types
- glacial features
- fossils

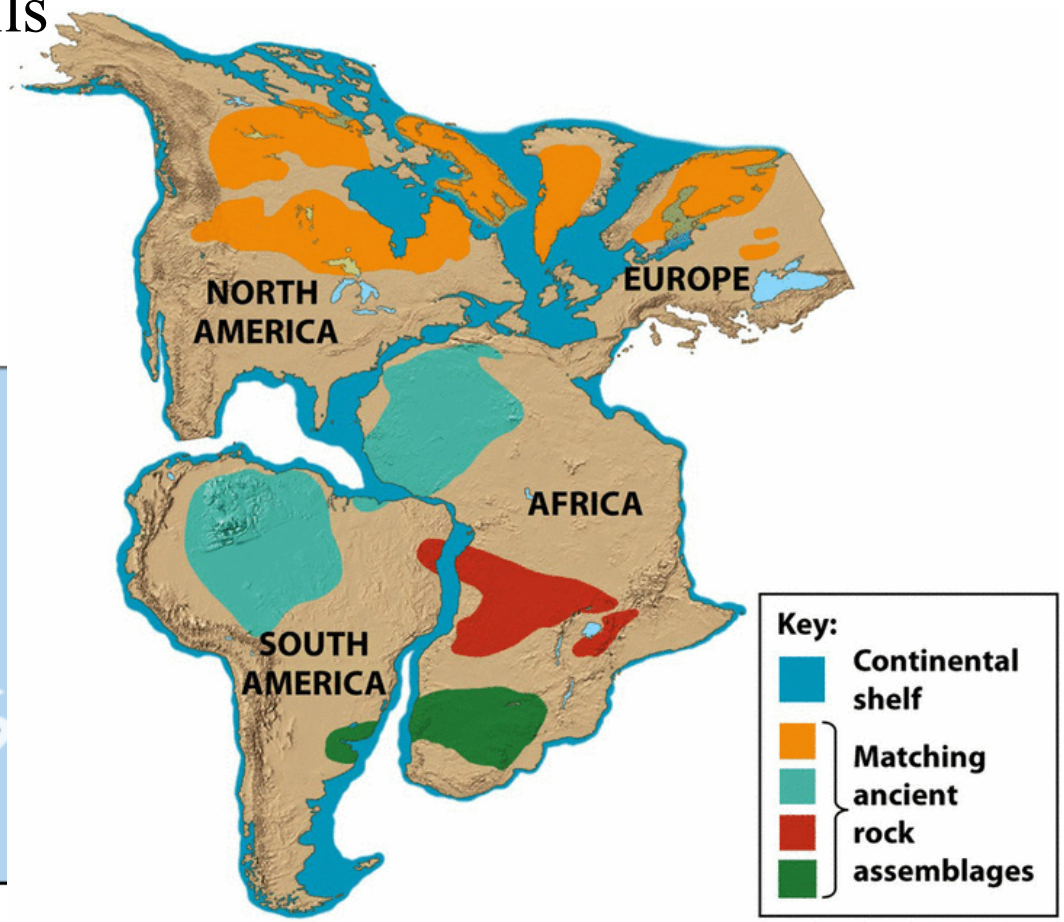

Continental drift rejection

Seismology:
the earth is solid (1920s-60s)

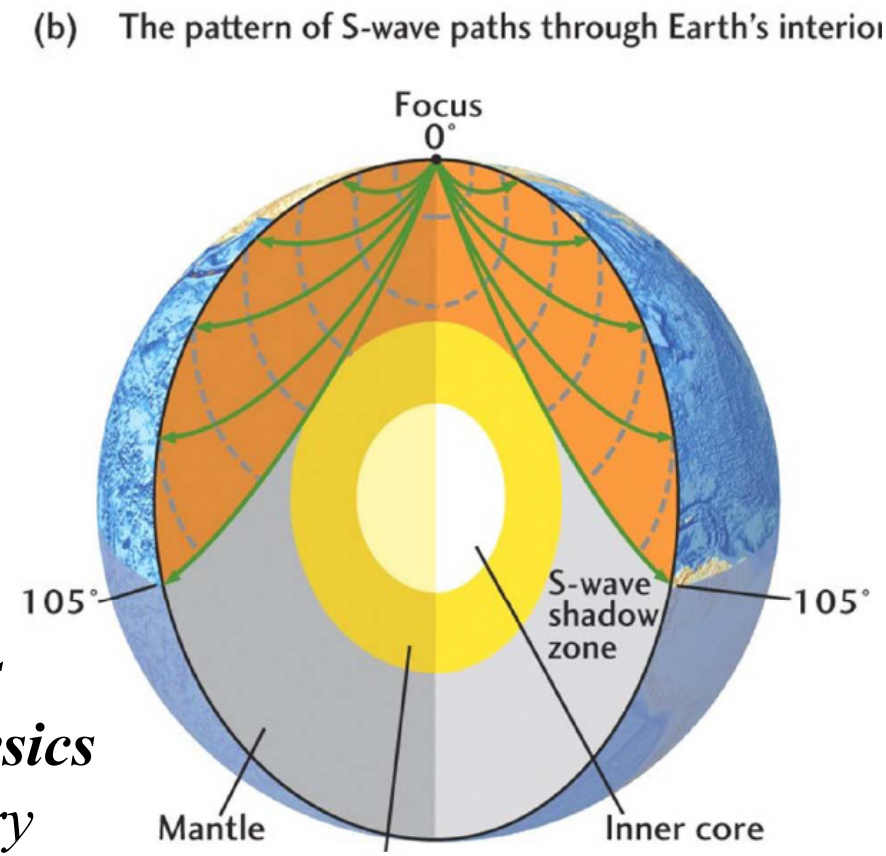

"I believe that the final resolution of the problem can only come from ***geophysics*** *since only that branch of science provides sufficiently precise methods. Were* ***geophysics*** *come to the conclusion that the drift theory is wrong, the theory would have to be abandoned by the systematic earth science as well, in spite of all corroboration, and another explanation for the facts would have to be sought"*

Wegener (1929)

Mantle convection fueled by radiogenic heating (1930s)

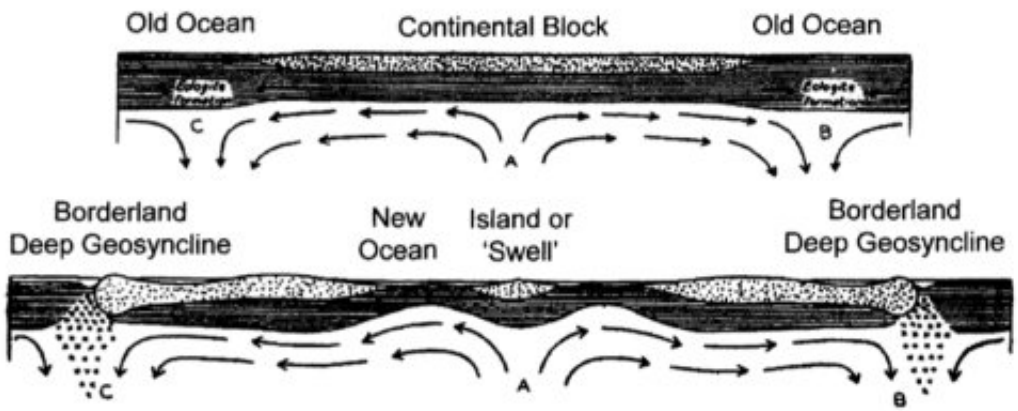

Arthur Holmes

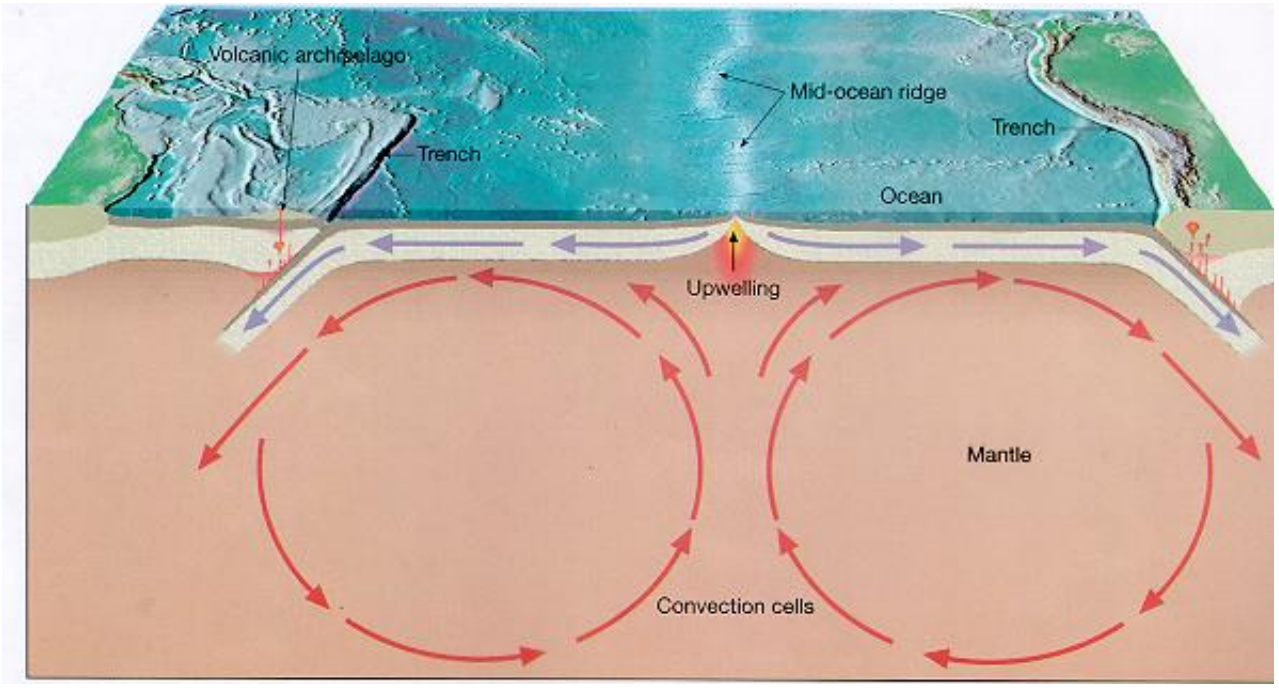

Trenches and active downwellings (1930s)

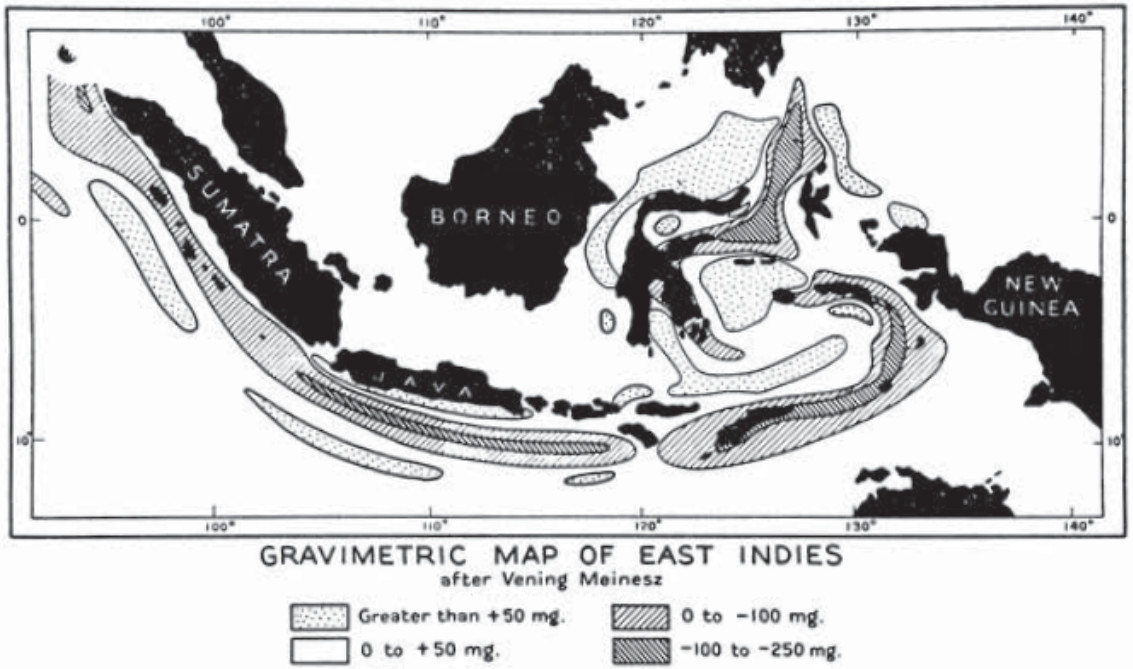

Fig. 2. Gravity Anomalies in the East Indies, Showing Belt of Gravity Deficiency Peripheral to the East Indian Archipelago, Flanked by Bands of Positive Anomalies.

Felix Vening Meinesz
(1887-1966)

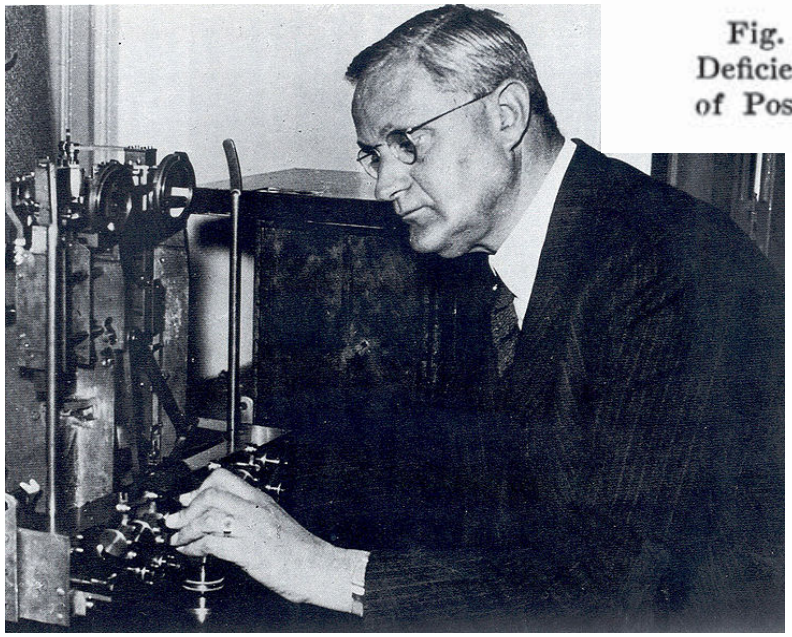

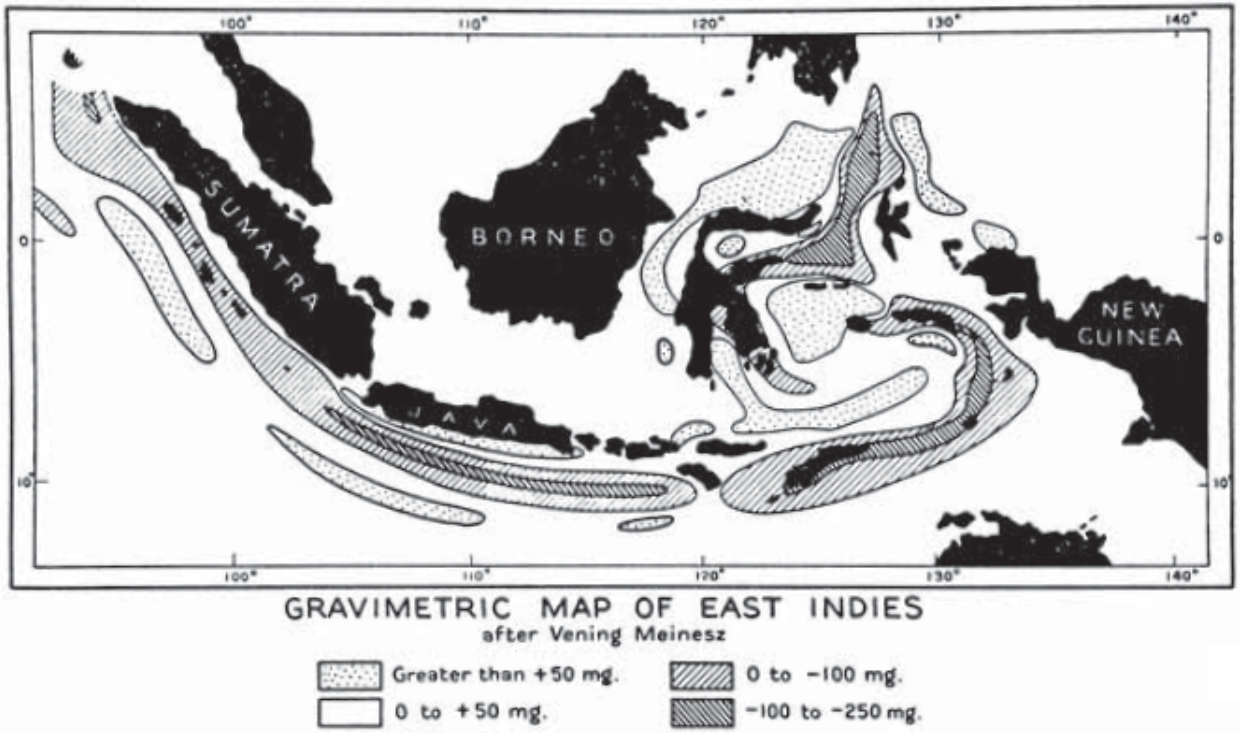

Fig. 2. Gravity Anomalies in the East Indies, Showing Belt of Gravity Deficiency Peripheral to the East Indian Archipelago, Flanked by Bands of Positive Anomalies.

very low gravity
indicates missing mass

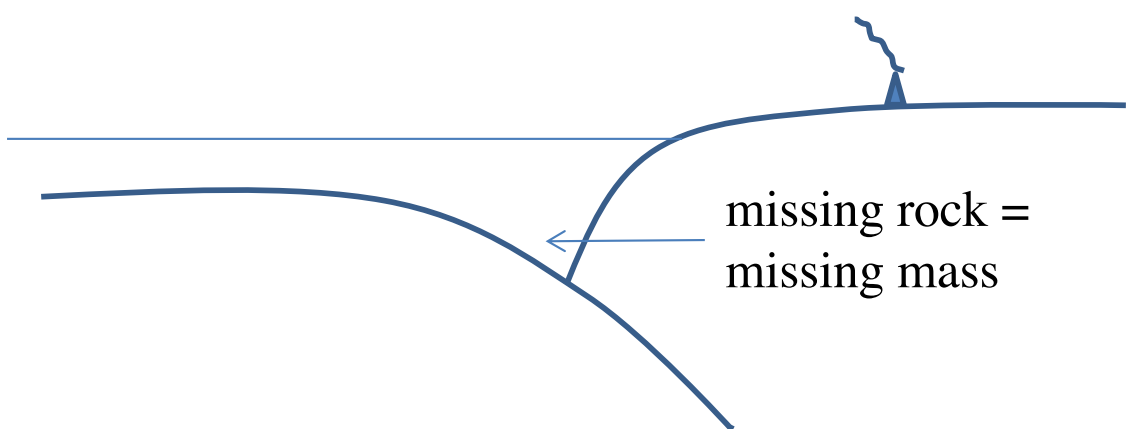

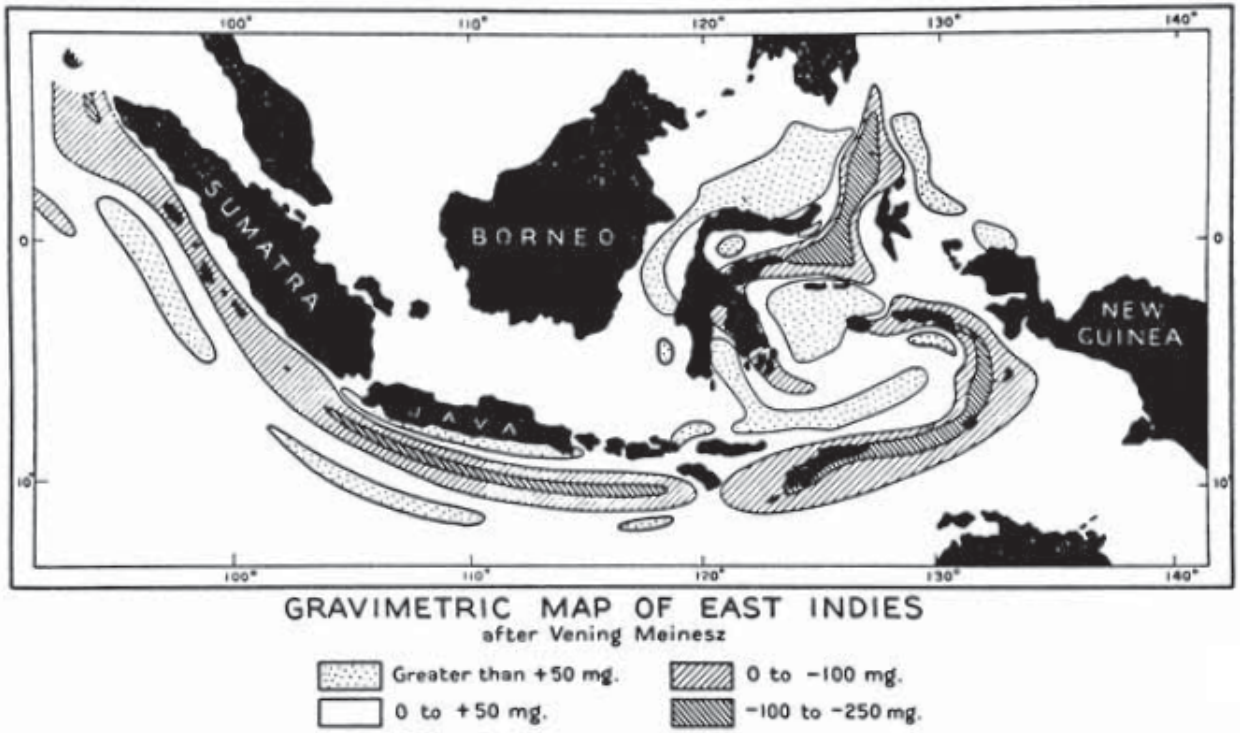

Fig. 2. Gravity Anomalies in the East Indies, Showing Belt of Gravity Deficiency Peripheral to the East Indian Archipelago, Flanked by Bands of Positive Anomalies.

very low gravity
indicates missing mass

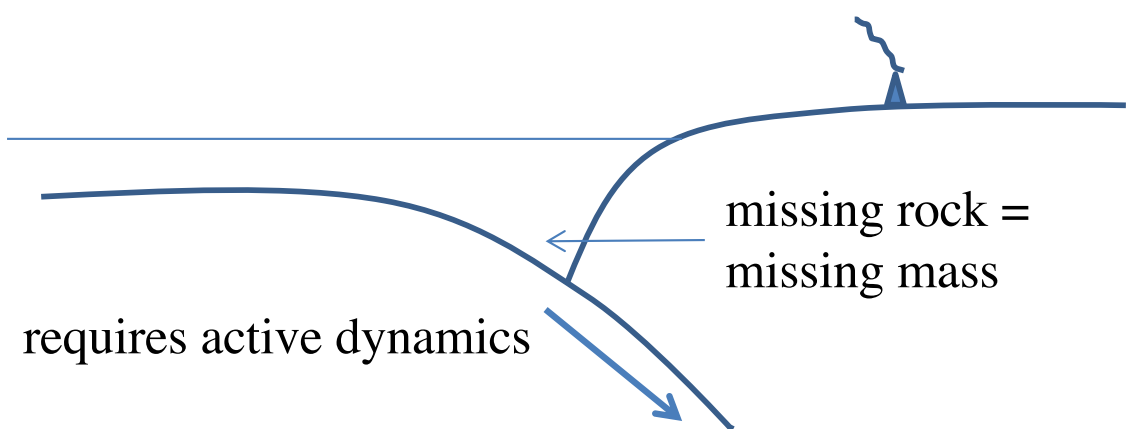

David Griggs:

The silicates in the Earth's mantle can deform very slowly

The earth's mantle acts like a liquid over geological time

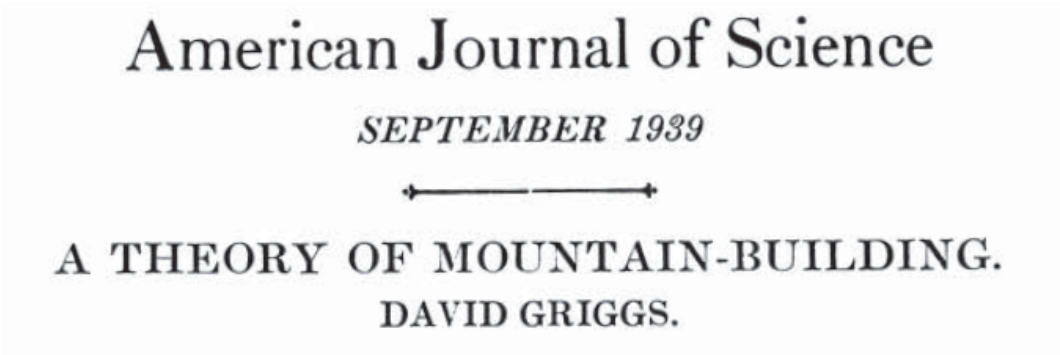
American Journal of Science

SEPTEMBER 1939

A THEORY OF MOUNTAIN-BUILDING.

DAVID GRIGGS.

David T. Griggs
(1911-1974)

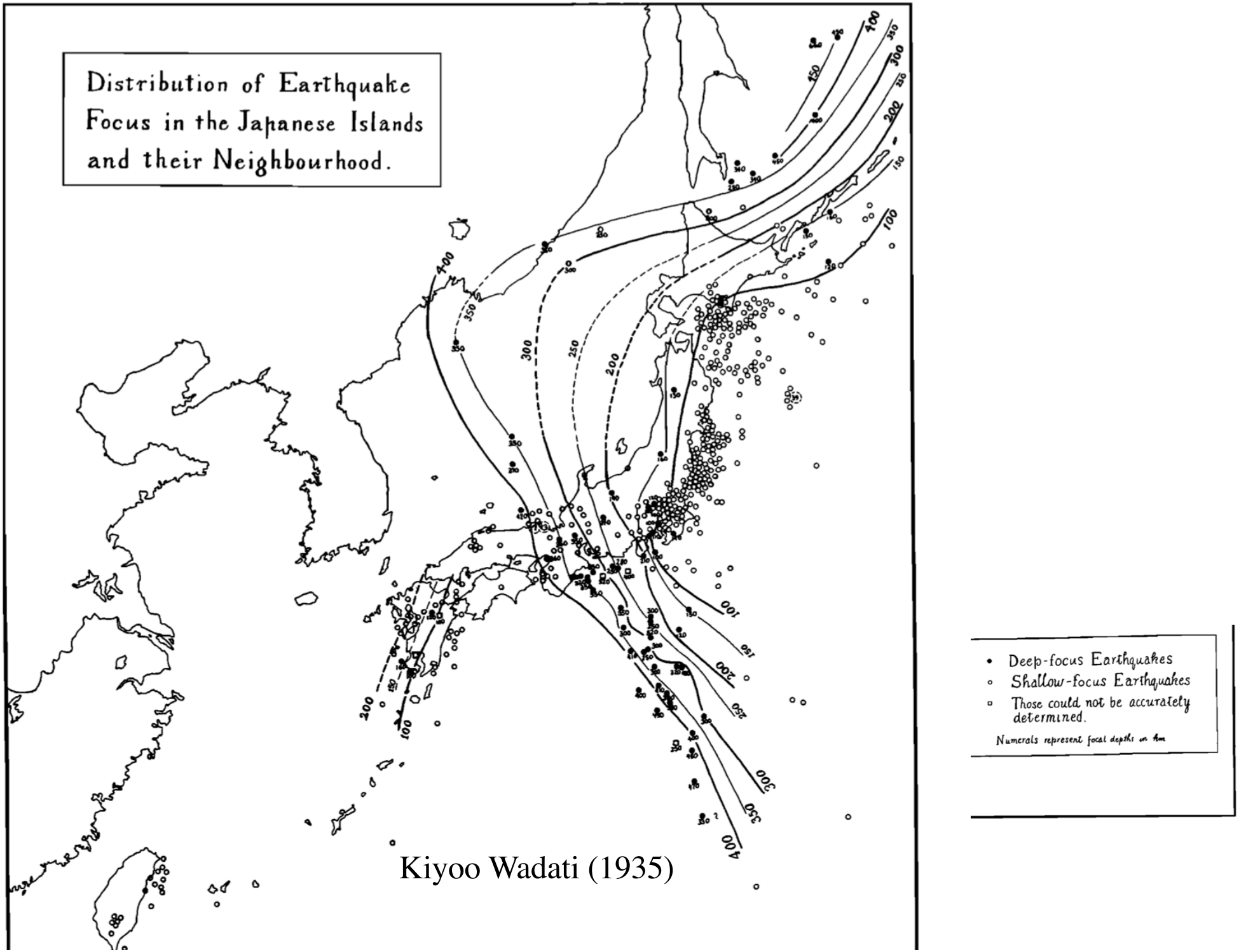
Distribution of Earthquake Focus in the Japanese Islands and their Neighbourhood.
Deep-focus Earthquakes
Shallow-focus Earthquakes
Those could not be accurately determined.
Numerals represent focal depths in km
Kiyoo Wadati (1935)

Tharp
&
Heezen

Marie Tharp (1920-2006)

From ship soundings:
North Atlantic (1957)
Entire Earth (1977)

Keith Runcorn (1922-1995)

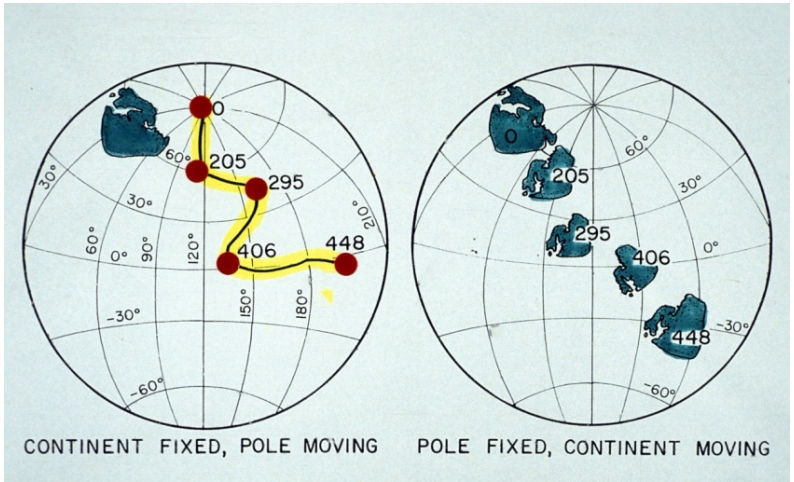

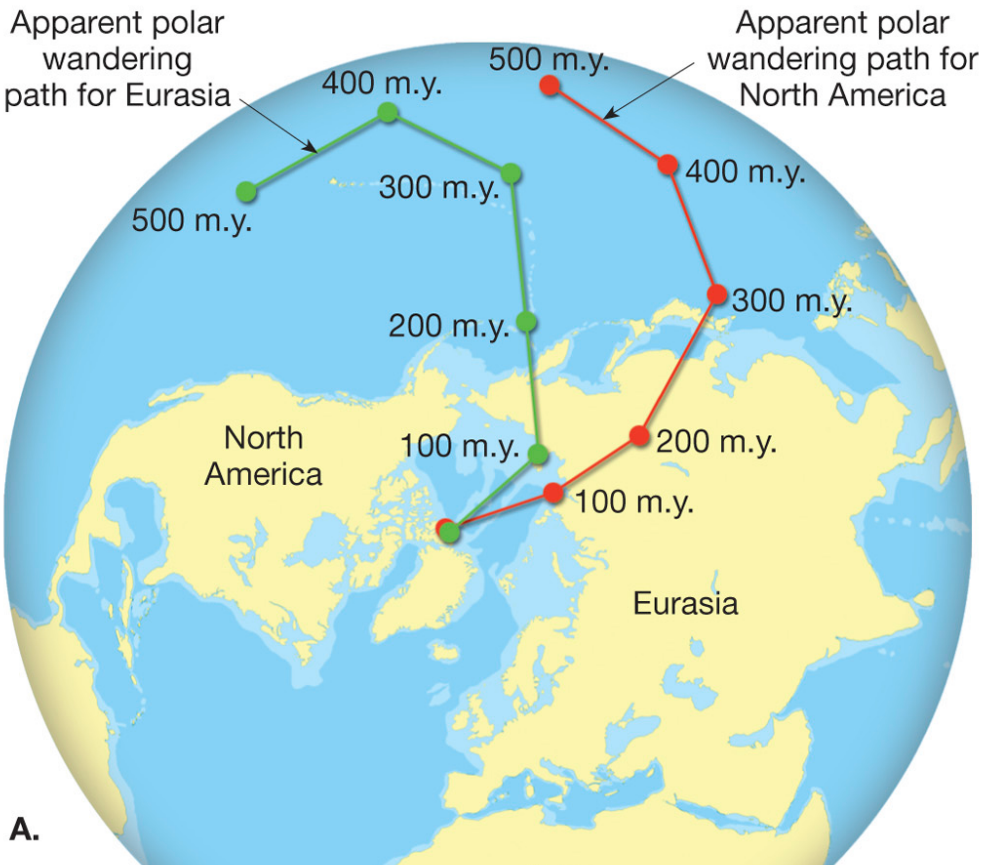

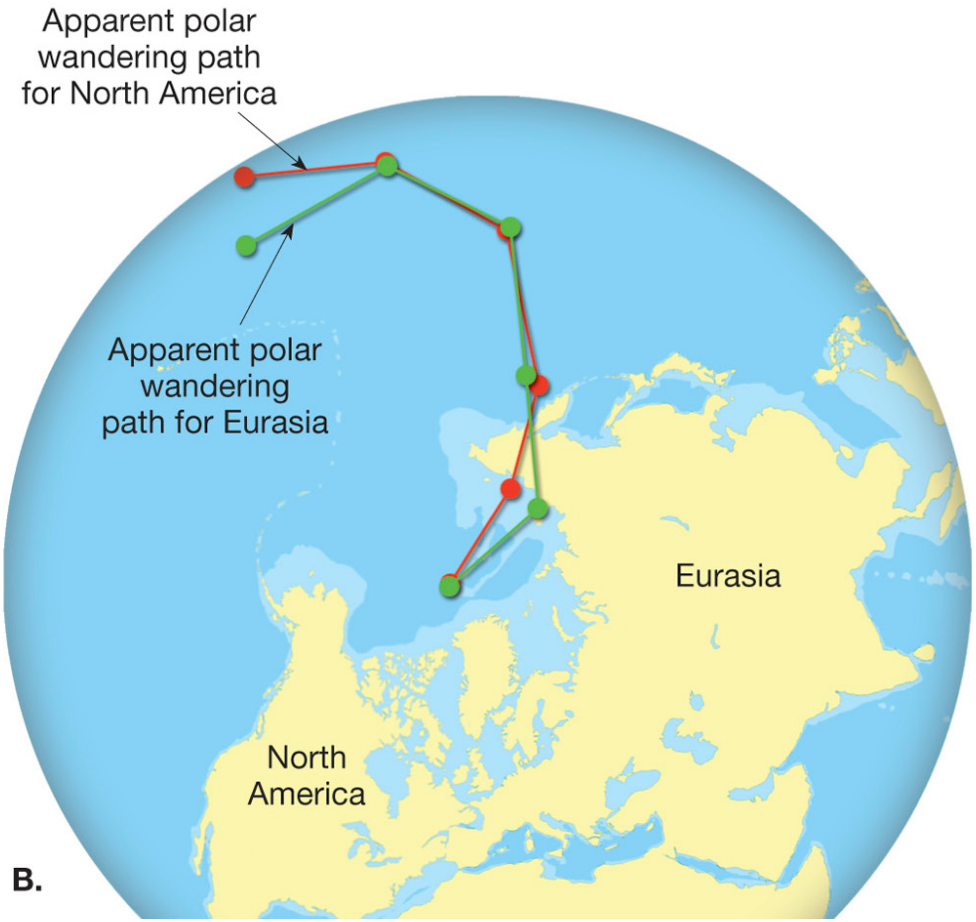

Paleomagnetic evidence for sea floor spreading (early 1960s)

Vines and Matthews (1970)

Vine and Matthews, 1963

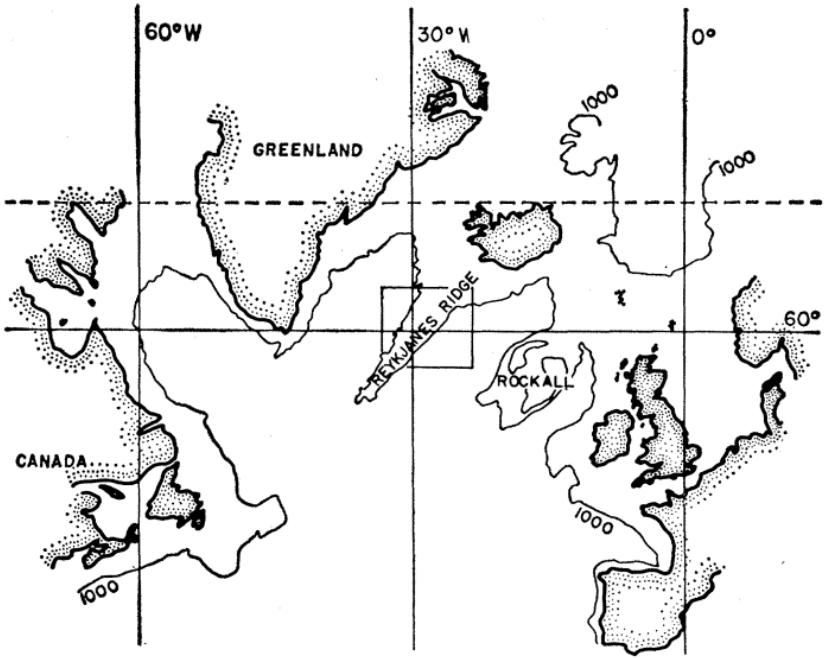

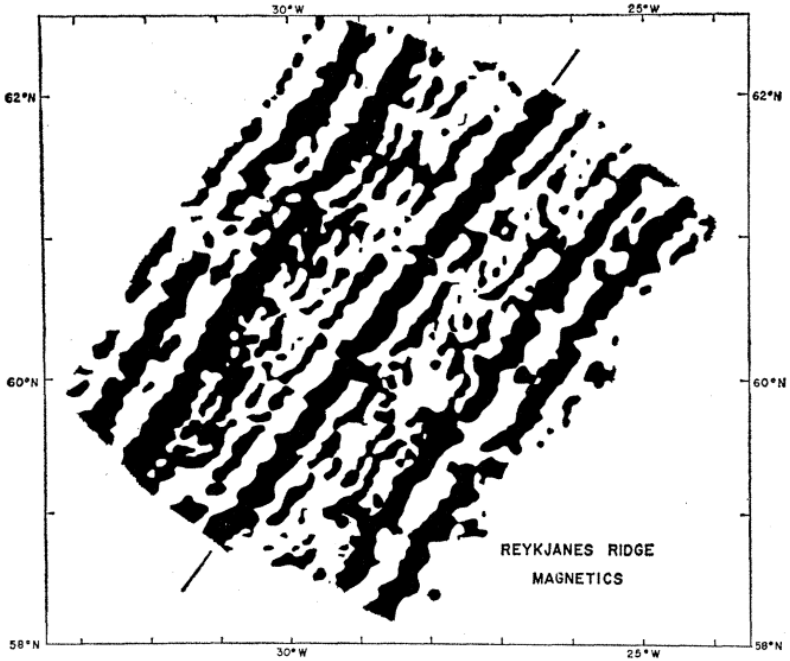

Fig. 2 (left). The location of Reykjanes Ridge, southwest of Iceland, and the area of Fig. 3. The 1000-fathom submarine contour is shown, together with the 500-fathom contours for Rockall Bank. Fig. 3 (right). Summary diagram of the magnetic anomalies observed over Reykjanes Ridge (see Fig. 2). Straight lines indicate the axis of the ridge and the central positive anomaly (*17*).

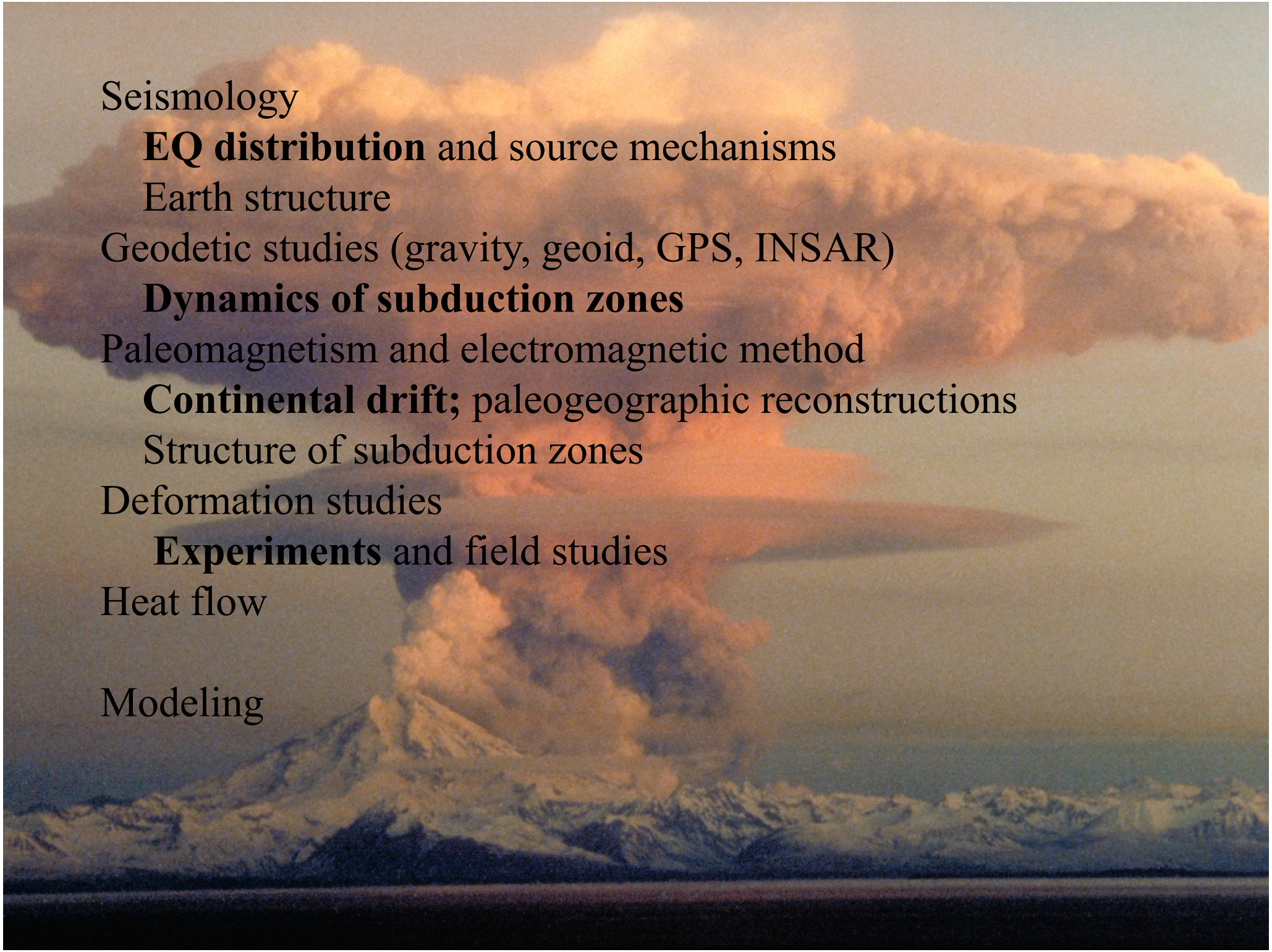

Seismology

- **EQ distribution** and source mechanisms
- Earth structure

Geodetic studies (gravity, geoid, GPS, INSAR)

- **Dynamics of subduction zones**

Paleomagnetism and electromagnetic method

- **Continental drift;** paleogeographic reconstructions
- Structure of subduction zones

Deformation studies

- **Experiments** and field studies

Heat flow

Modeling

The Subducting Oceanic Plate

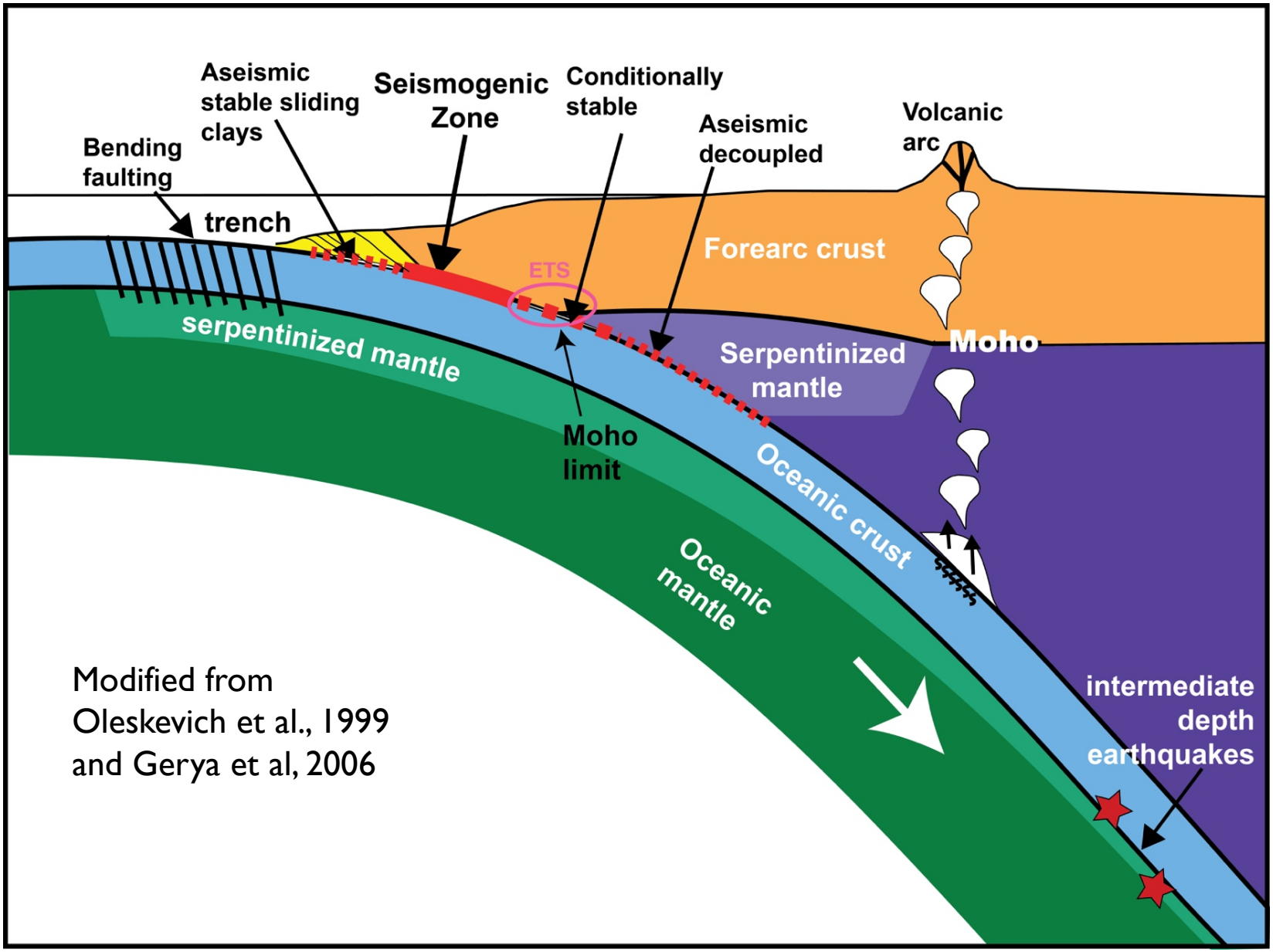

Modified from
Oleskevich et al., 1999
and Gerya et al, 2006

Subduction Cycles and Deformation

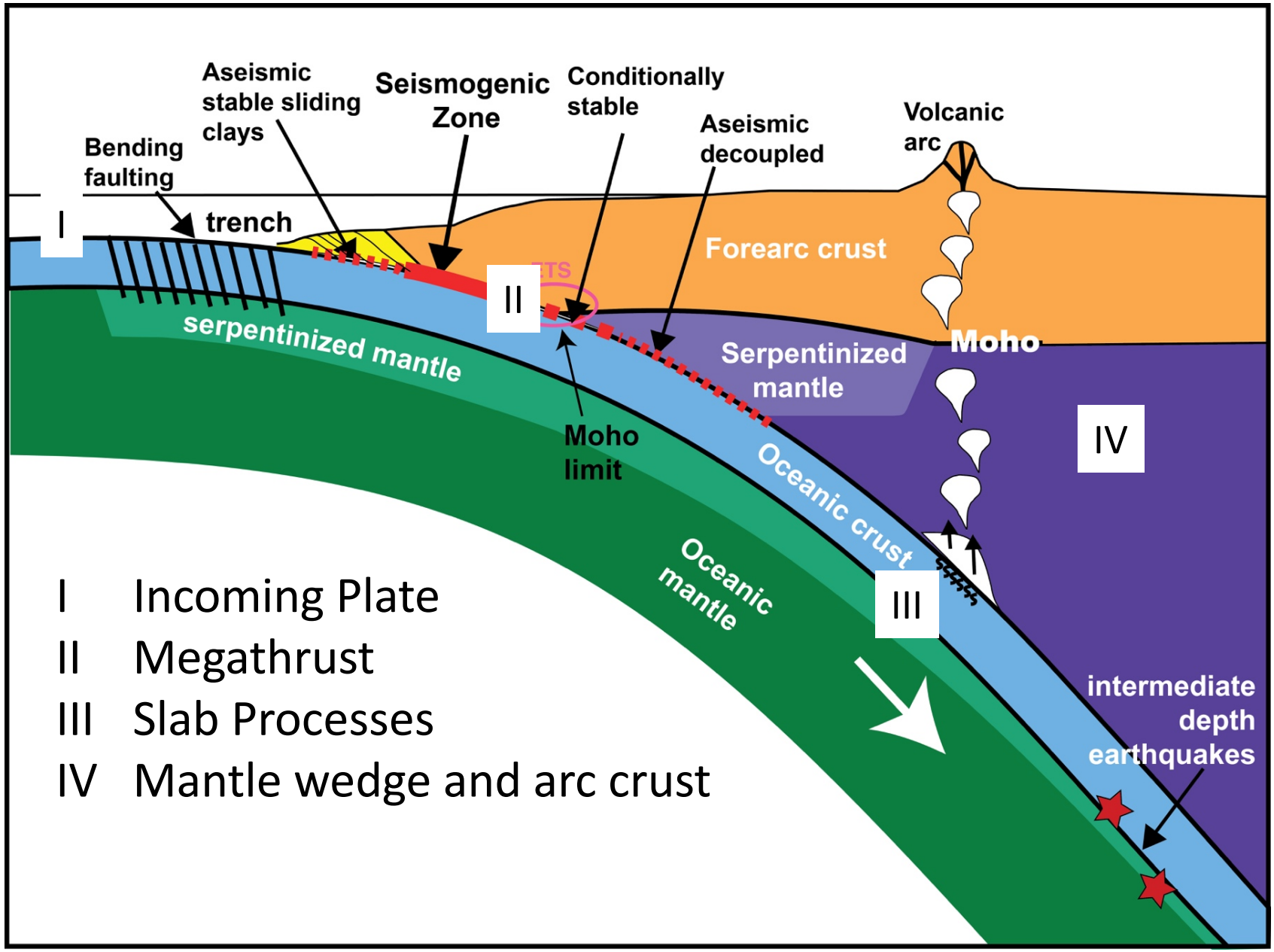

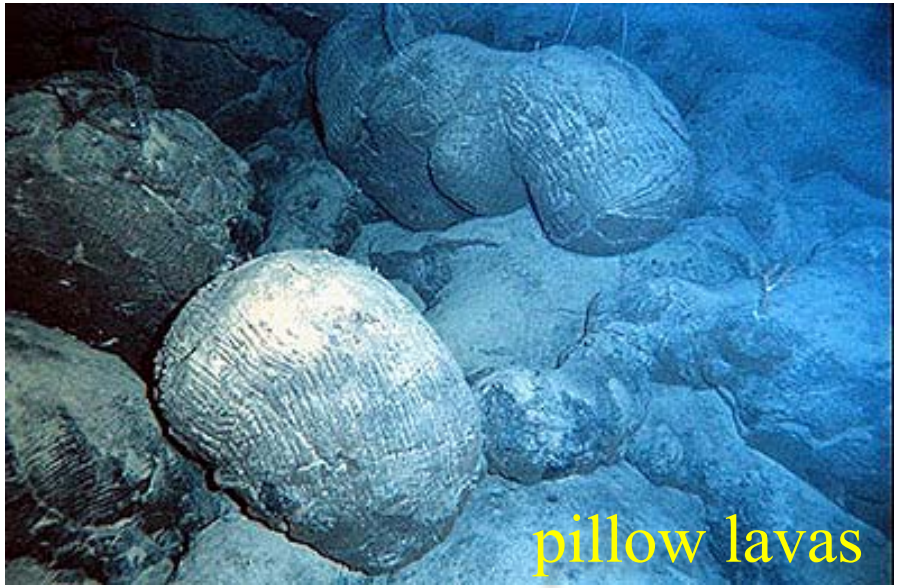
pillow lavas

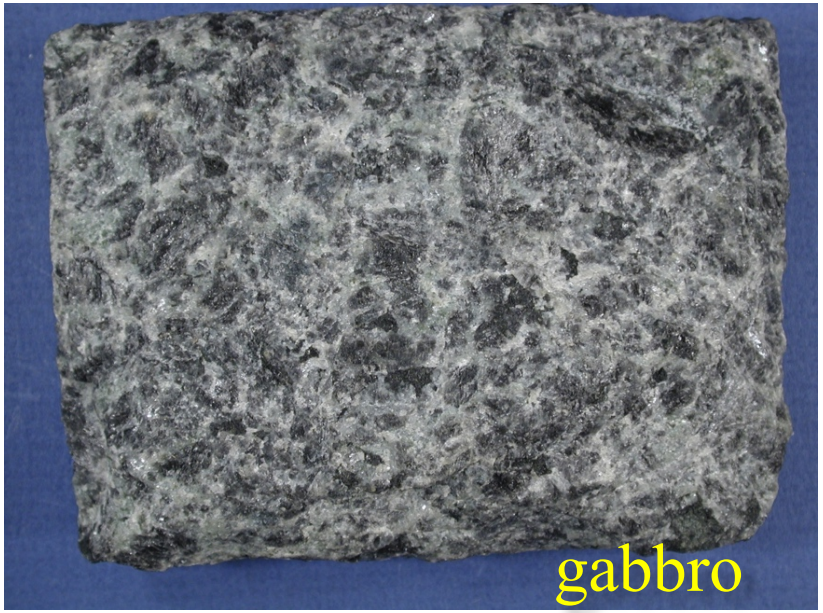
gabbro

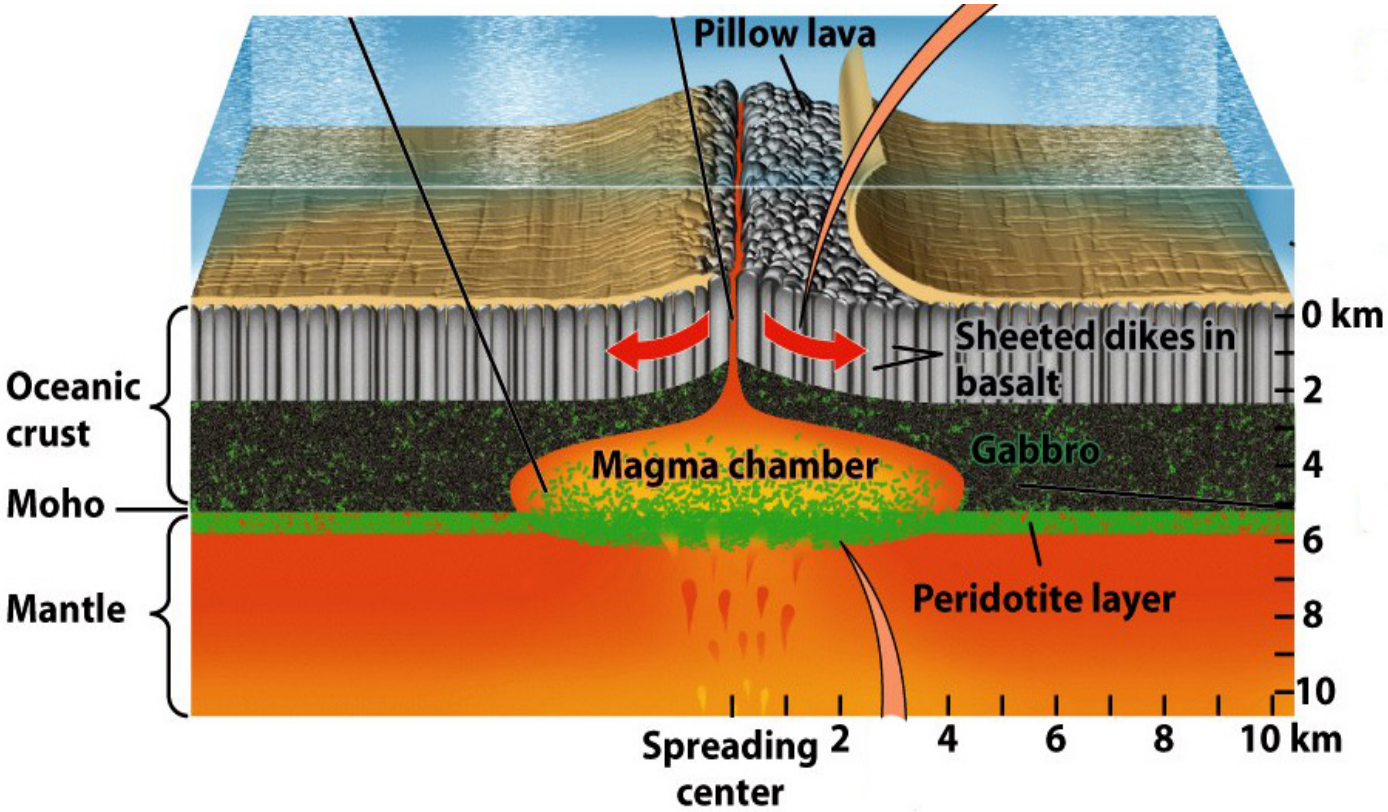
Pillow lava
Sheeted dikes in basalt
Oceanic crust
Moho
Mantle
Magma chamber
Gabbro
Peridotite layer
Spreading center
0 km
2
4
6
8
10
2
4
6
8
10 km

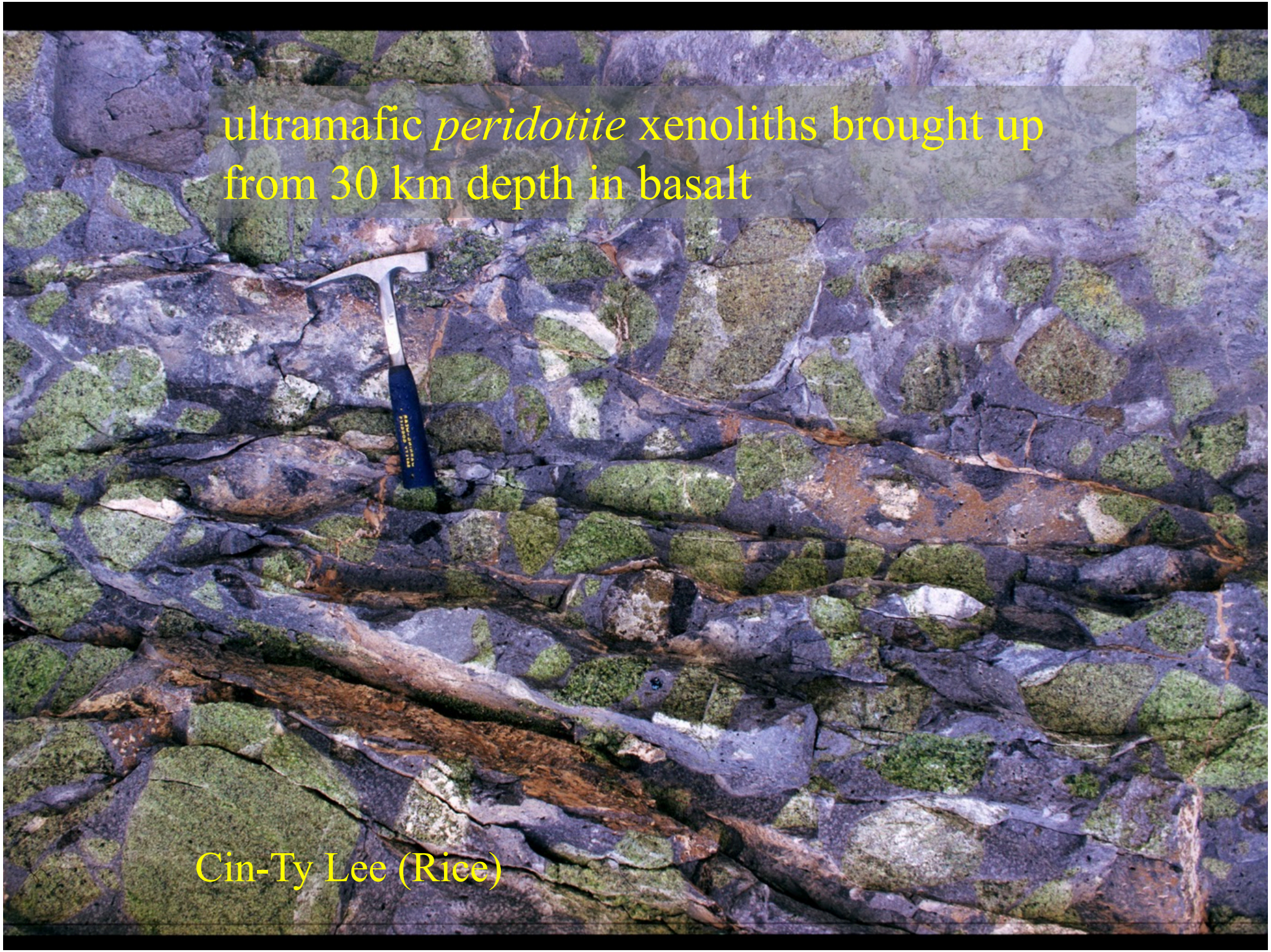
ultramafic *peridotite* xenoliths brought up
from 30 km depth in basalt
Cin-Ty Lee (Rice)

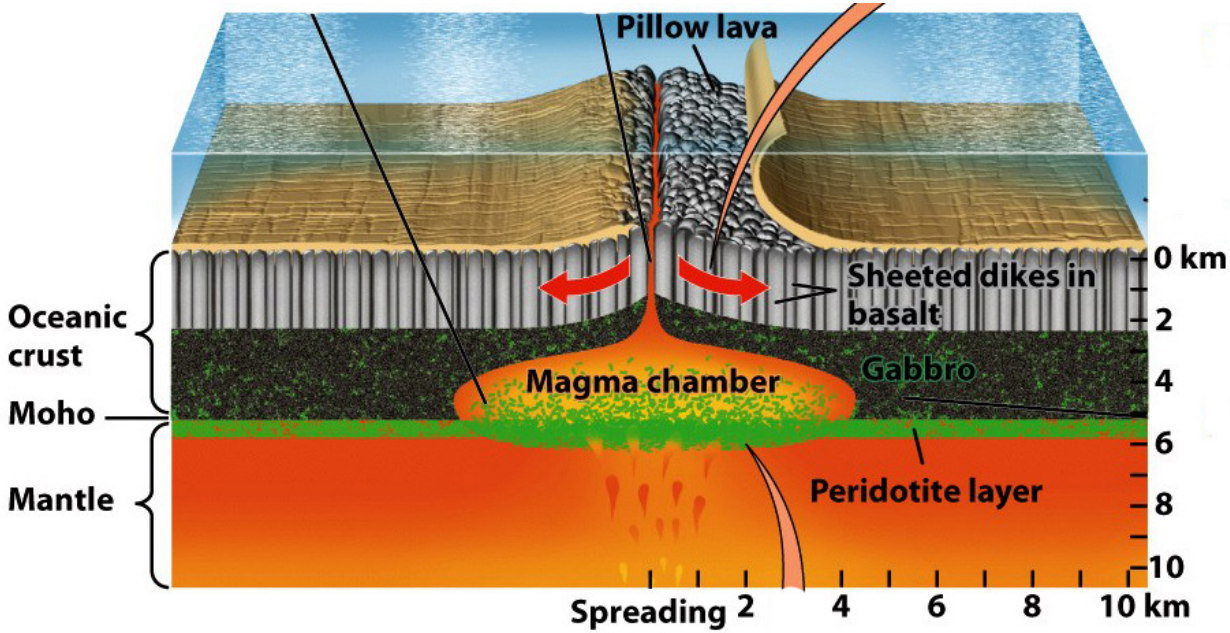
Pillow lava
Sheeted dikes in basalt
Oceanic crust
Moho
Mantle
Magma chamber
Gabbro
Peridotite layer
0 km
2
4
6
8
10
Spreading
2
4
6
8
10 km

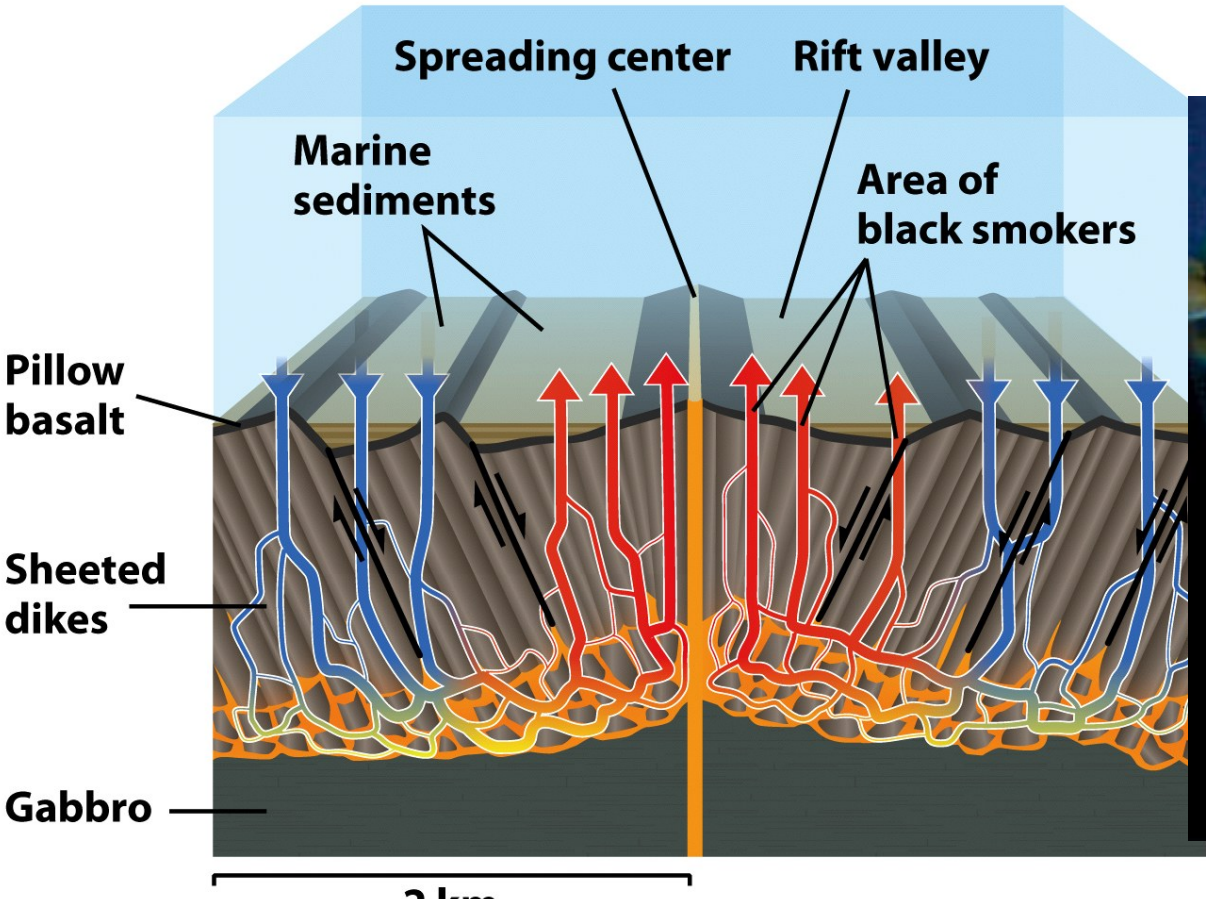
Spreading center
Rift valley
Marine sediments
Area of black smokers
Pillow basalt
Sheeted dikes
Gabbro

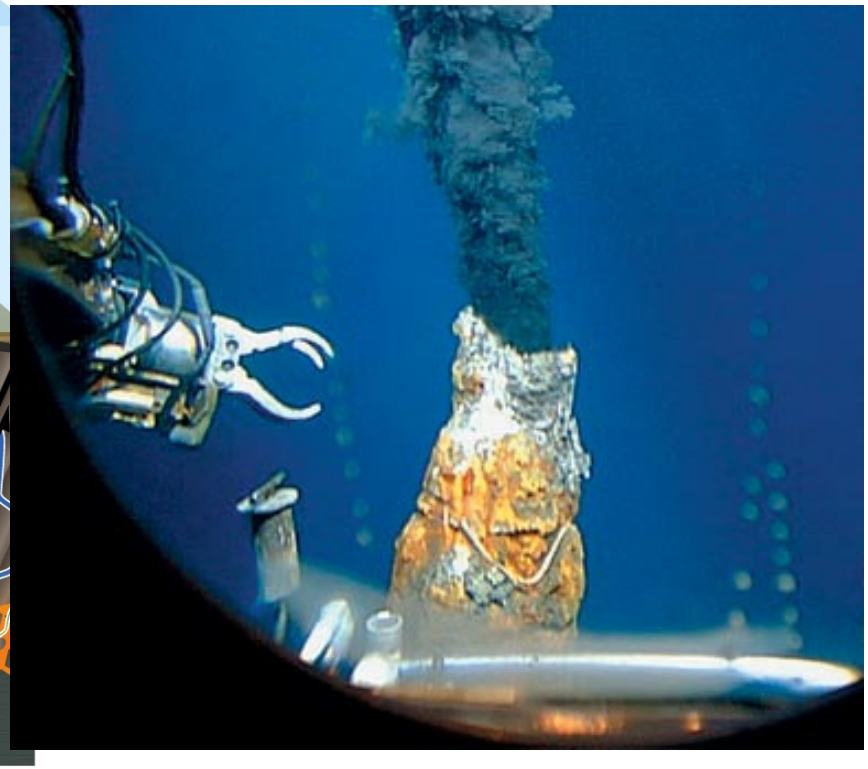

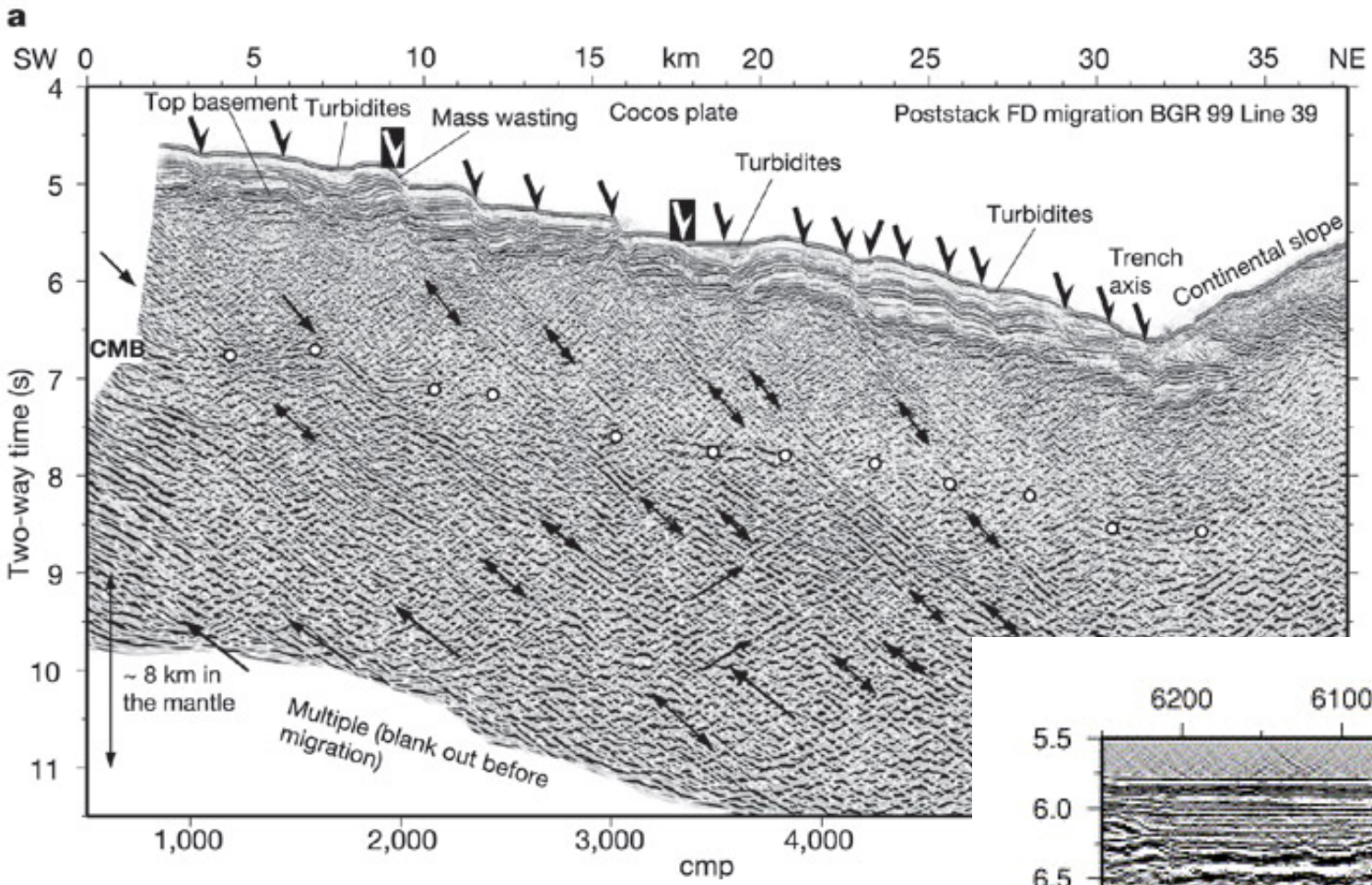

Ranero et al., Nature, 2003

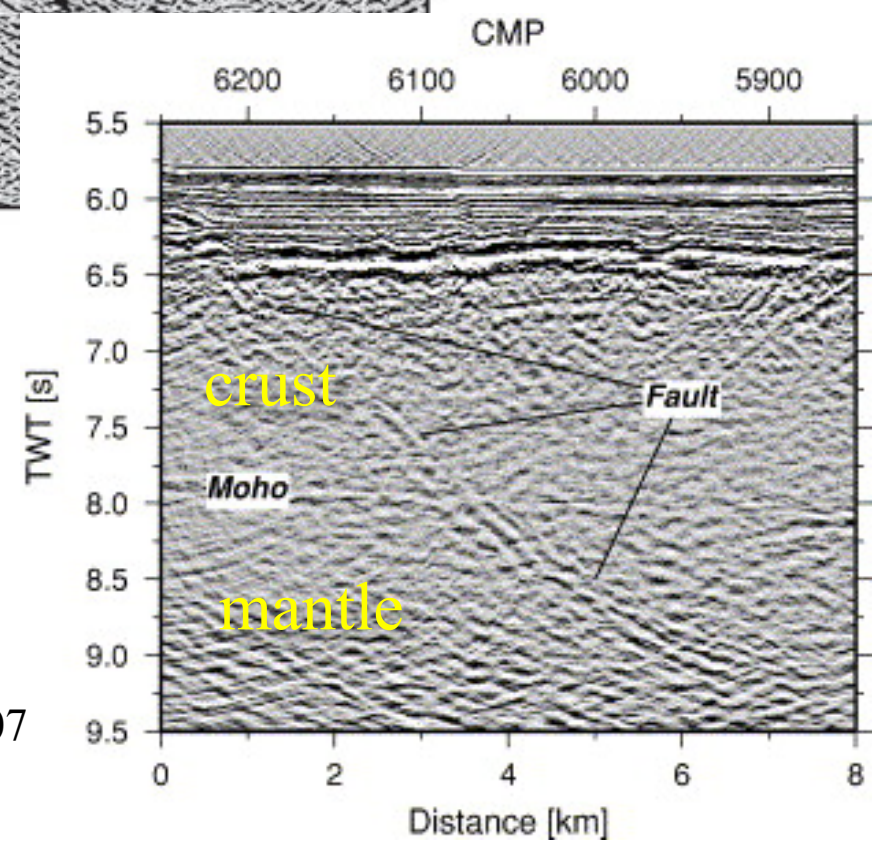

Bend faulting in Nicaragua provides fluid pathways to mantle below crust

Grevemeyer et al., EPSL, 2007

Estimated water distribution in incoming slab

Compacted sediments: 0.4-5 wt% (variable composition)

Volcanics and sheeted dikes: 2 wt%

Gabbro: 0.7 wt%

Serpentinite in upper mantle: X wt% in Y km thick layer

Slab structure outboard of trench at Nicaragua (Ivandic et al., 2008)

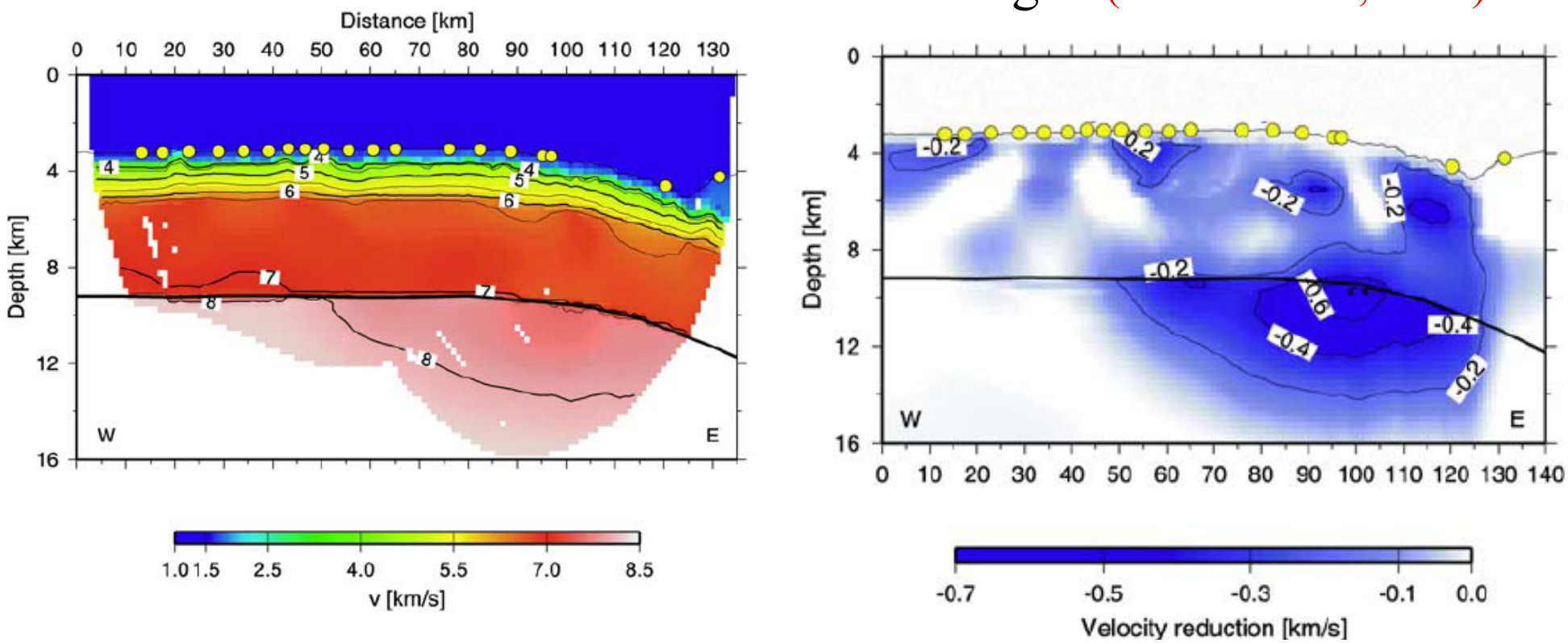

Shillington et al., Nature GS, 2015

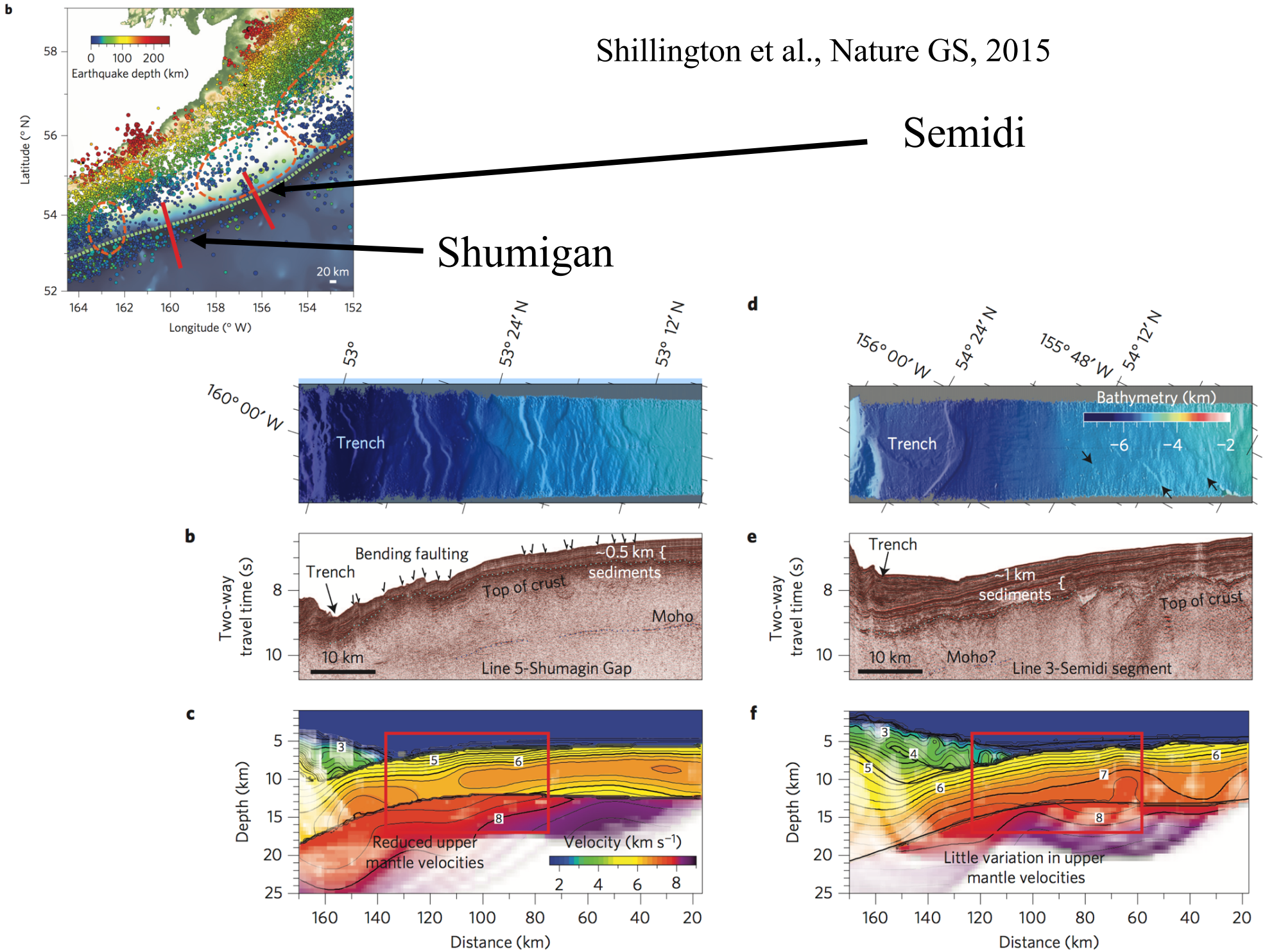

Seafloor EM studies show high conductivity regions

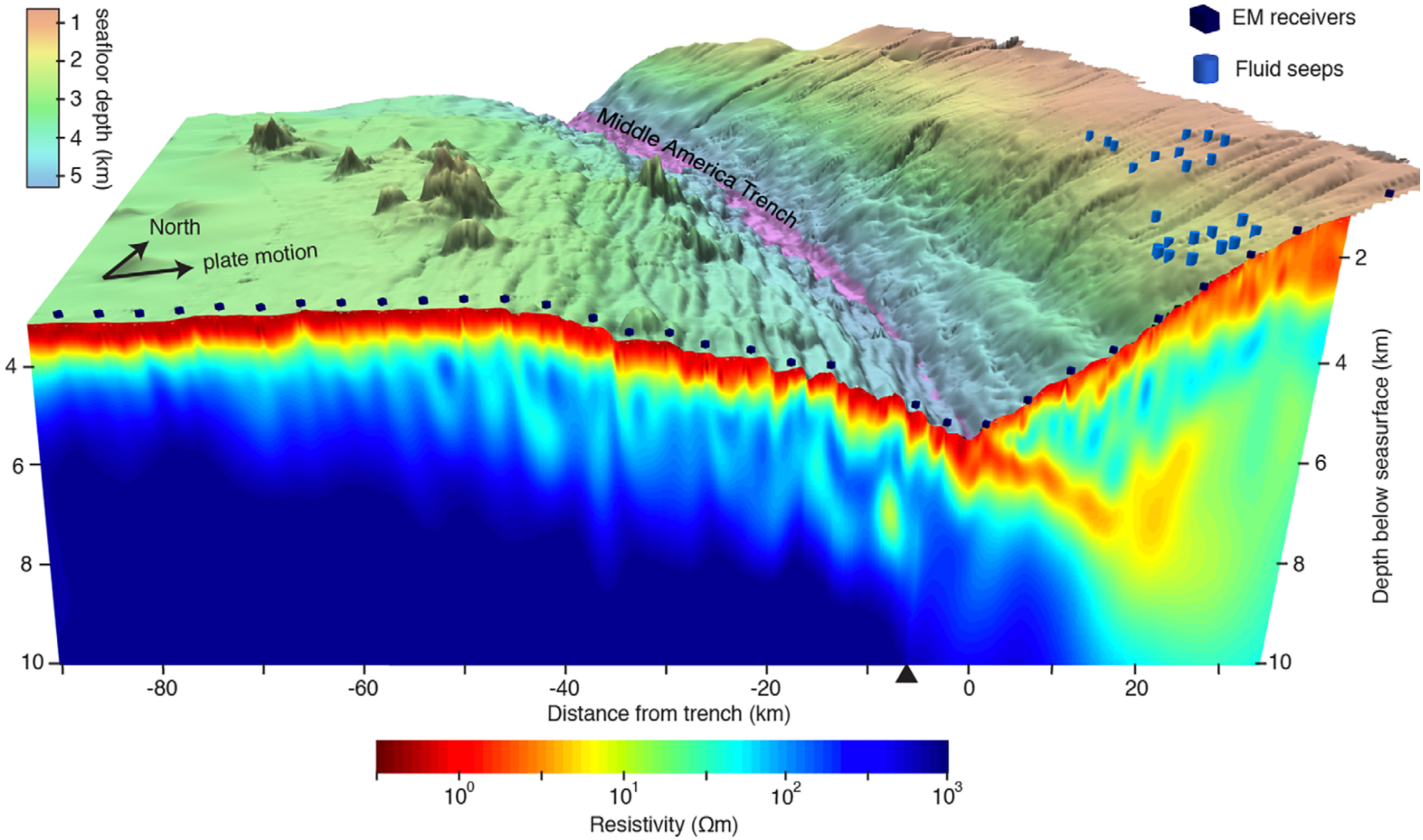

Naif et al., G3, 2015, 2016

Shallow slip in the forearc

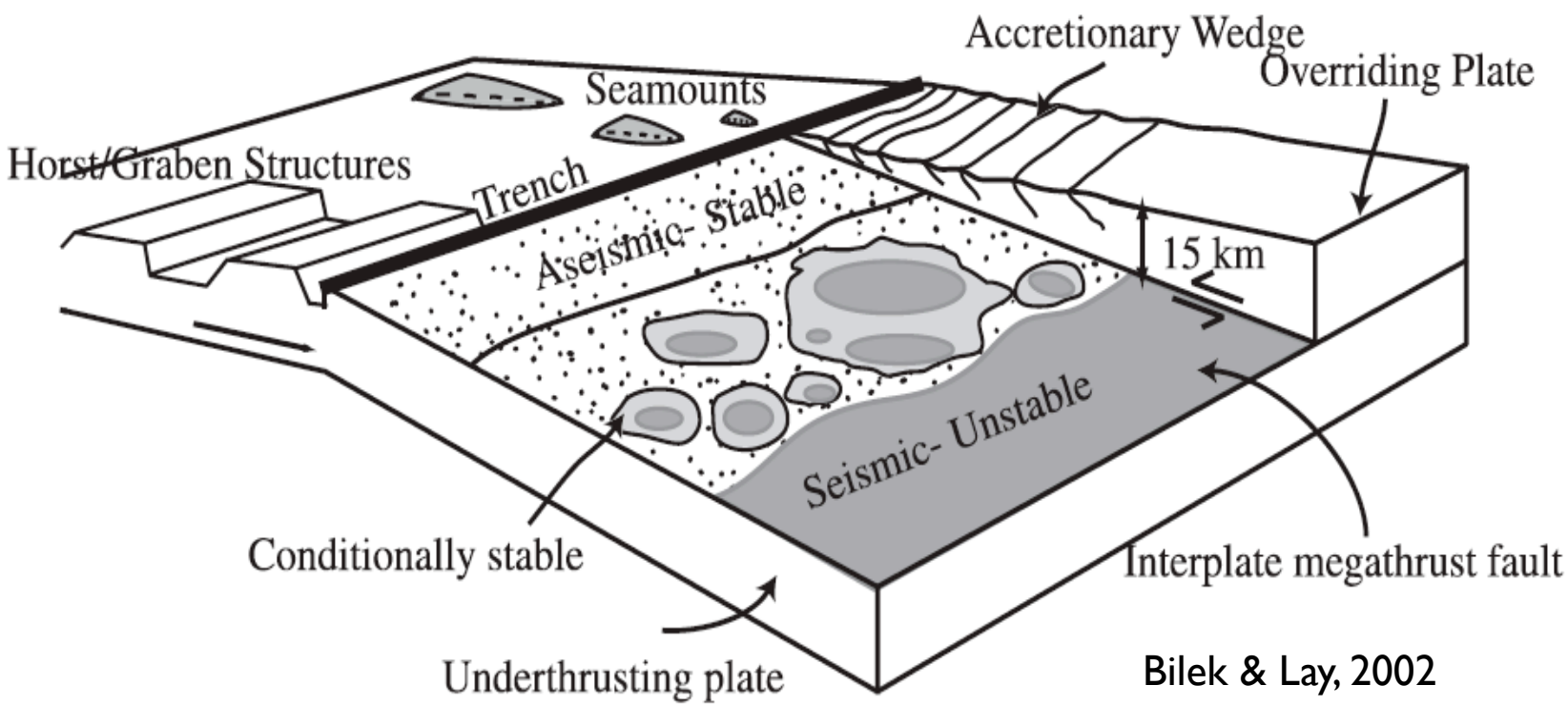

Bilek & Lay, 2002

Episodic tremor and slip in Cascadia

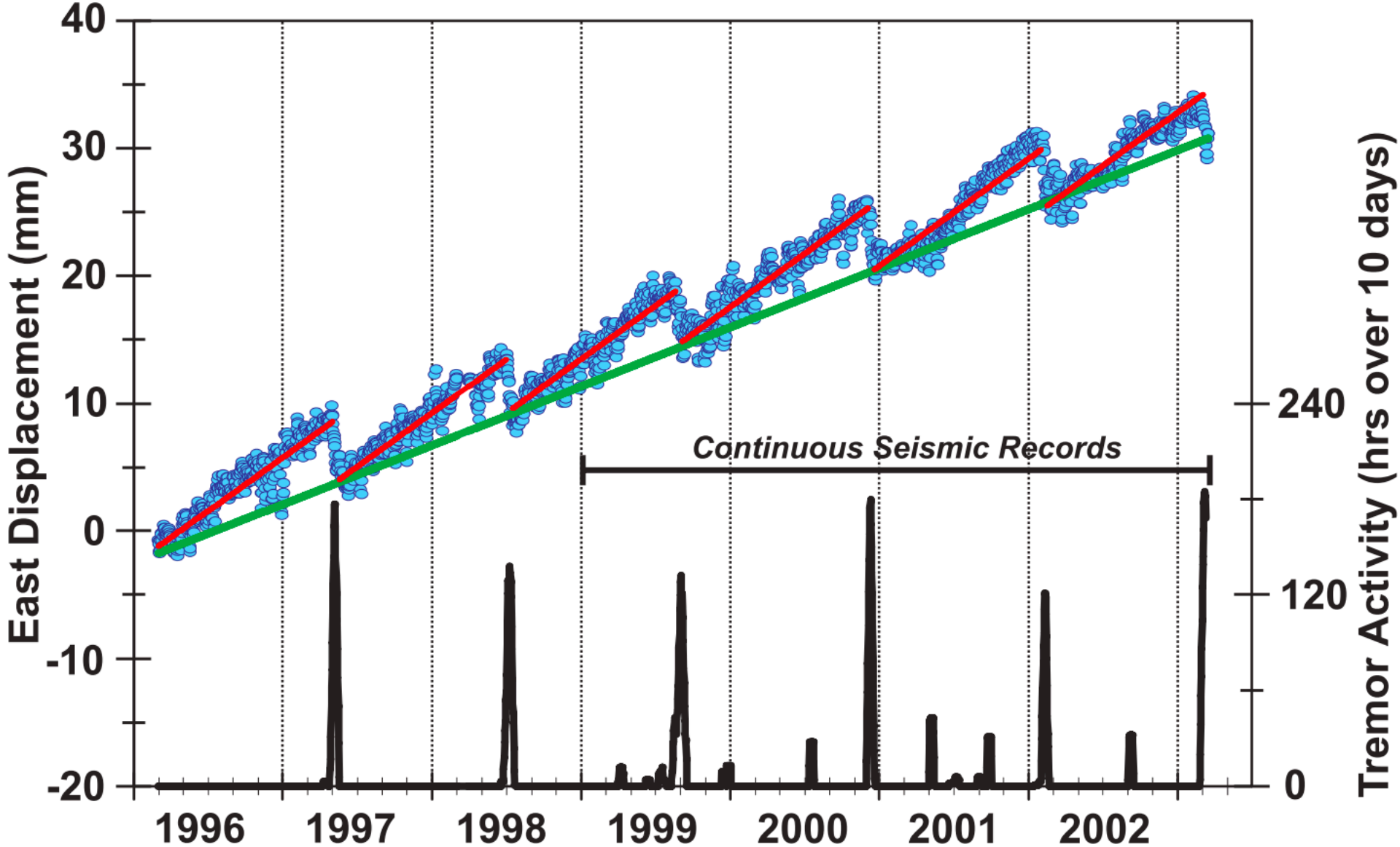

Rodgers and Dragert, Science, 2003

Estimated Plate Coupling

from GPS data 1995-2000

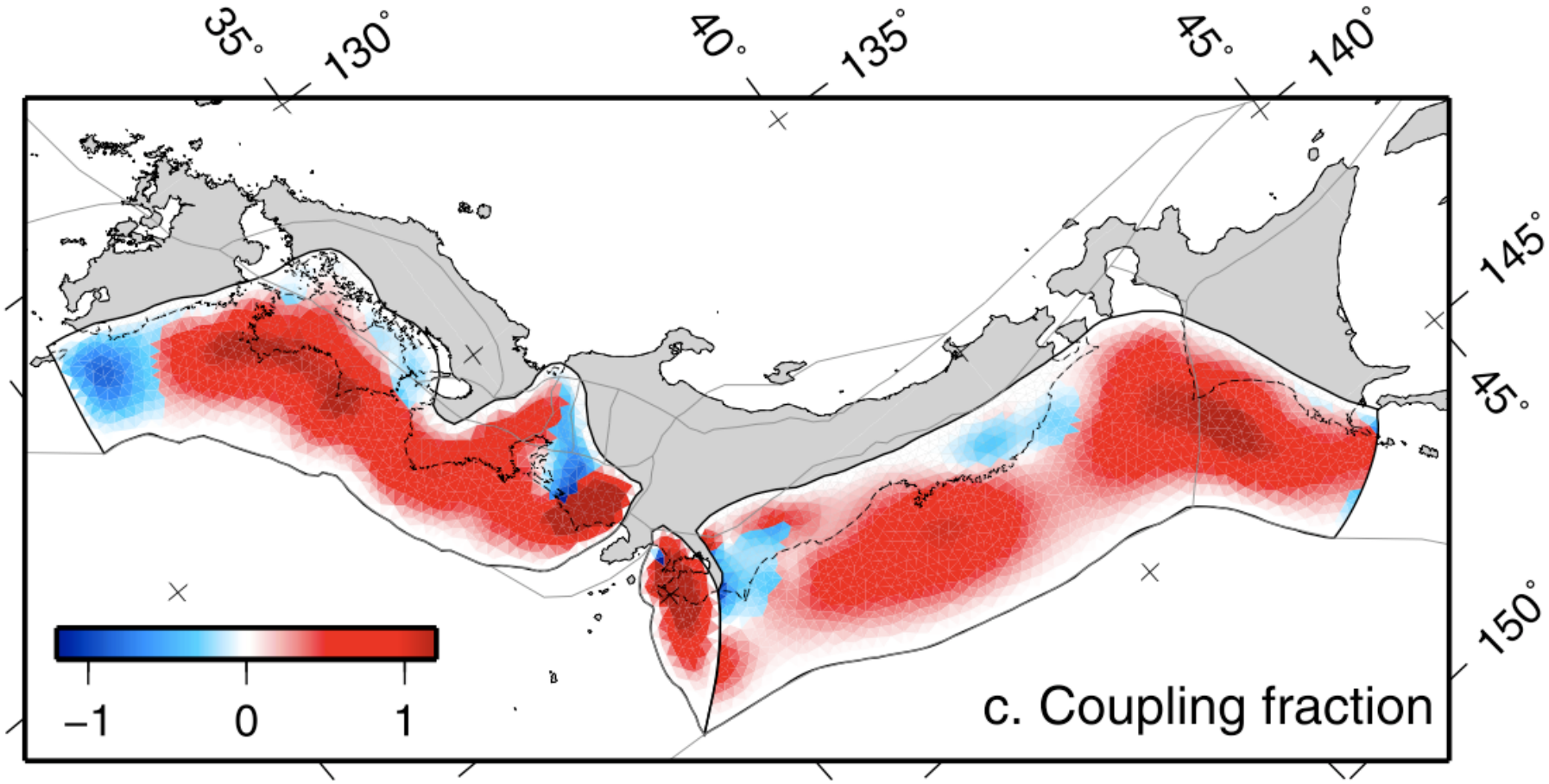

slide from Jeff Freymueller
(SCD TEI student symposium 2015)

Meade and Loveless (2010)

Estimated Plate Coupling

from GPS data 1995-2000

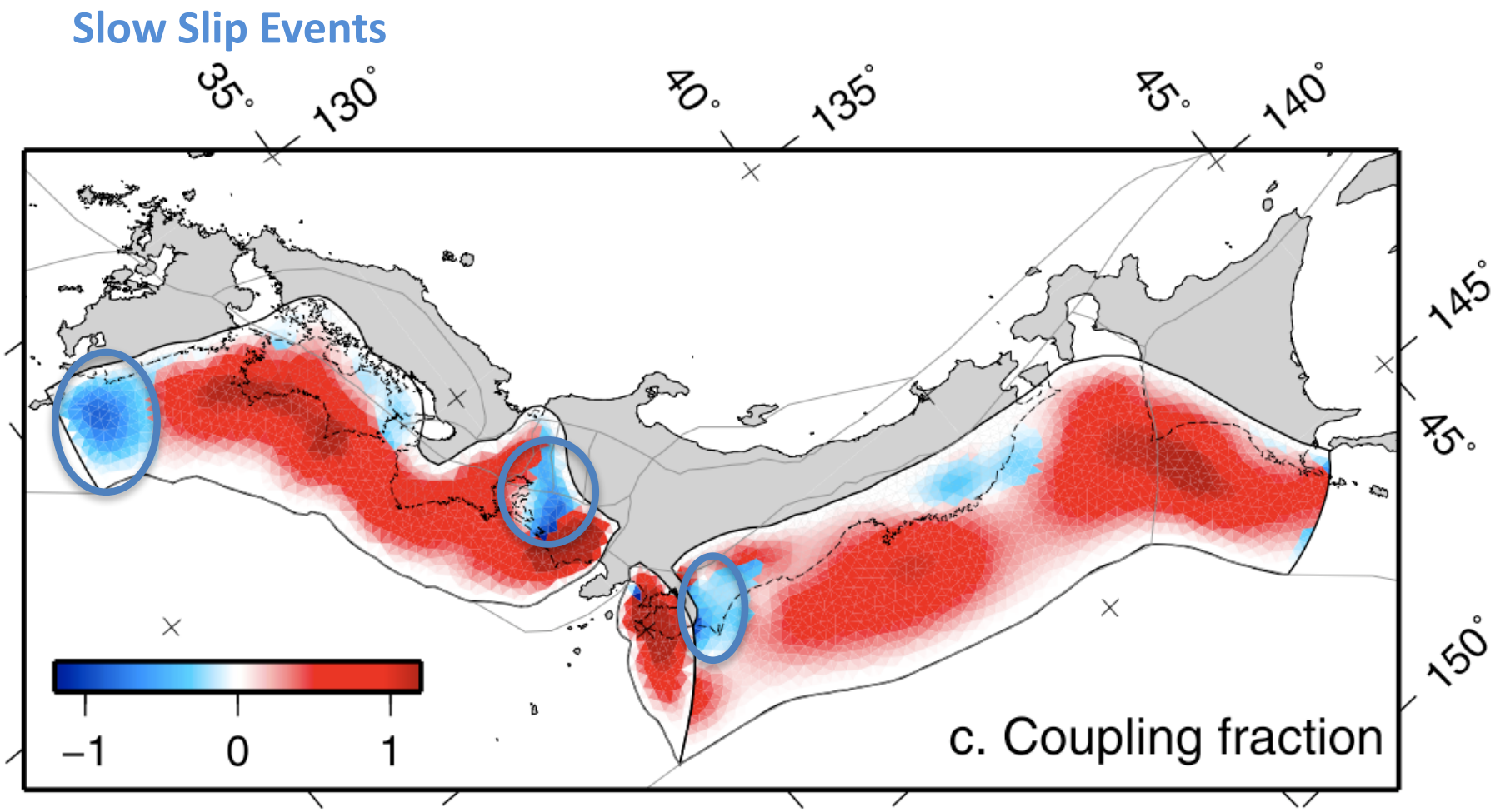

slide from Jeff Freymueller
(SCD TEI student symposium 2015)

Meade and Loveless (2010)

Estimated Plate Coupling

from GPS data 1995-2000

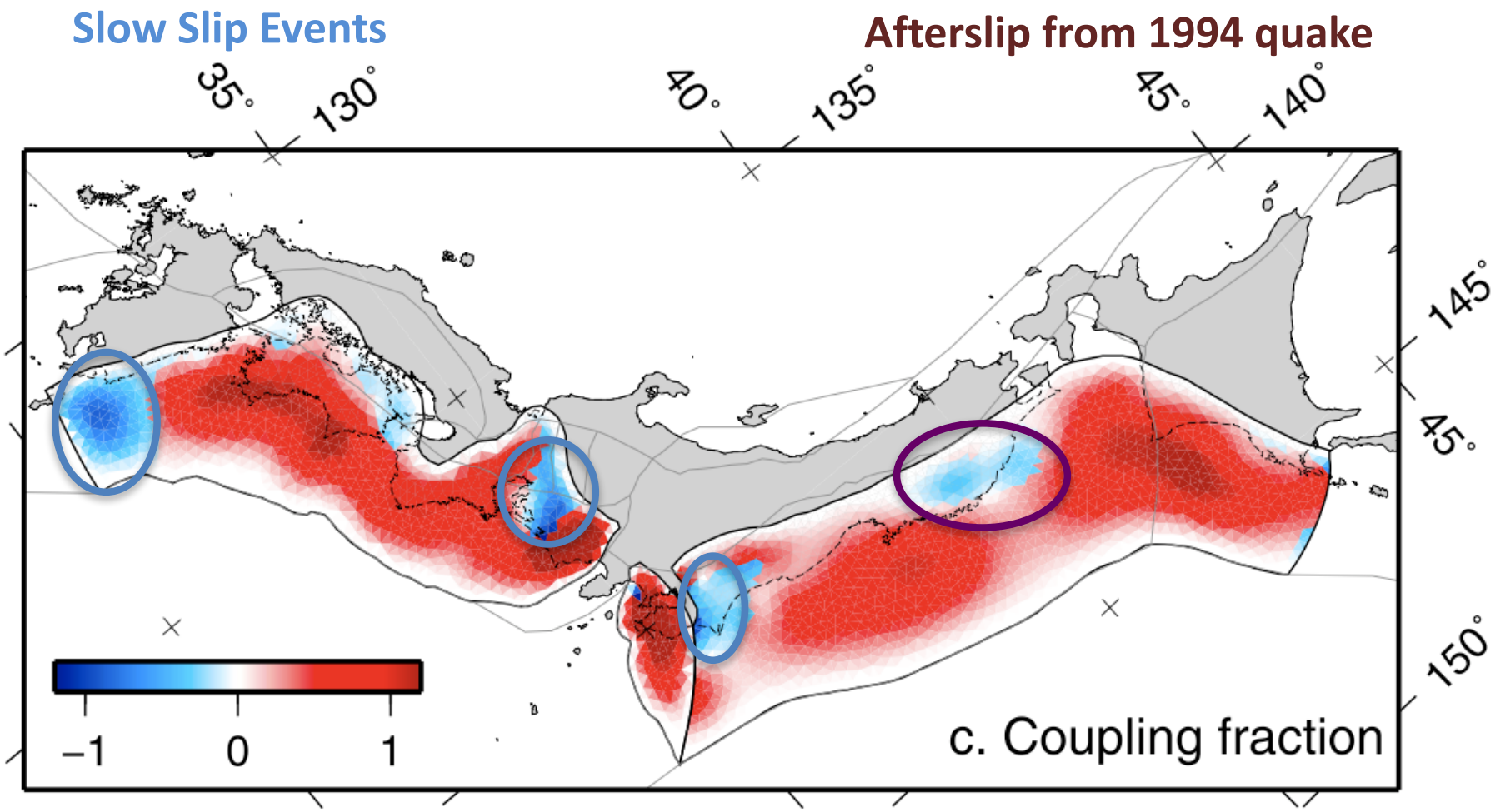

slide from Jeff Freymueller
(SCD TEI student symposium 2015)

Meade and Loveless (2010)

Estimated Plate Coupling

from GPS data 1995-2000

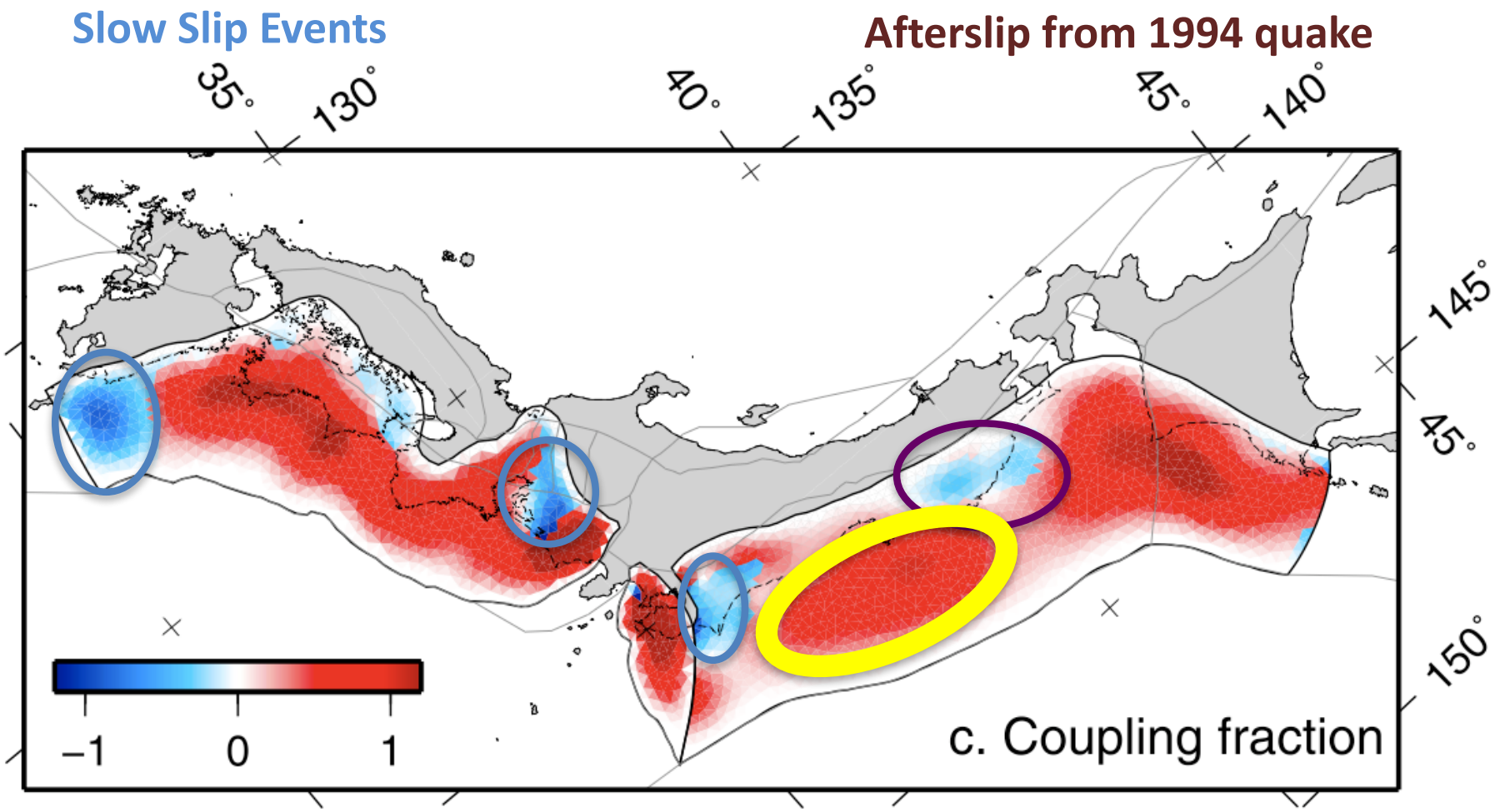

slide from Jeff Freymueller
(SCD TEI student symposium 2015)

Meade and Loveless (2010)

Comparison of Locked Zone to Slip

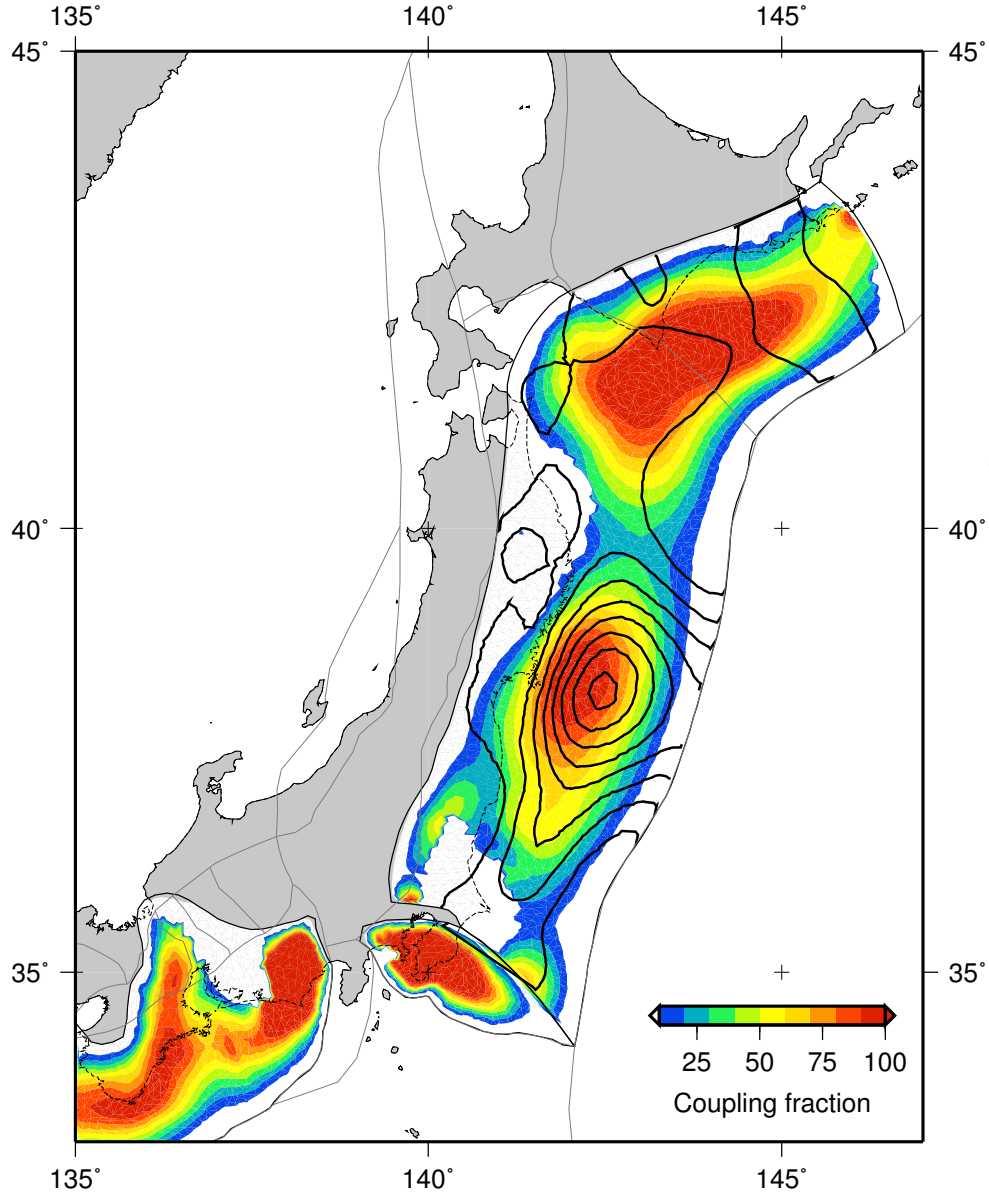

Colors: Loveless and Meade (2010) interseismic model

Contours: Jack Loveless' slip model contours

To first order, the rupture area of the earthquake is the same as the interseismic locked zone

Loveless and Meade, 3/14/11
Loveless and Meade (2011)

slide from Jeff Freymueller
(SCD TEI student symposium 2015)

Stachnik et al., 2004

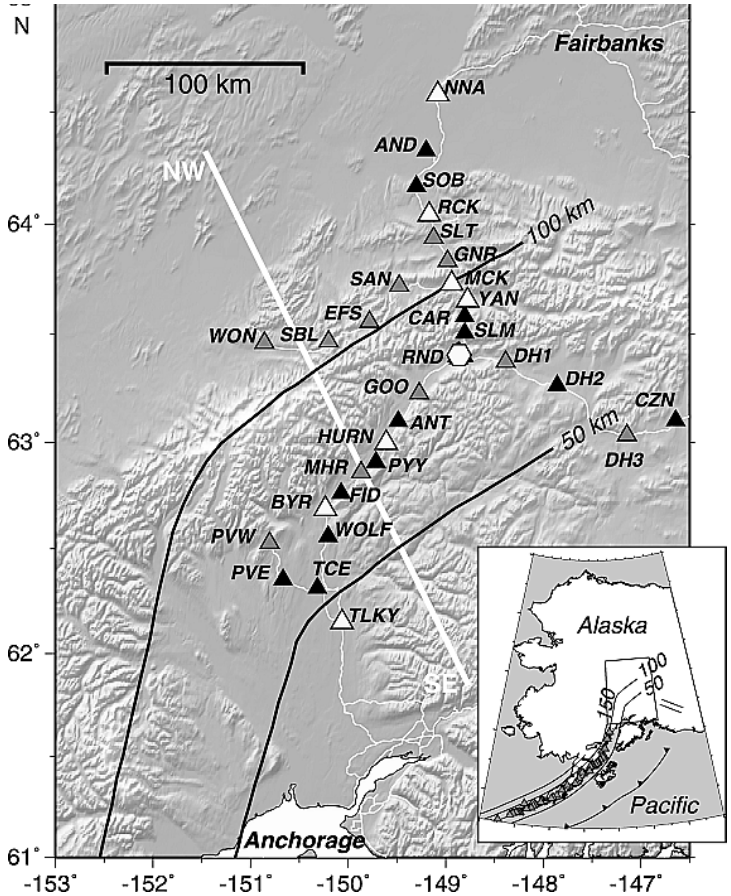

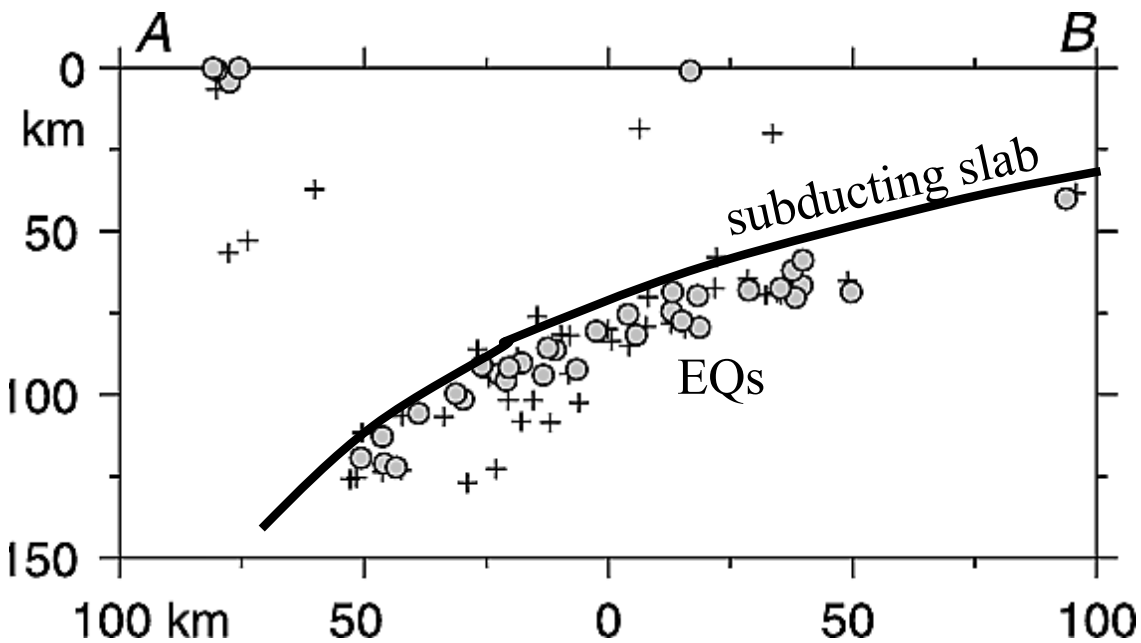

Stachnik et al., 2004

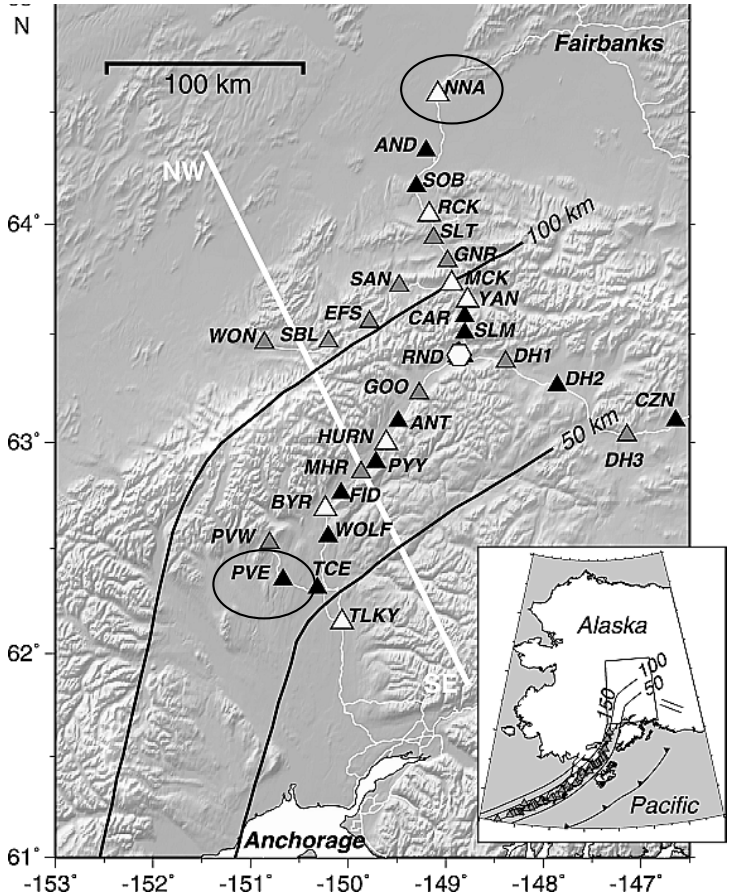

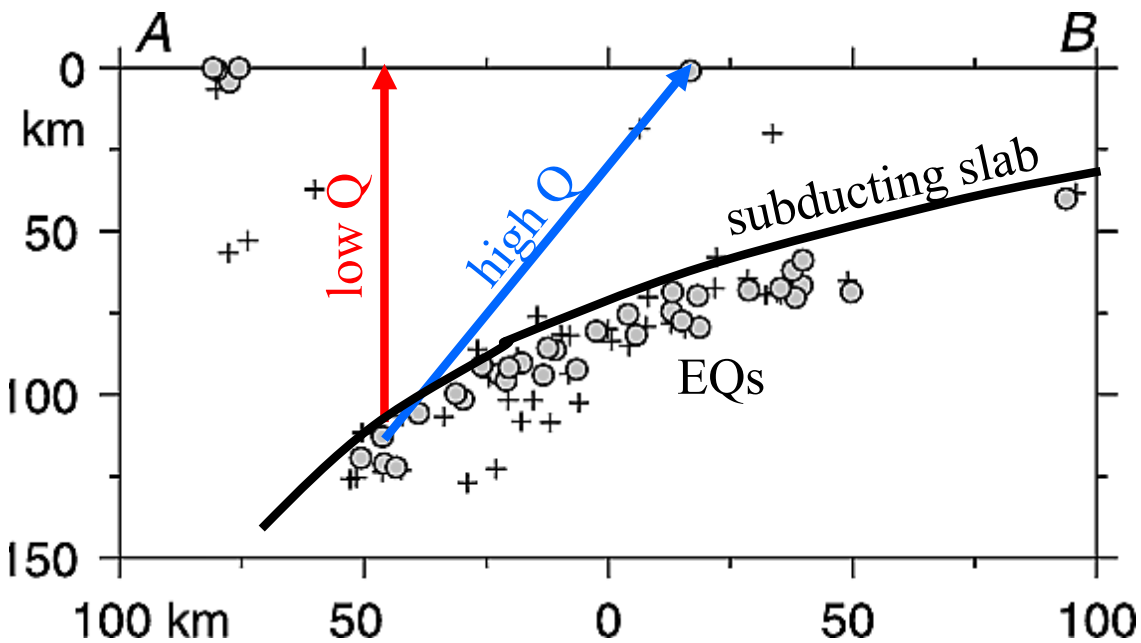

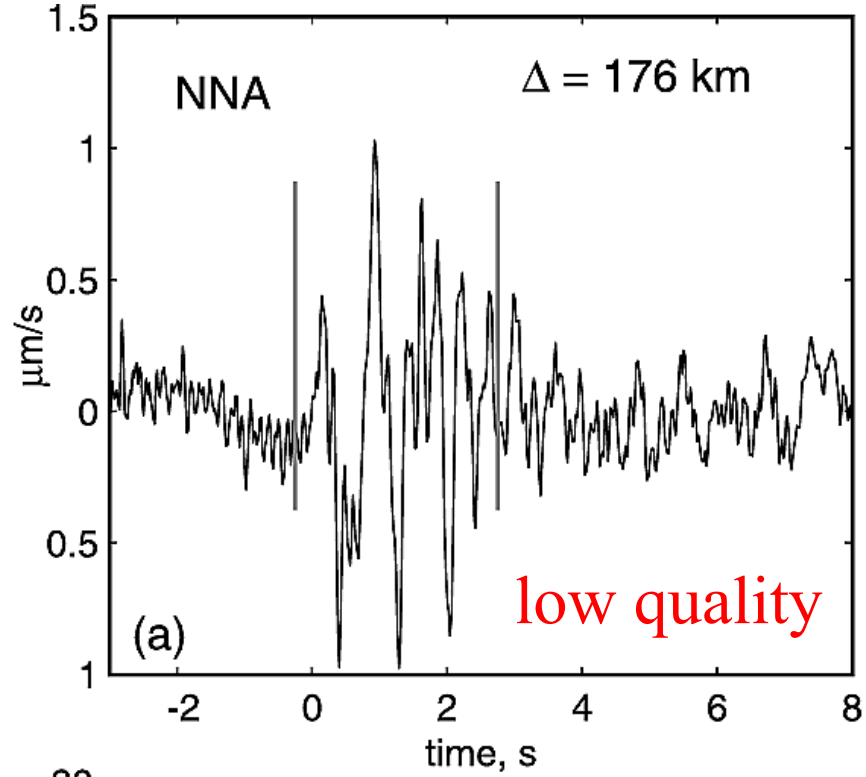

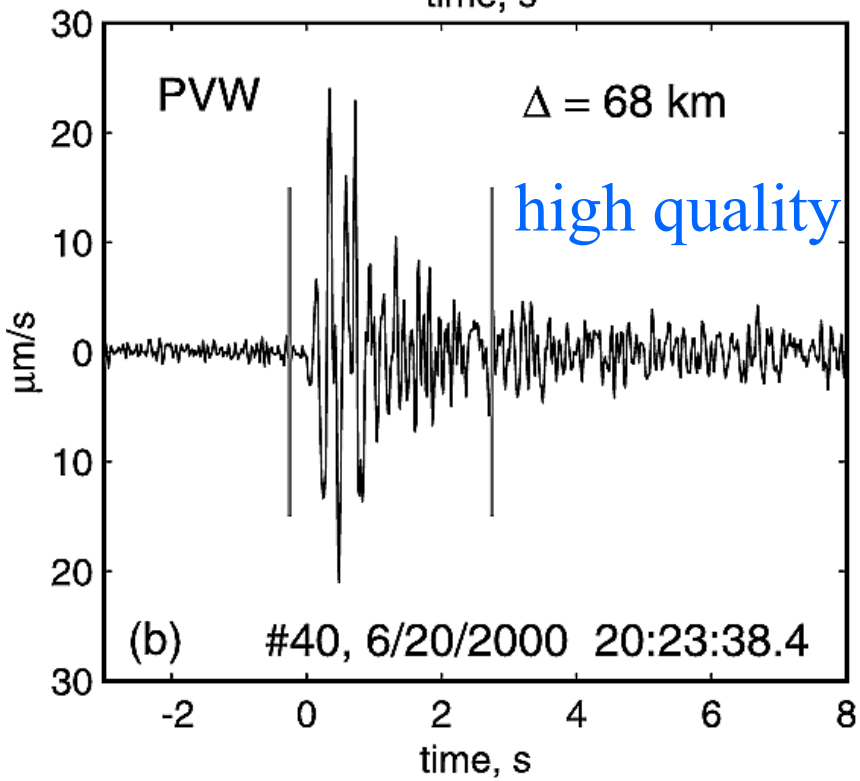

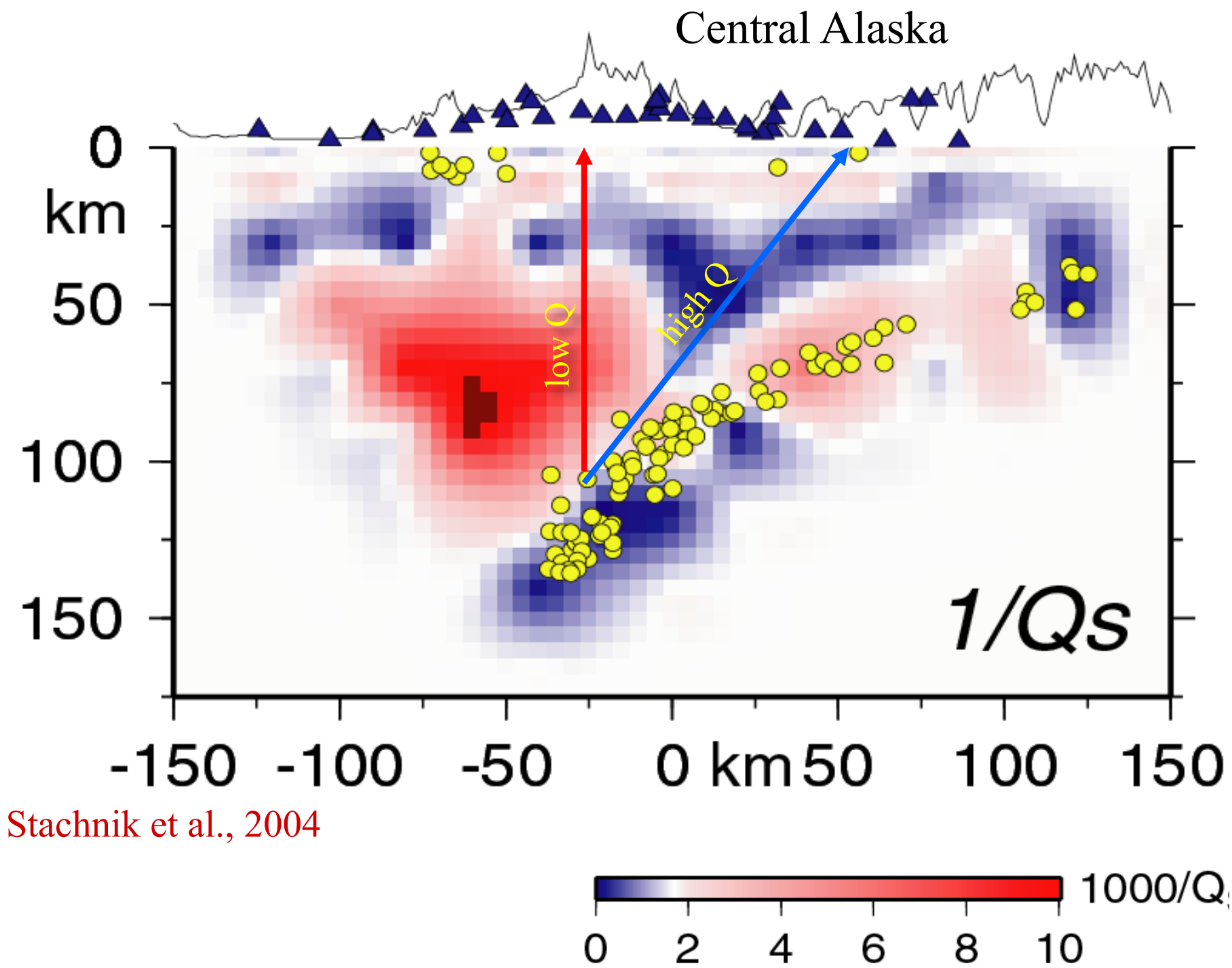

Stachnik et al., 2004

Q (1/attenuation)

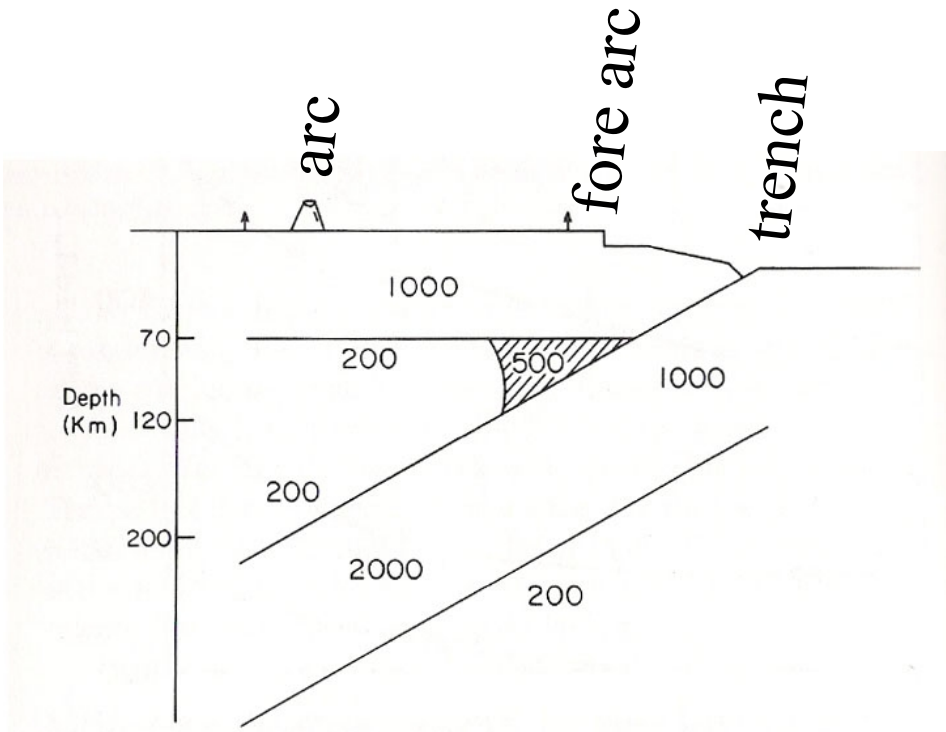

FIGURE 3.5 Q model for the Japan region. The hatched region has an anomalously high Q for the asthenosphere, $Q_p = 500$; normal oceanic asthenosphere has $Q_p = 200$.

Sacks, 1984

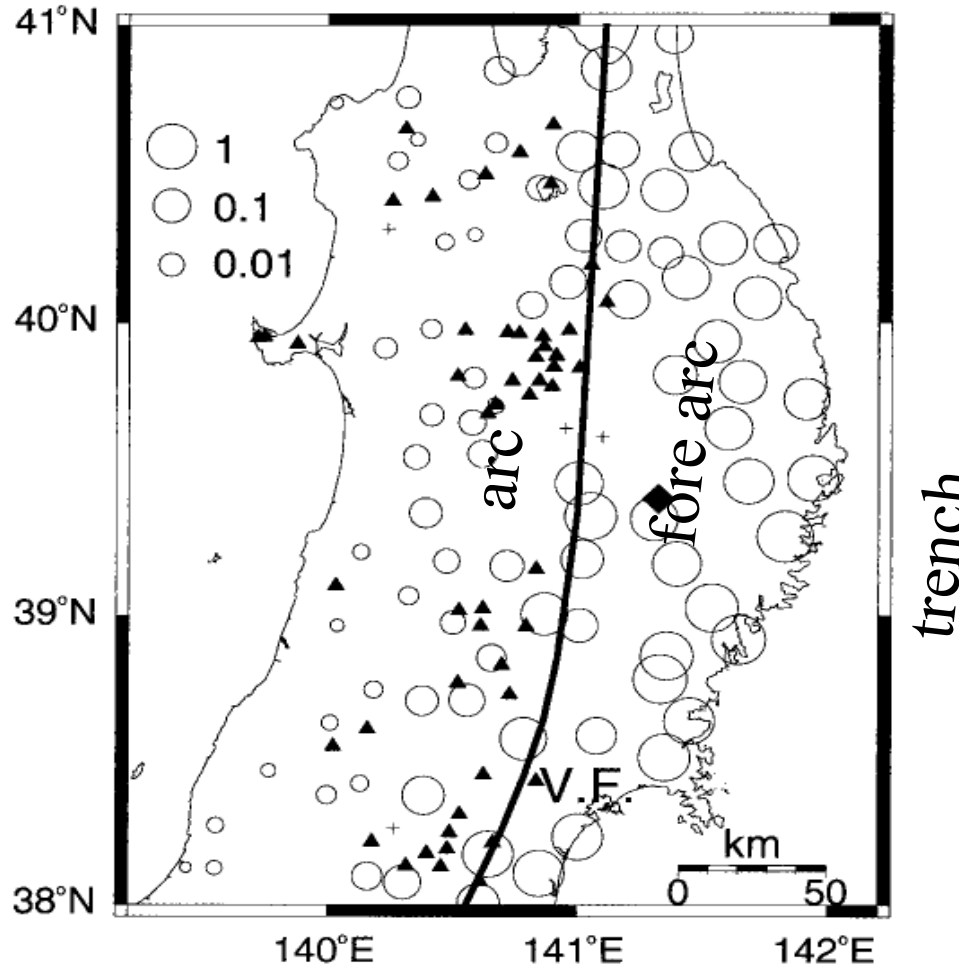

Figure 4. Map showing the spatial distribution of S-coda-wave energy at a lapse time of 180 sec. The epicenter of the earthquake analyzed is denoted by a filled diamond. The open circles are normalized and scaled in proportion to the S-coda-wave energy calculated at each borehole station. The filled triangles show locations of the Quaternary volcanoes. The thick solid line indicates the volcanic front.

Yoshimoto, BSSA, 2006

heatflow

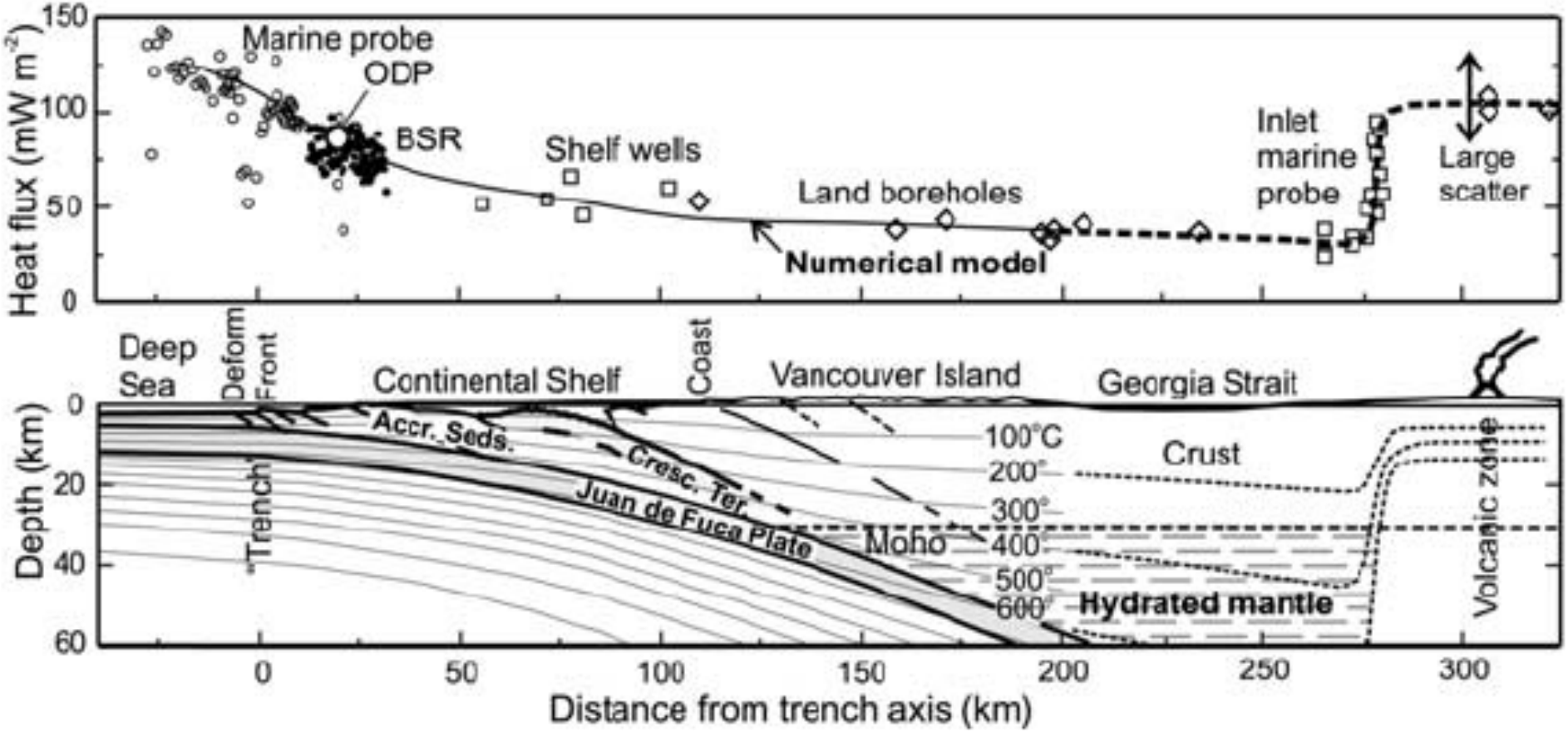

Figure for Cascadia subduction zone (young + slow = warm subduction)
Hyndman & Peacock EPSL 2003

van Keken, Kita, Nakajima,
Solid Earth, 2012

Heatflow data from
Tanaka et al., 2004.

Fast subduction of old lithosphere
below Tōhoku and Hokkaido:
example of cold subduction

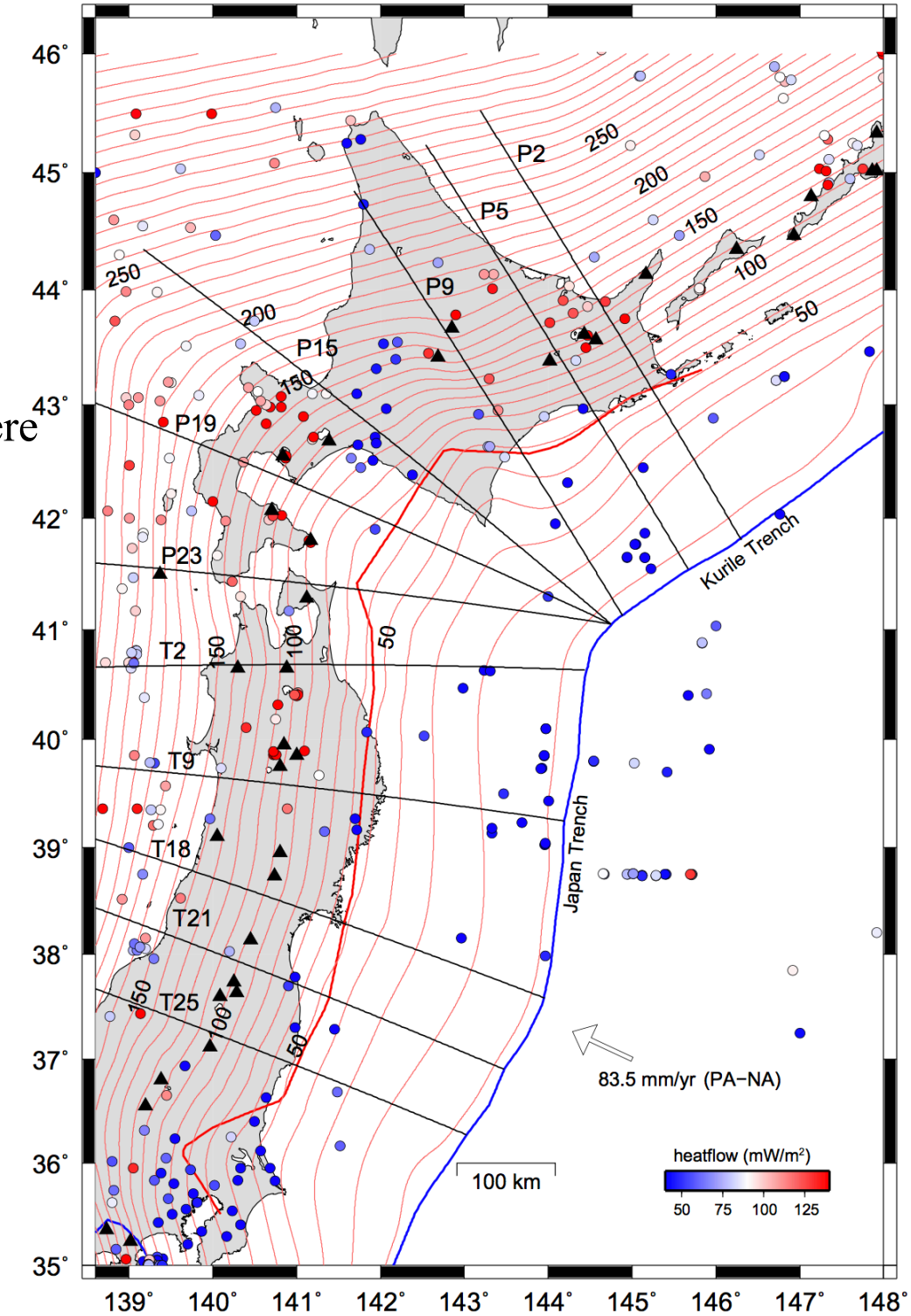

Cascadia

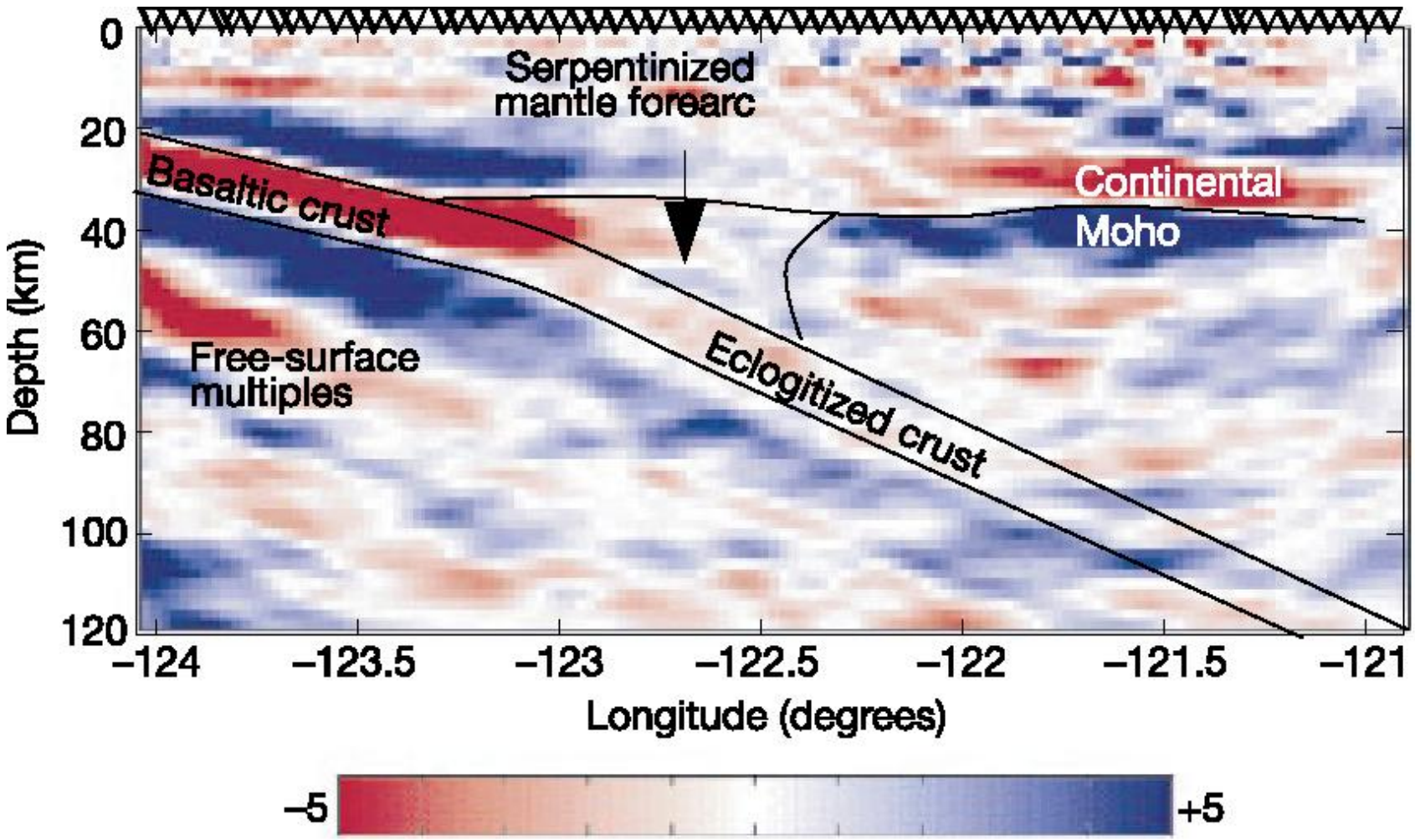

S perturbation (%)

Bostock et al., 2002

Olivine + water ⟶ **serpentinite** + magnetite

PNAS 2017

Subduction zone forearc serpentinites as incubators for deep microbial life

Oliver Plümper[a,1], Helen E. King[a], Thorsten Geisler[b], Yang Liu[a,c], Sonja Pabst[d], Ivan P. Savov[e], Detlef Rost[f], and Thomas Zack[g]

[a]Department of Earth Sciences, Utrecht University, 3584 CD Utrecht, The Netherlands; [b]Steinmann Institut für Geologie, Mineralogie und Paläontologie, University of Bonn, 53115 Bonn, Germany; [c]Debye Institute for Nanomaterials Science, Utrecht University, 3584 CC Utrecht, The Netherlands; [d]BHP Billiton Western Australia Iron Ore, Perth, WA 6000, Australia; [e]Institute of Geophysics and Tectonics, School of Earth and Environment, University of Leeds, Leeds LS2 9JT, United Kingdom; [f]Department of Physics, University of Auckland, Auckland 1010, New Zealand; and [g]Department of Earth Sciences, University of Gothenburg, 40530 Gothenburg, Sweden

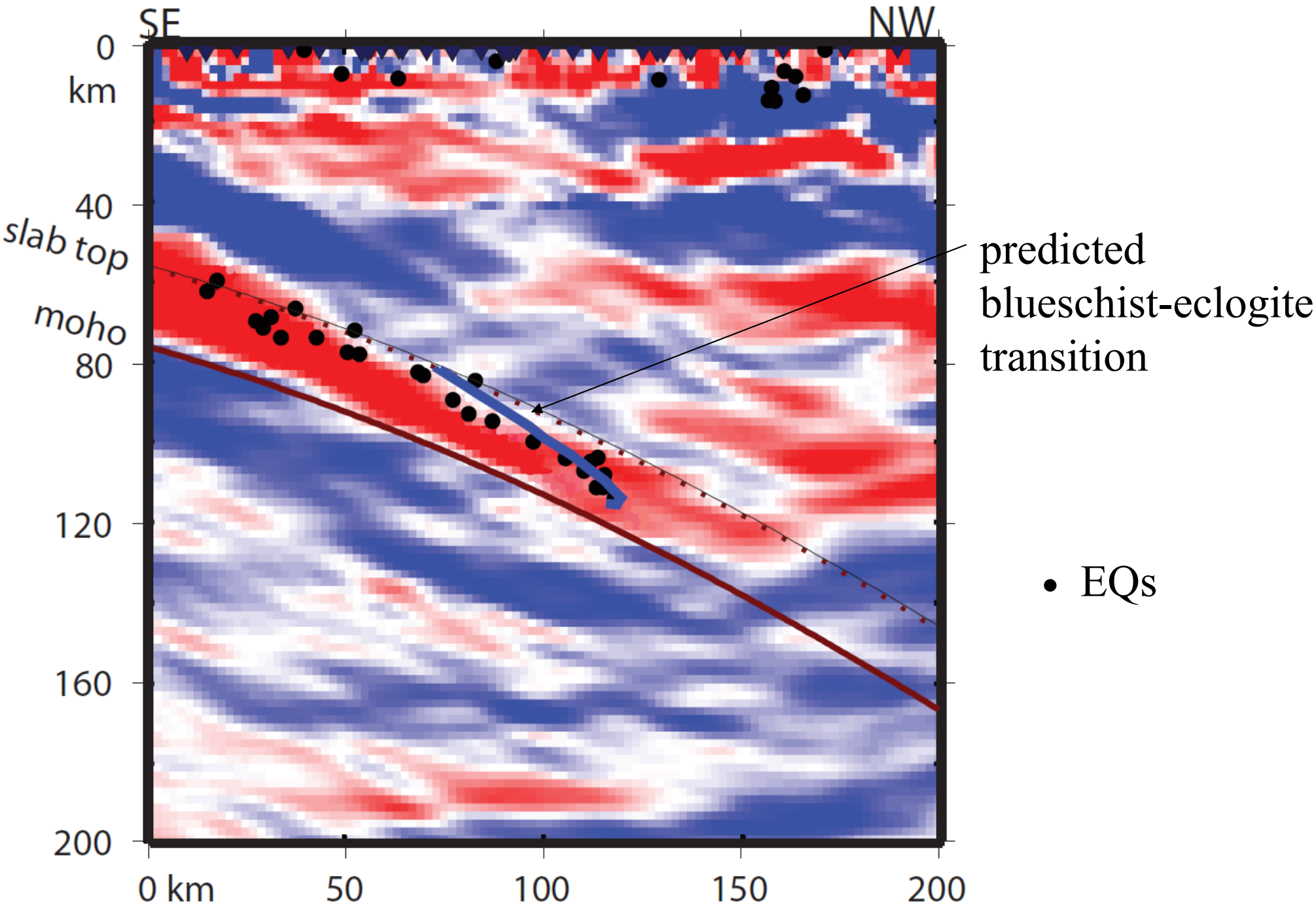

Central Alaska (Rondenay, Abers and van Keken, Geology, 2008)

Blueschist

Photo by Sarah Penniston-Dorland

increasing p,T

H_2O

Eclogite

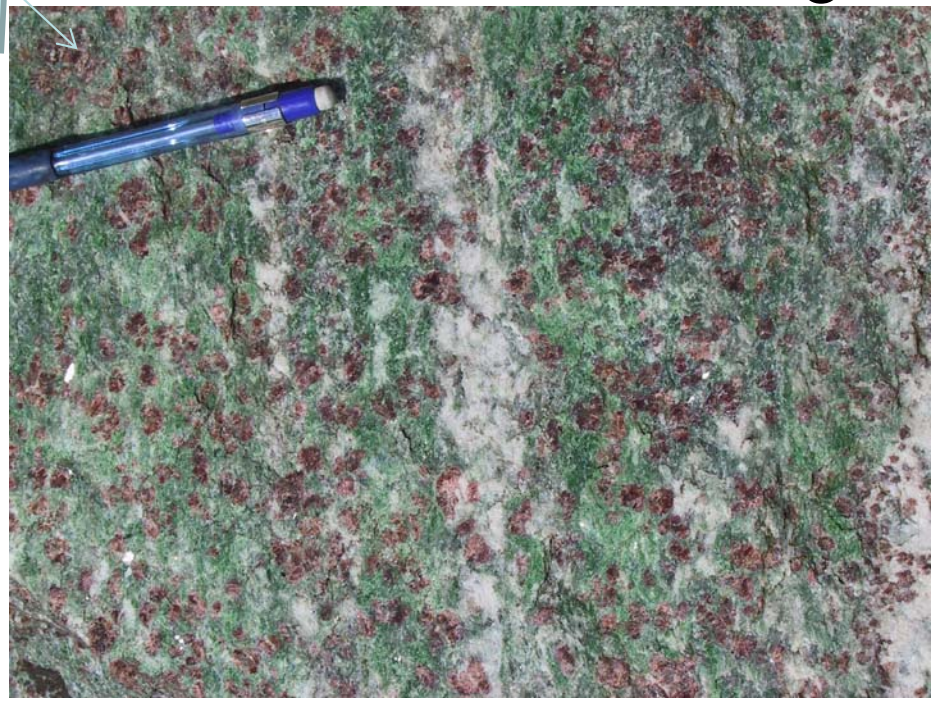

Photo by Brad Hacker

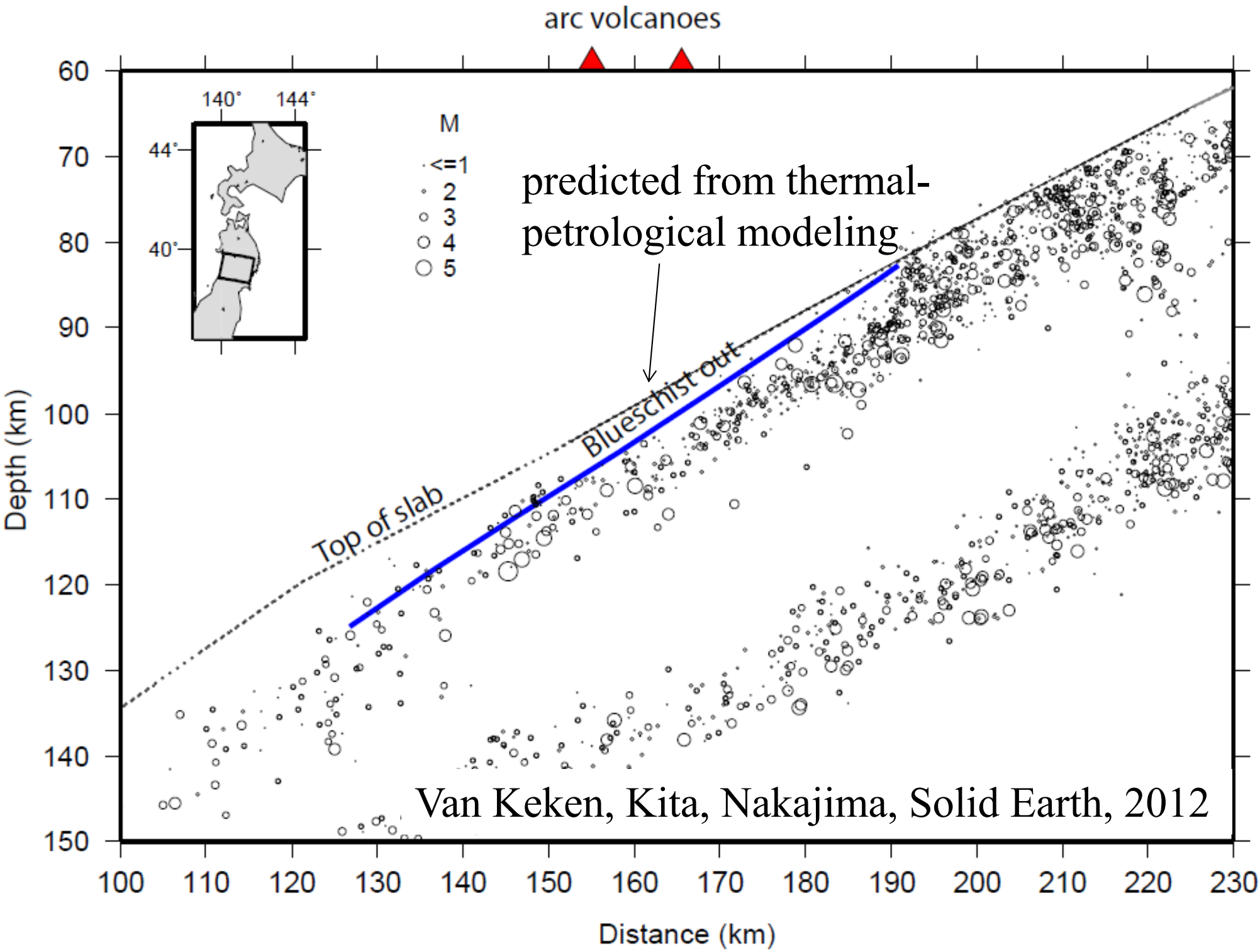
arc volcanoes
140°
144°
44°
40°
M
<=1
2
3
4
5
predicted from thermal-petrological modeling
Bluschist out
Top of slab
Van Keken, Kita, Nakajima, Solid Earth, 2012
Depth (km)
Distance (km)
60
70
80
90
100
110
120
130
140
150
100
110
120
130
140
150
160
170
180
190
200
210
220
230

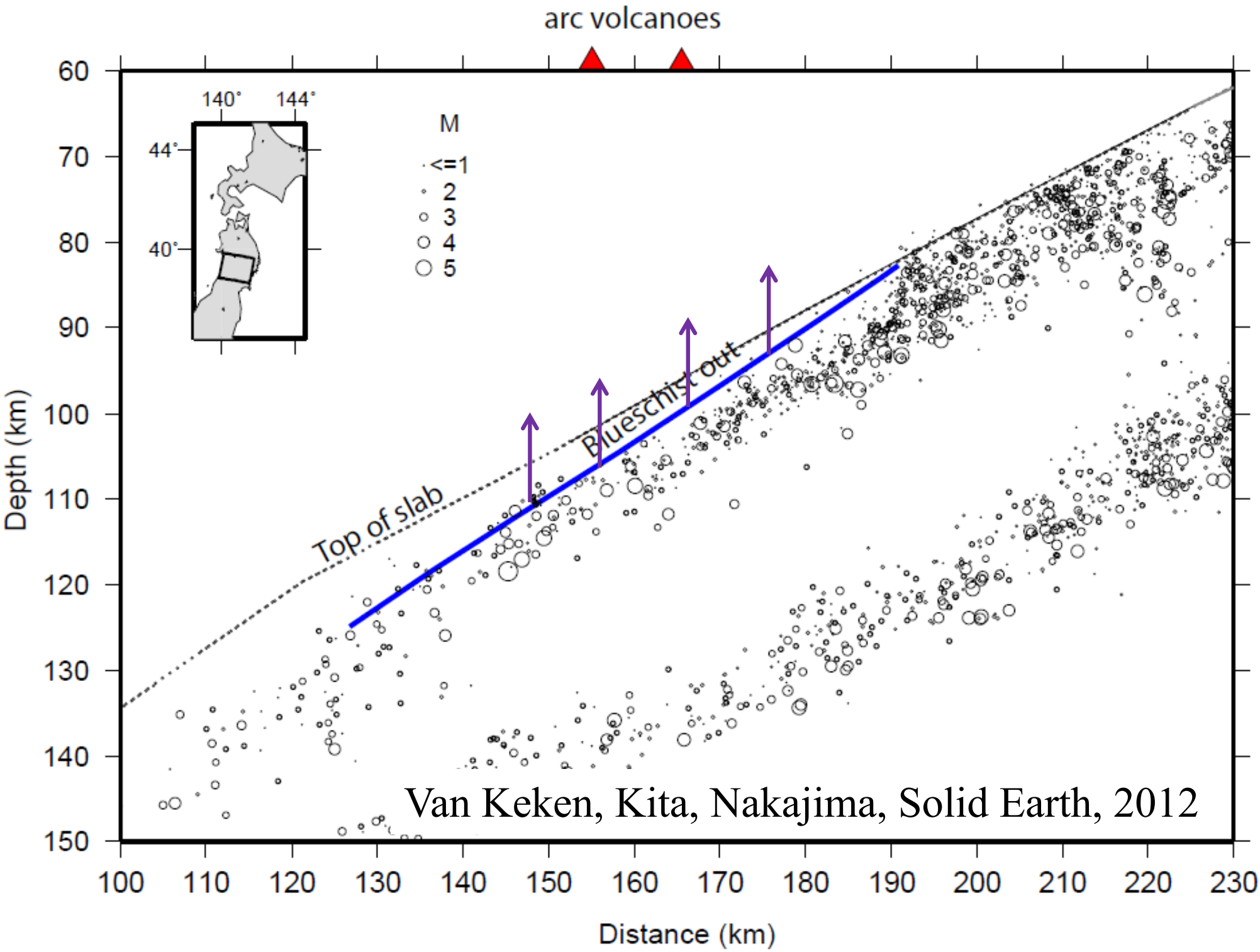
arc volcanoes
140°
144°
44°
40°
M
<=1
2
3
4
5
Top of slab
Blueschist out
Depth (km)
Distance (km)
60
70
80
90
100
110
120
130
140
150
100
110
120
130
140
150
160
170
180
190
200
210
220
230
Van Keken, Kita, Nakajima, Solid Earth, 2012

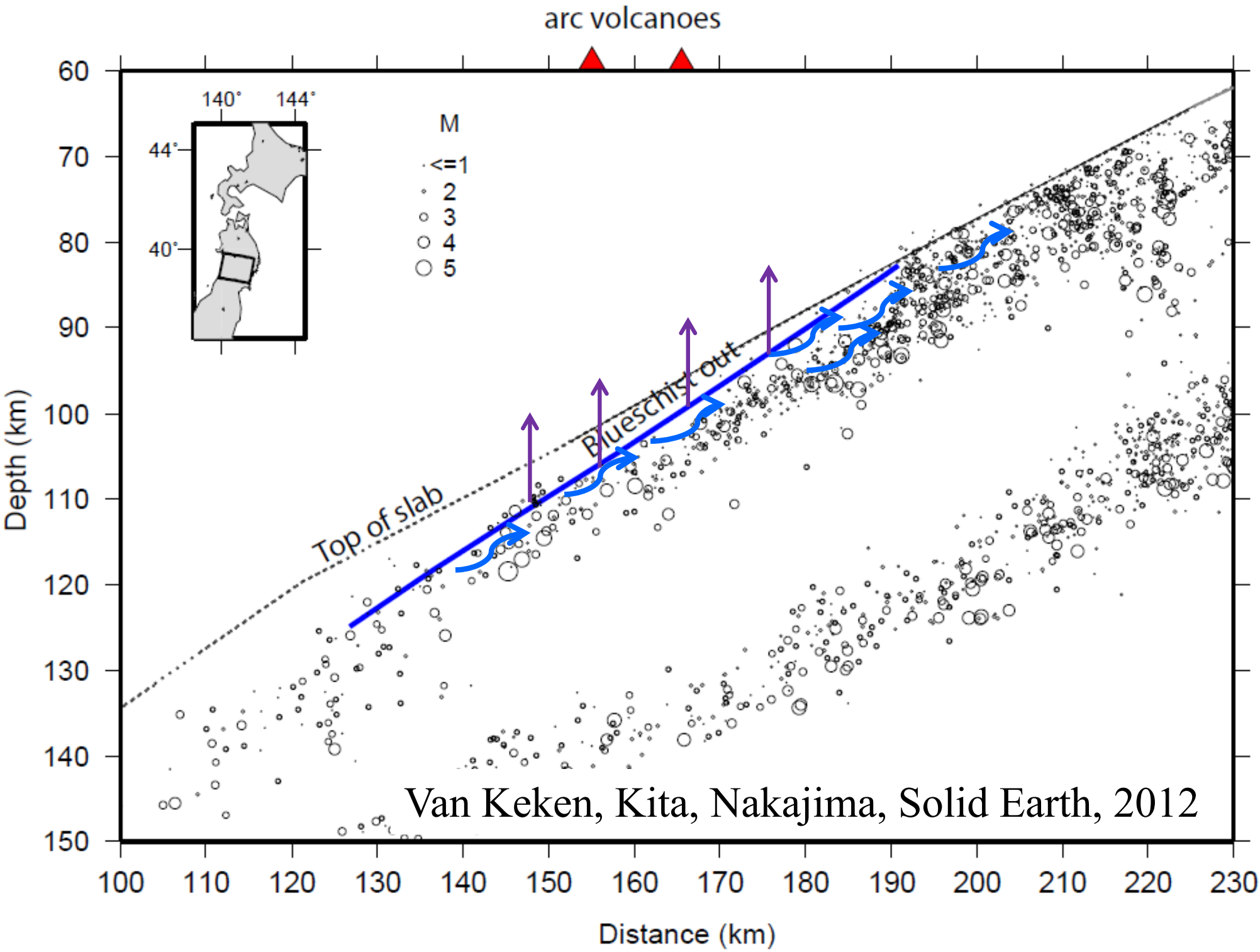
arc volcanoes
140°
144°
44°
40°
M
<=1
2
3
4
5
Top of slab
Blueschist out
Depth (km)
Distance (km)
60
70
80
90
100
110
120
130
140
150
100
110
120
130
140
150
160
170
180
190
200
210
220
230
Van Keken, Kita, Nakajima, Solid Earth, 2012

Very low P-wave velocity in upper crust below Tohoku

(Shiina et al., GRL, 2013)

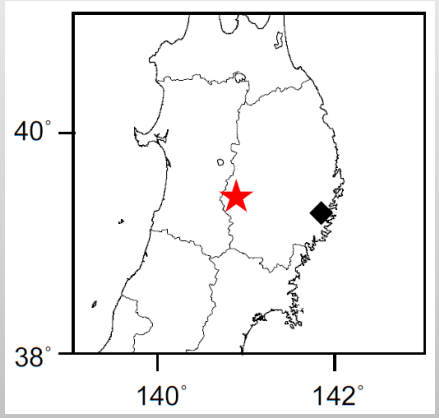

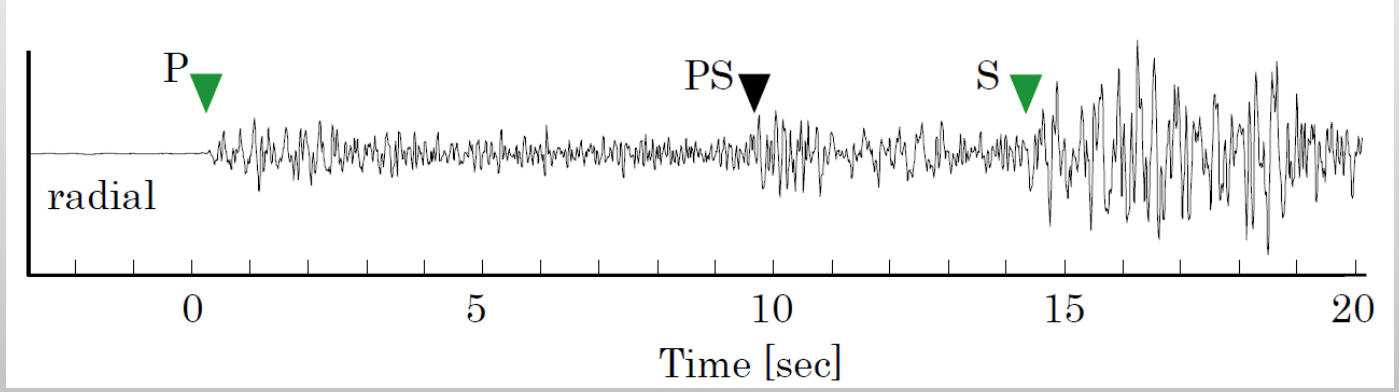

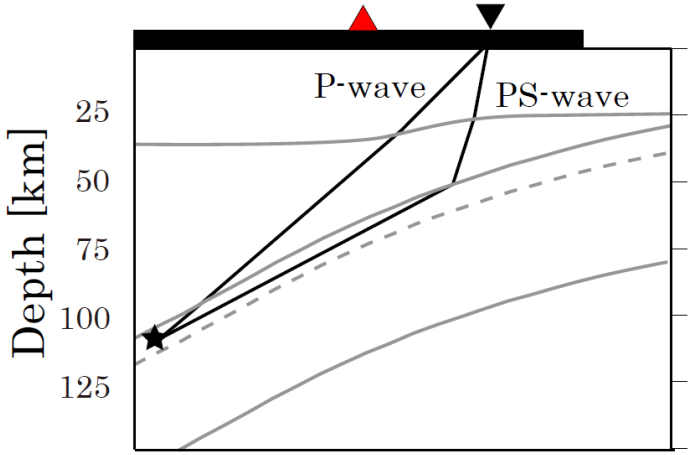

A schematic figure of a PS wave

P-wave velocity < 7.2 km/s suggest presence of free fluids

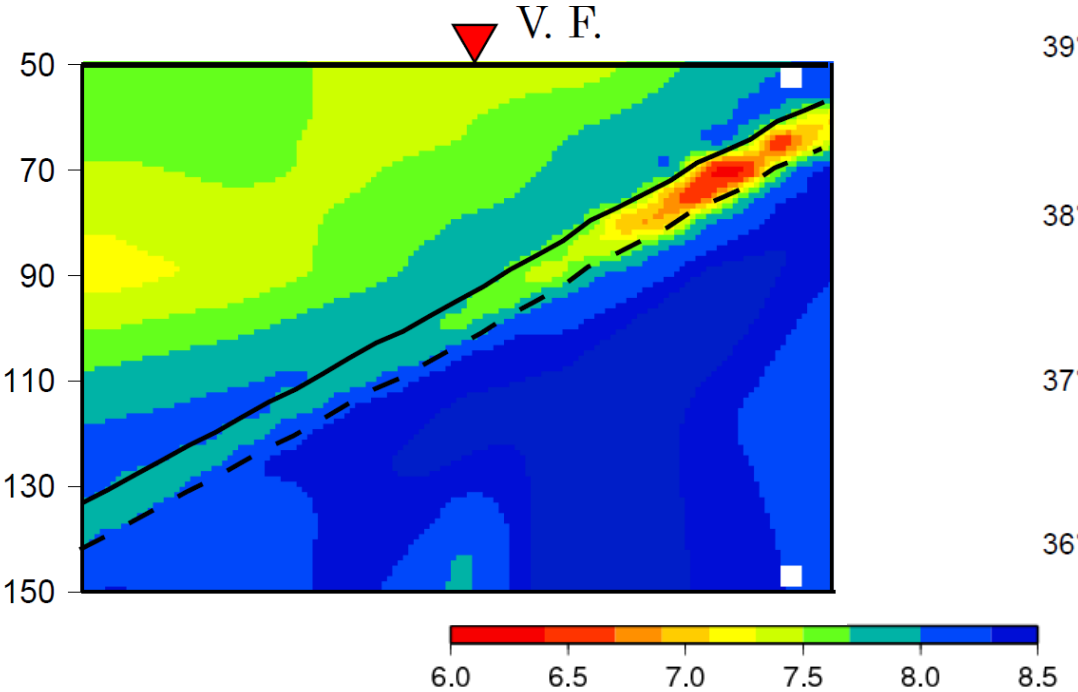

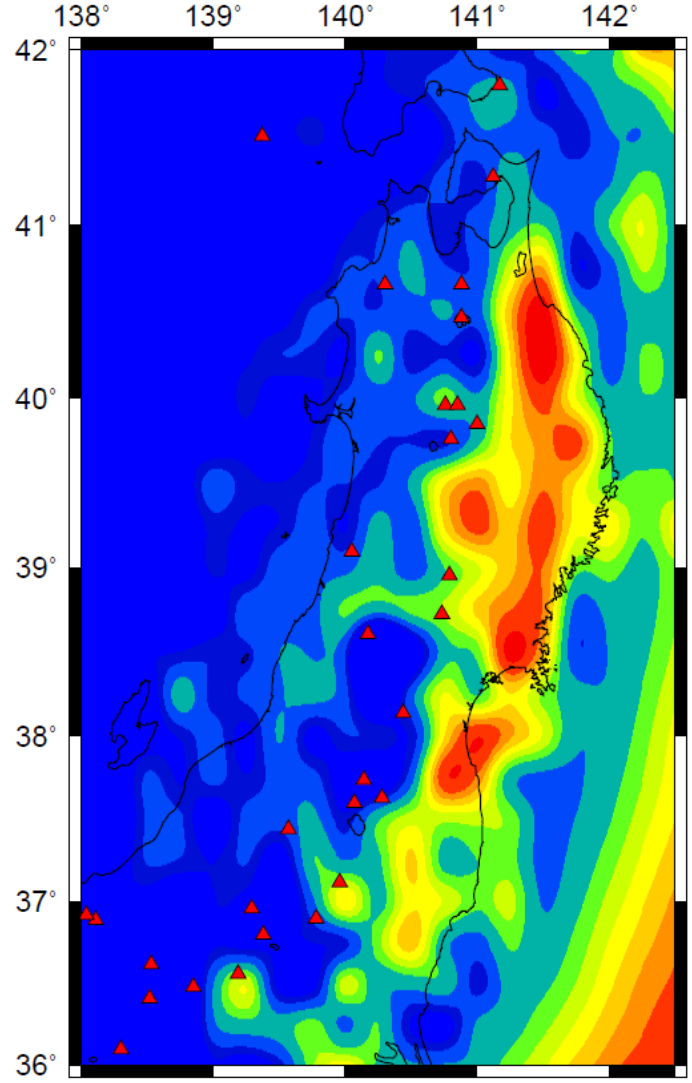

Shiina et al., 2013

Further slides were not discussed since the lecture time was reduced

The mantle wedge

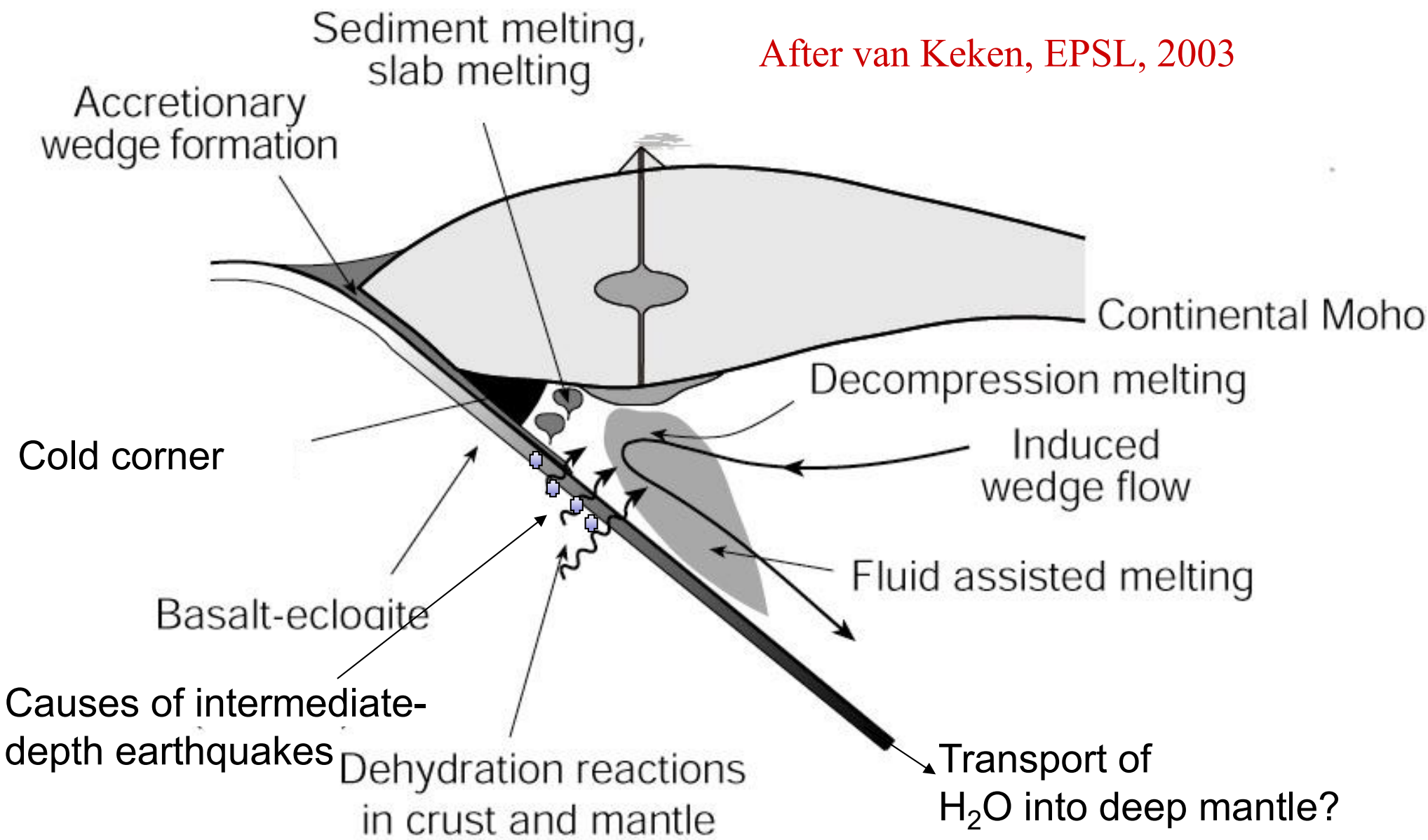

Liu and Zhao, PEPI, 2016

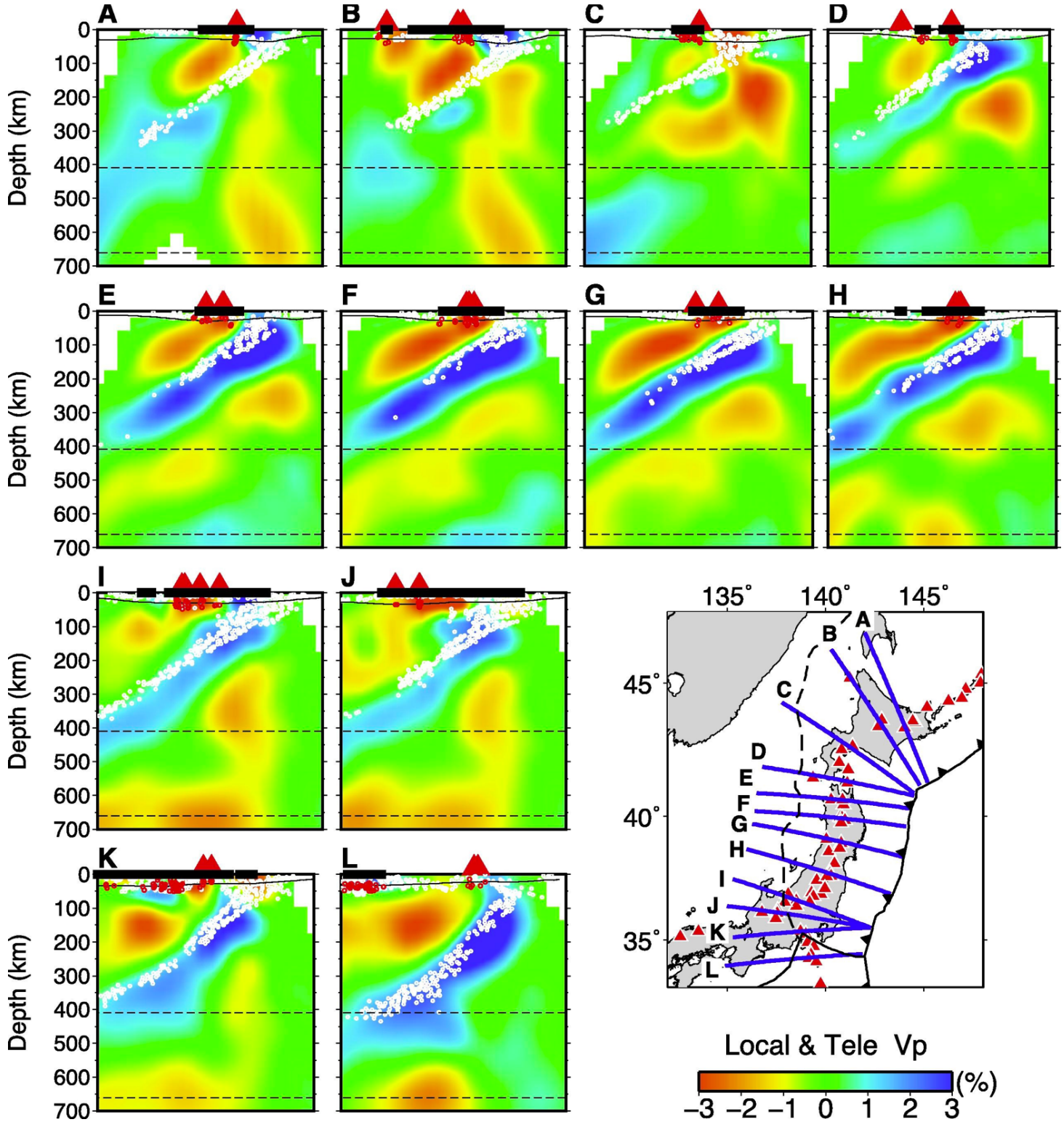

Kawakatsu and Watada, 2007
(interpretation by Brad Hacker, SCD TEI, 2015)

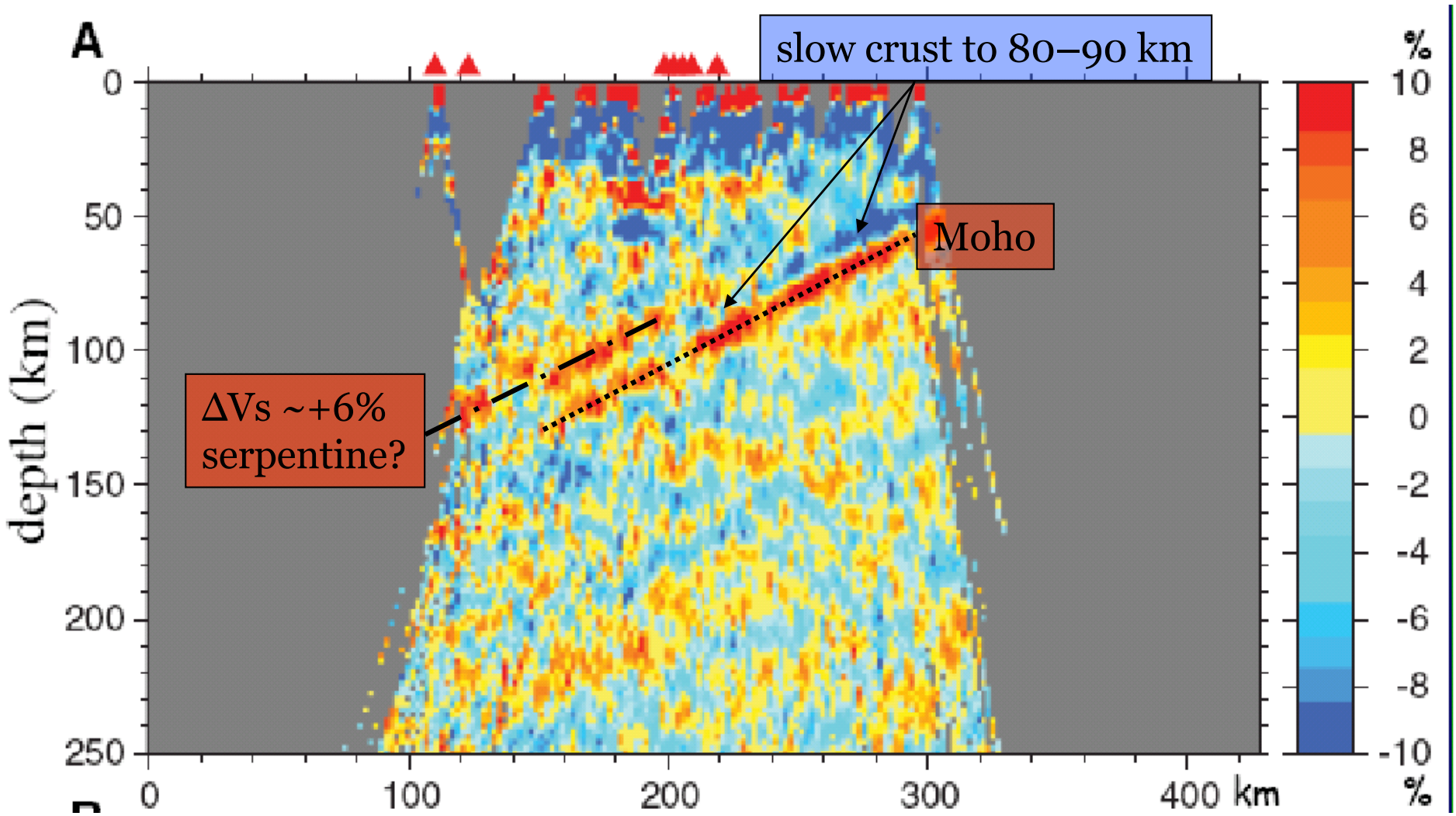

Tamura et al.,
EPSL, 2002

low seismic velocity
(='hot') fingers
below volcano clusters
in Tohoku.

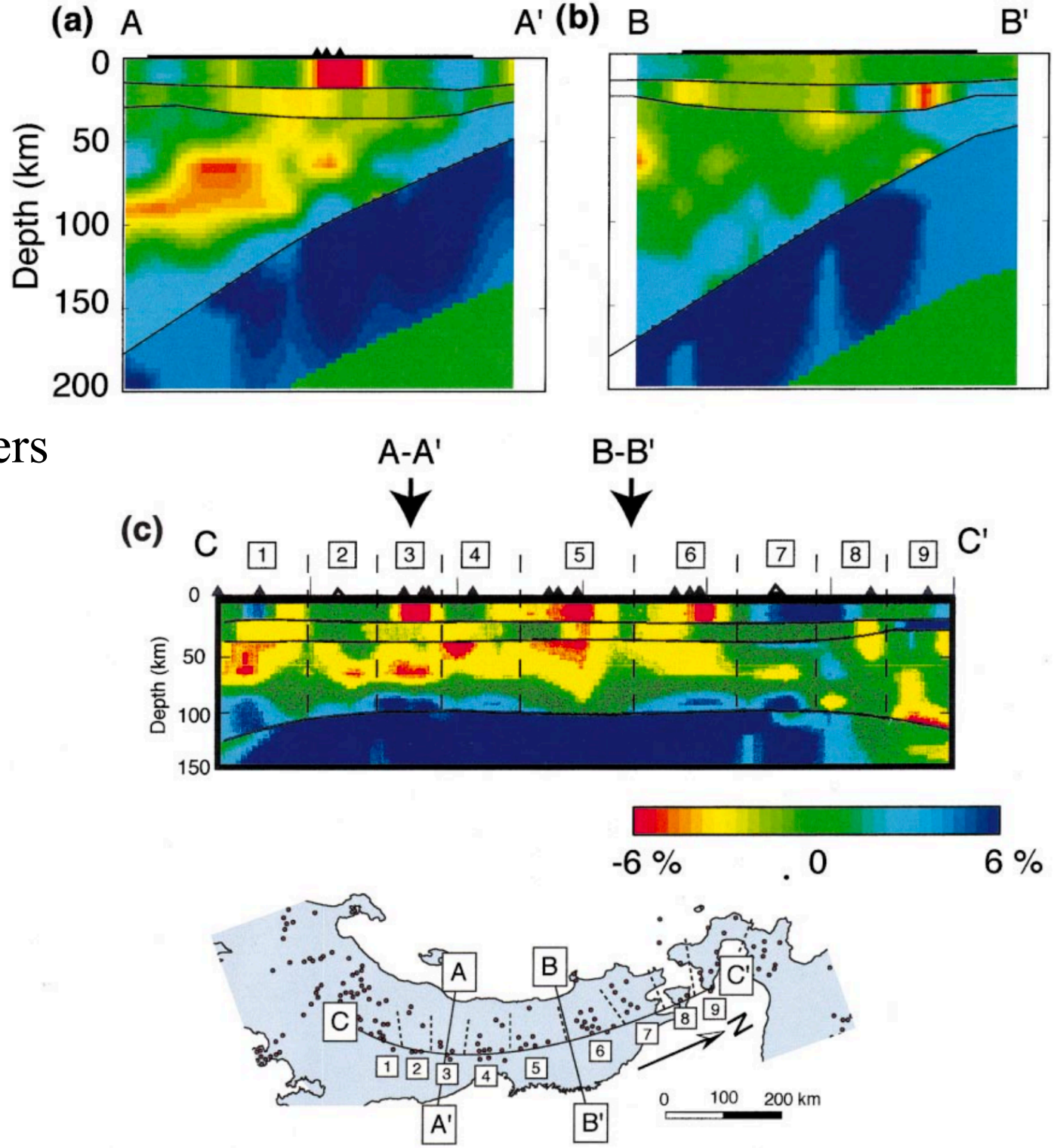

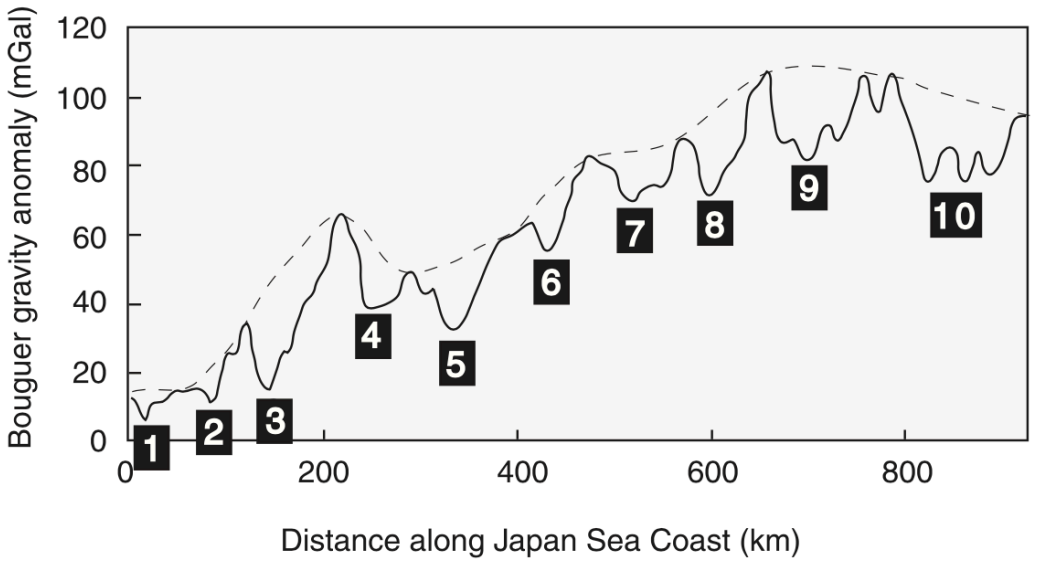

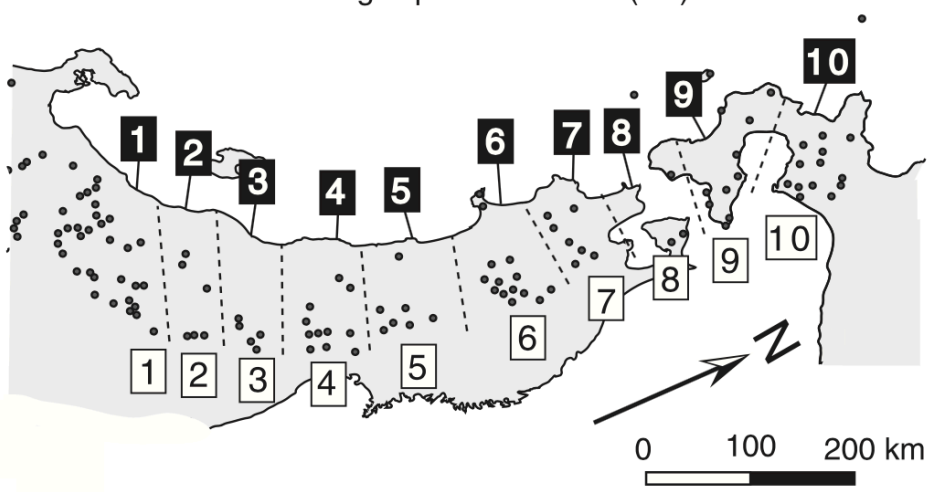

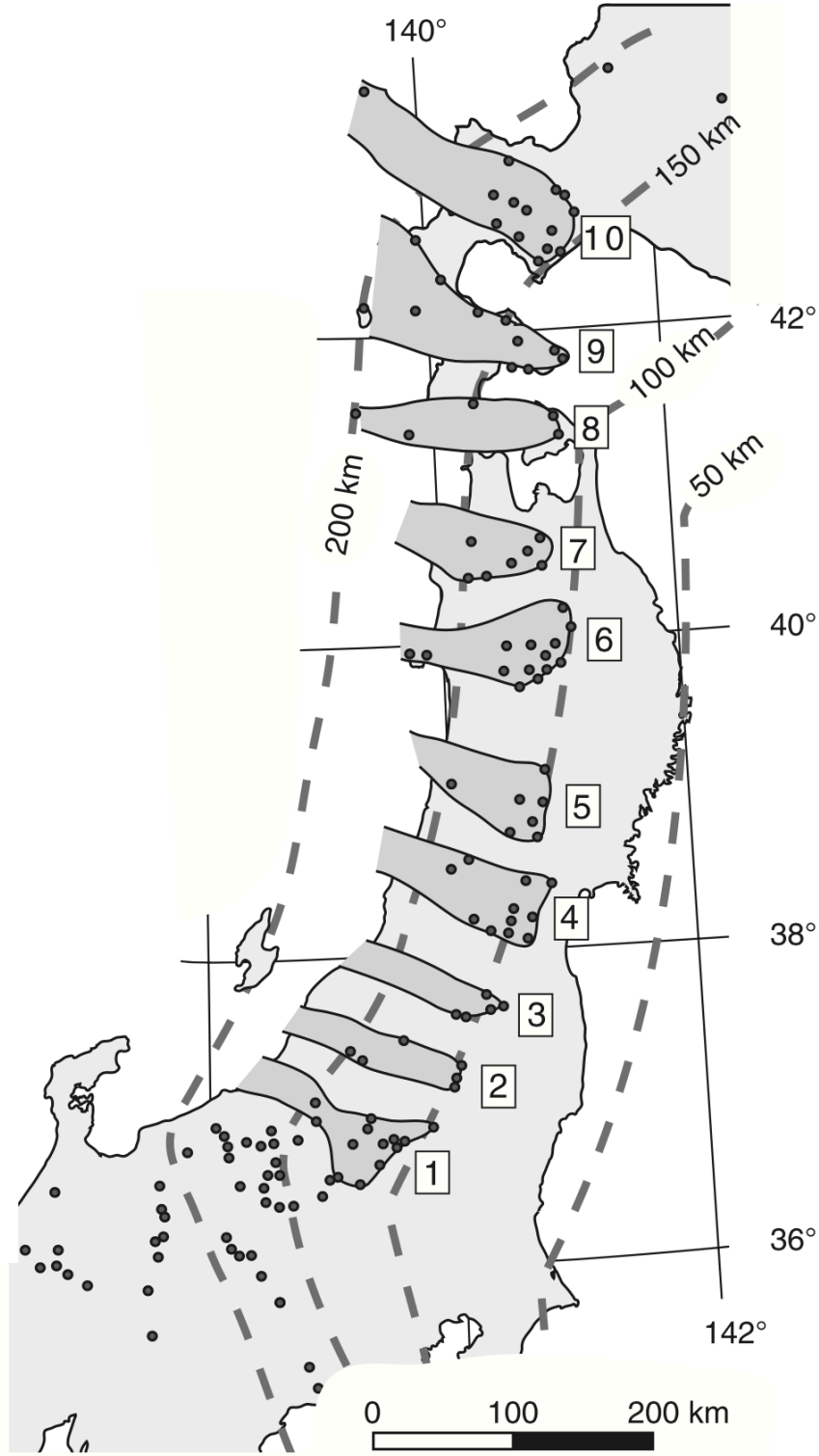

Tamura et al., EPSL, 2002

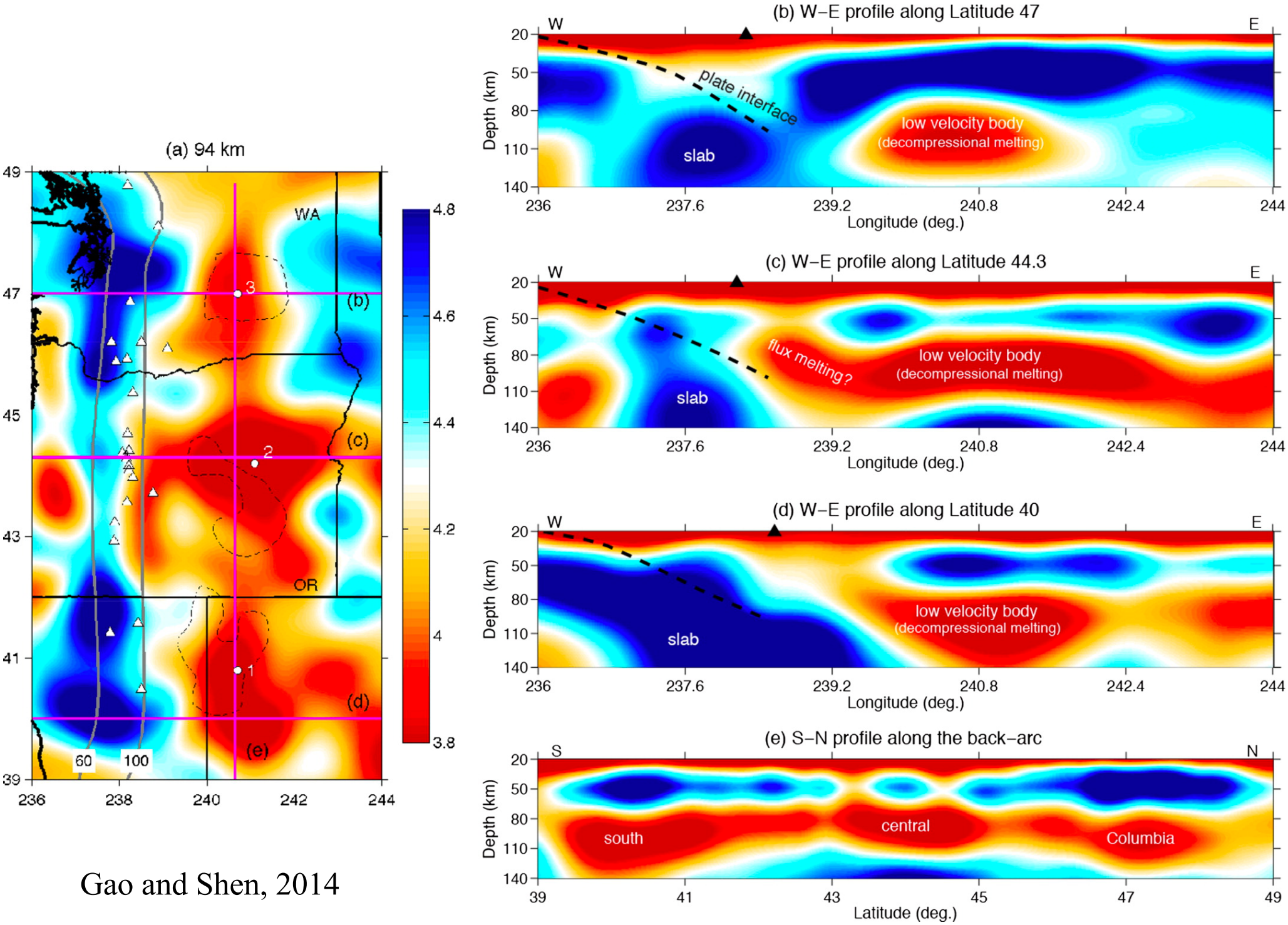

Gao and Shen, 2014

Bostock et al., 2002

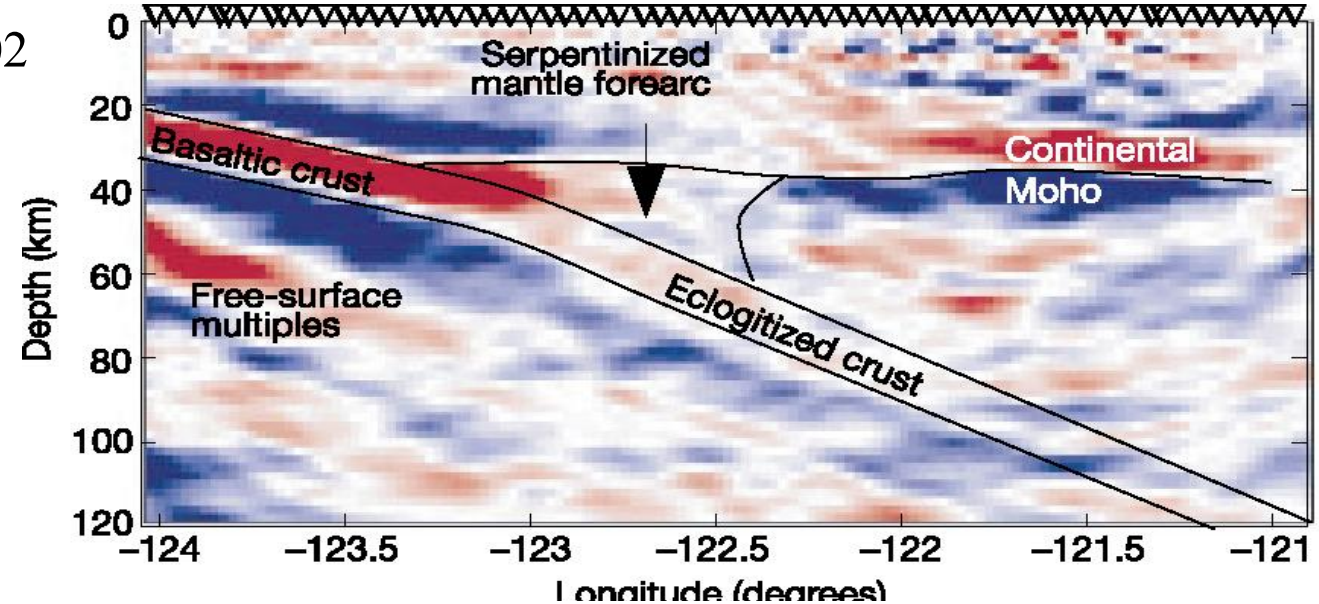

Hansen et al., 2016

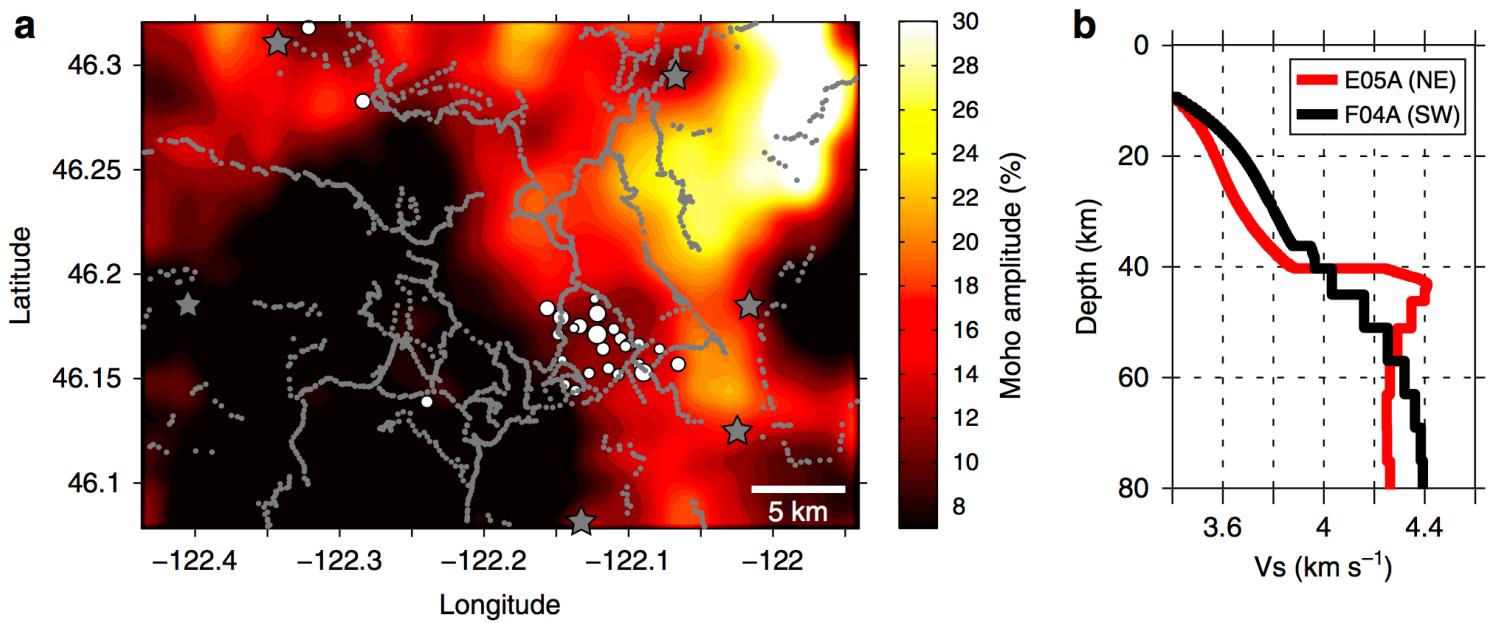

Figure 5 | Spatial variations in the Moho reflectivity. Moho amplitudes derived from common midpoint stacking of the PmP phase are shown in (**a**). Grey dots denote station locations and stars are the shot locations. The locations of deep long period earthquakes from the Pacific Northwest Seismic Network catalogue are plotted as white dots whose size scales with magnitude. Reported hypocenter uncertainties are all less than 6 km, however, mislocations and/or misidentifications are possible due to the emergent low frequency arrivals[34]. S-wave velocity models[16] for the two Transportable Array stations northeast (E05A) and southwest (F05A) of the image region are shown on in (**b**) (see Fig. 2 for their locations).

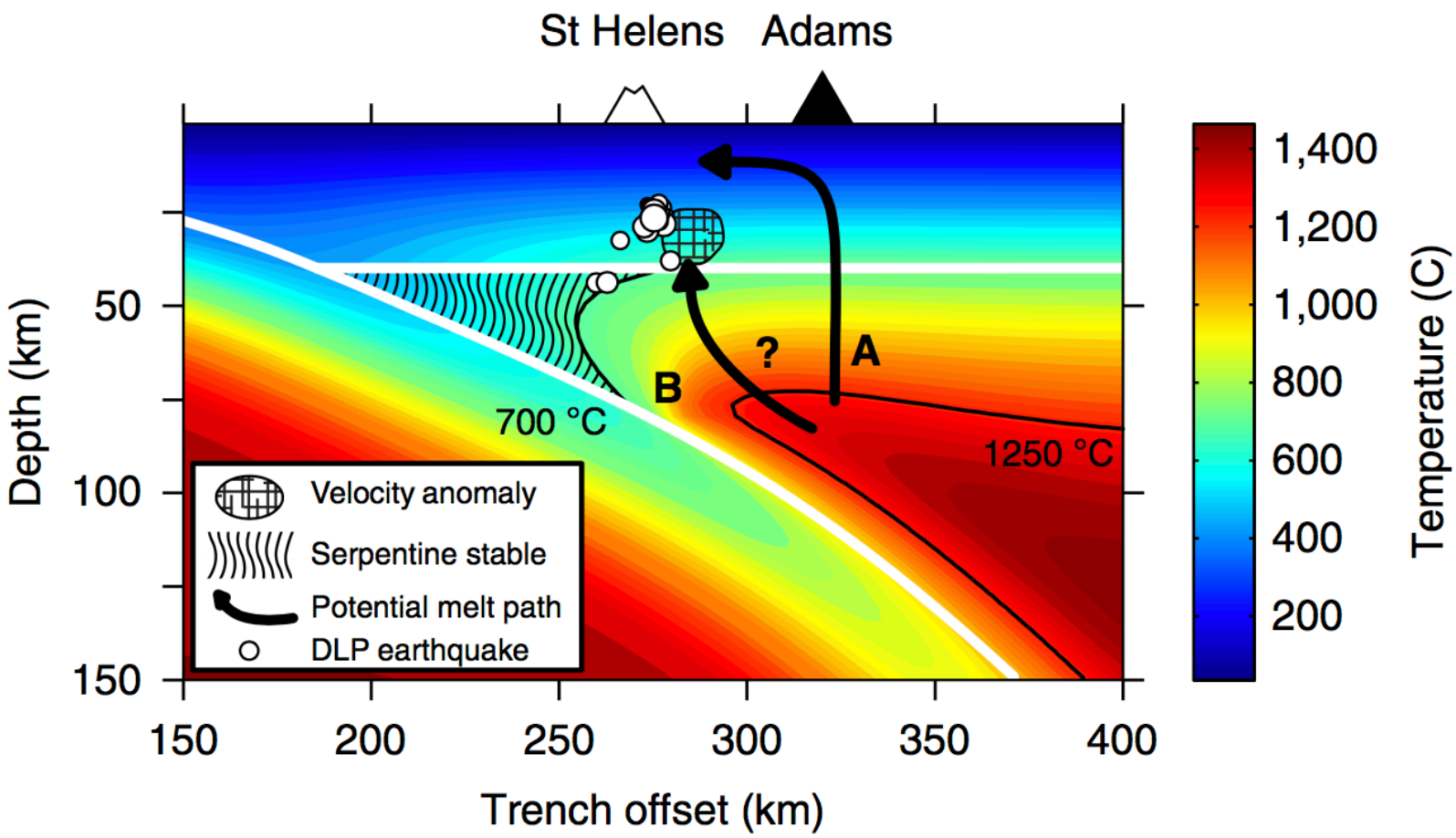

Hansen et al., 2016

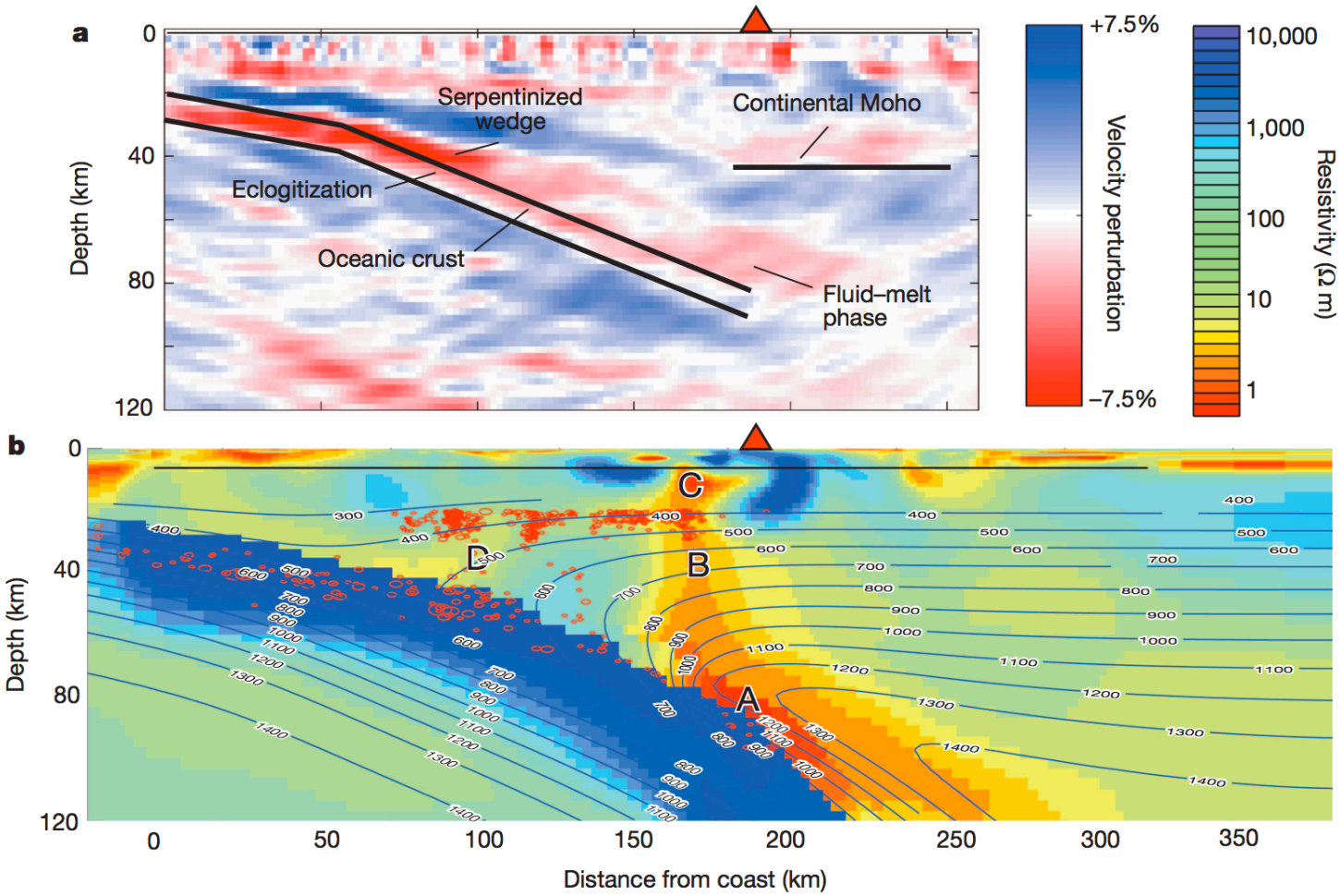

Figure 2 | Primary seismic (a) and magnetotelluric (b) models. Panel **b** includes both a thermal profile (contours, labelled in degrees Celsius) and earthquake hypocentre locations (red circles) within 20 km of our profile line[23]. Fluid released from the subducting slab enters the mantle wedge at A. Melt initiated at or very near the interface is transported upward by buoyancy and dragged down. The fluid/melt phase rises through the mantle wedge (B) until it reaches the crust, joining fluids released from shallower reactions (D). The combined fluid/melt continues to rise until reaching a reservoir (C) in the crust. Mount Rainier is shown as a red triangle.

McGary et al., 2014

Geophysical imaging of volcano activity and structure

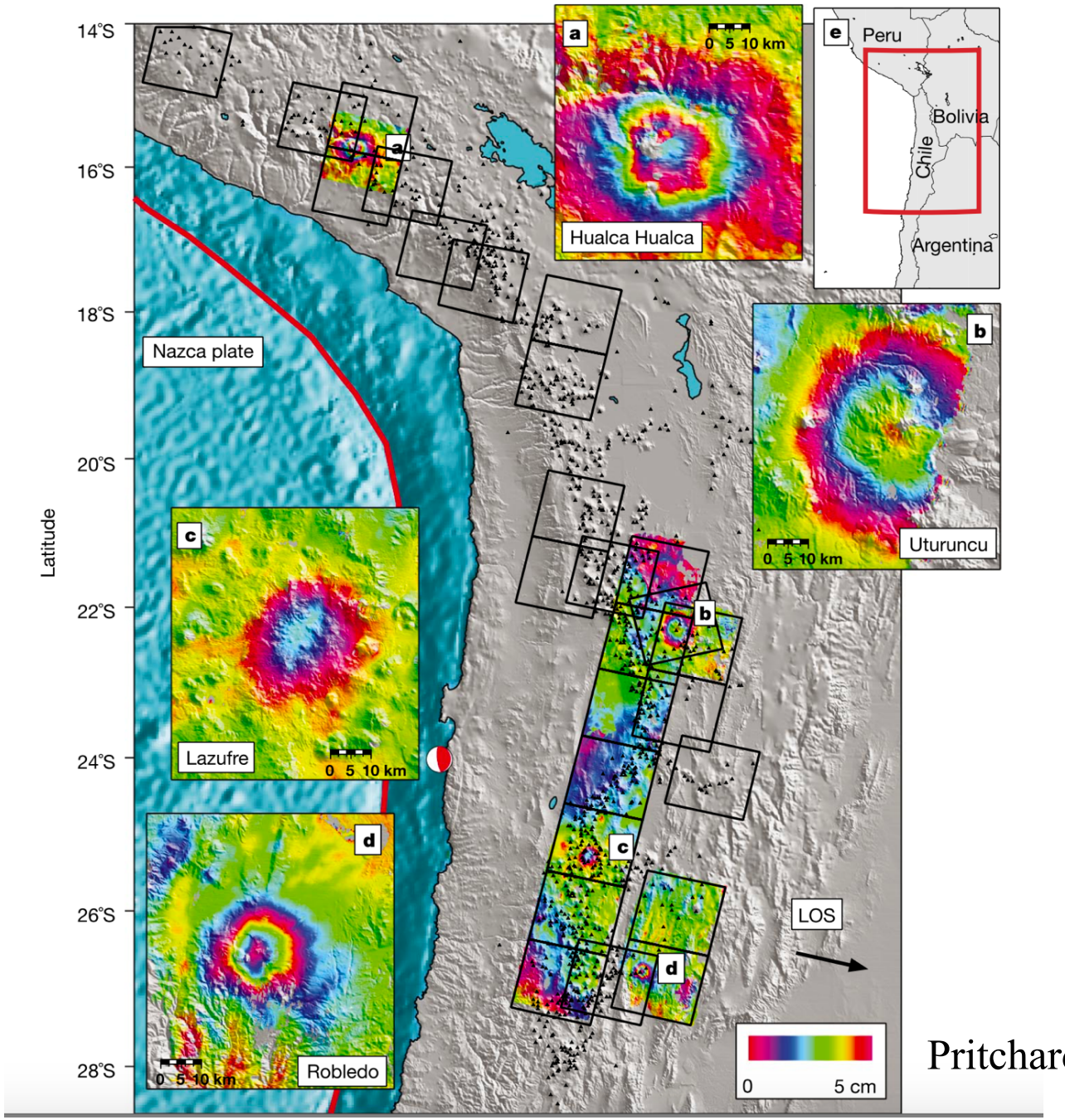

M. Kaufman/AVO/UAF

Pritchard and Simons, 2002

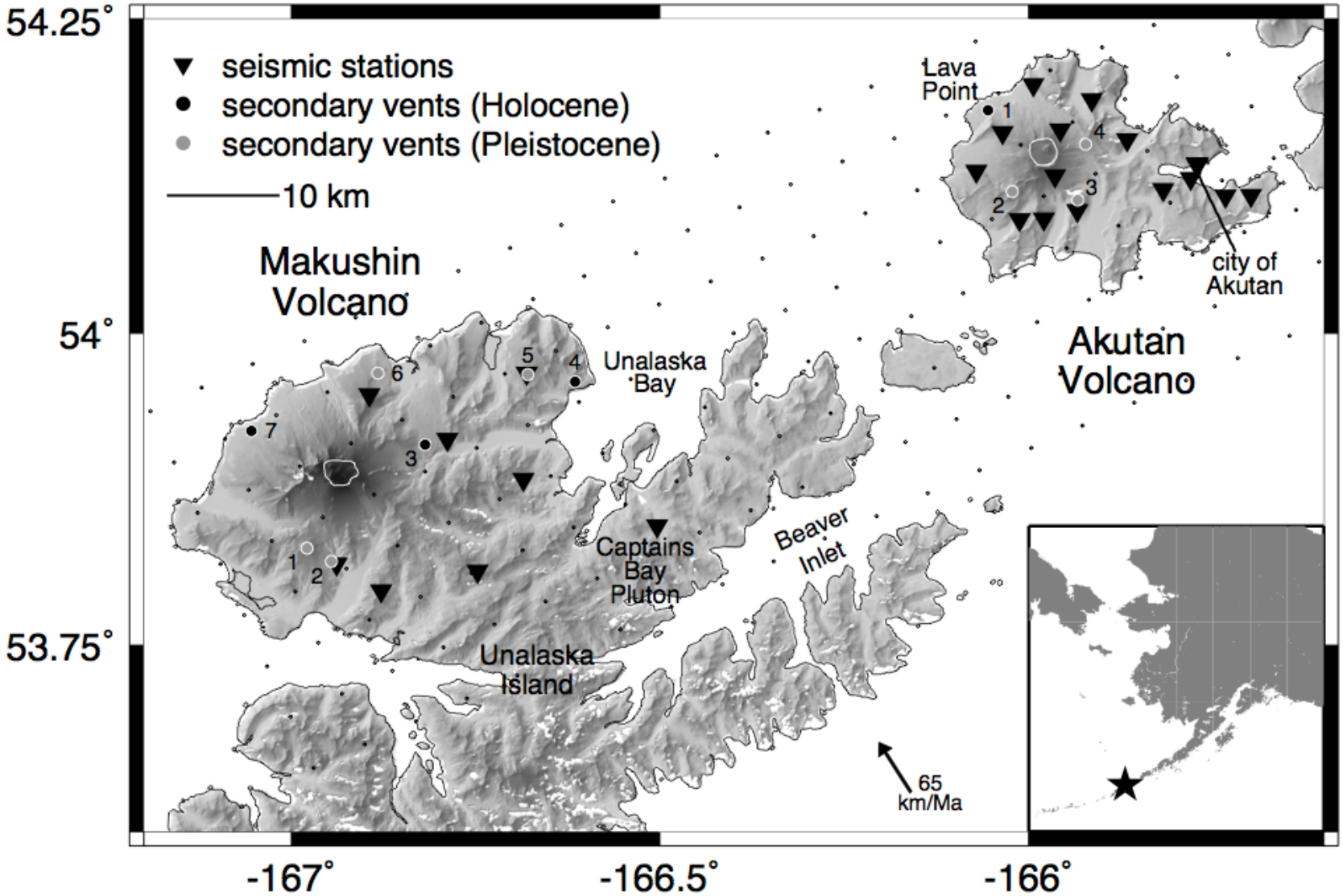

Syracuse et al., 2015

Akutan:
most recent eruption: 1992
magma chamber depth:

13 km (InSAR; Lu et al., 2000)
4 km (GPS; Ji and Herring, 2011)
4.5 km (petrologic; Zimmer, 2009)

Makushin:
most recent eruption: 1995
magma chamber depth:

7 km (InSAR; Lu et al., 2002)
5-6 km (petrologic; Zimmer, 2009)

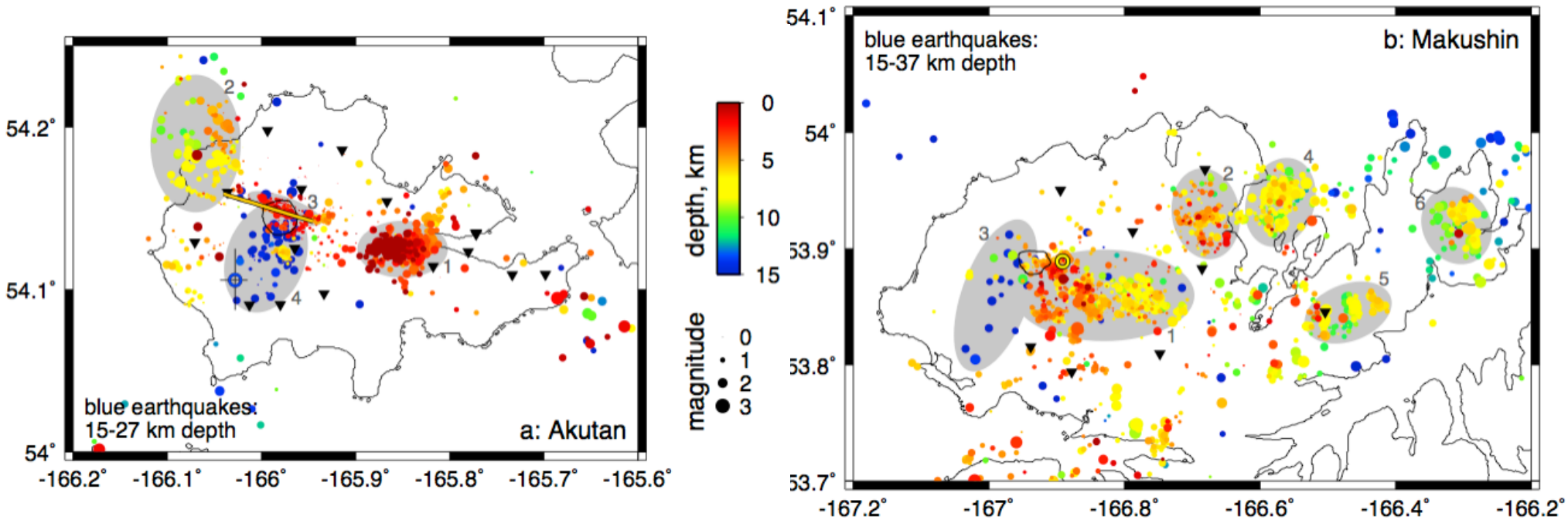

Syracuse et al., 2015

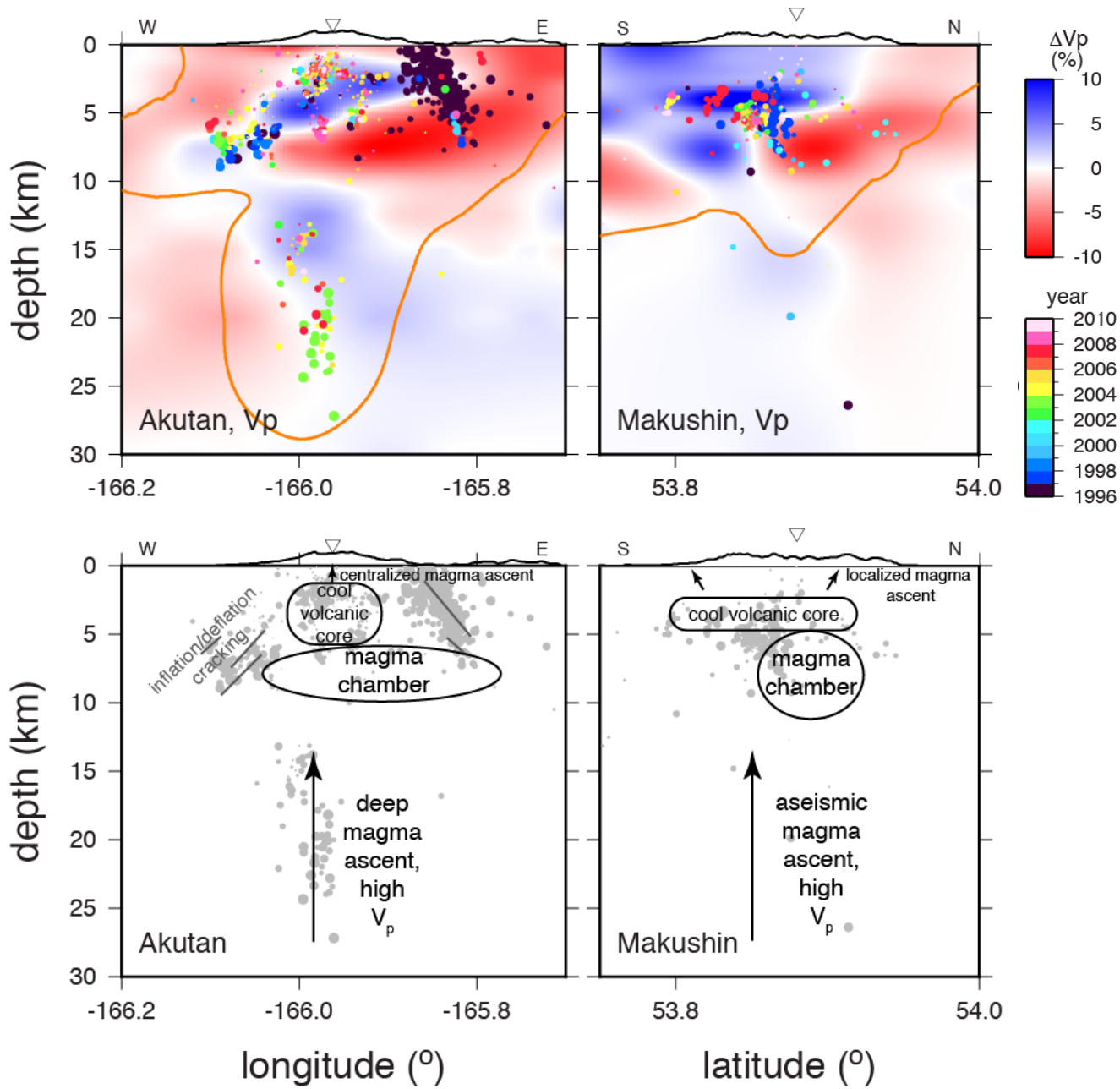

Syracuse et al., 2015

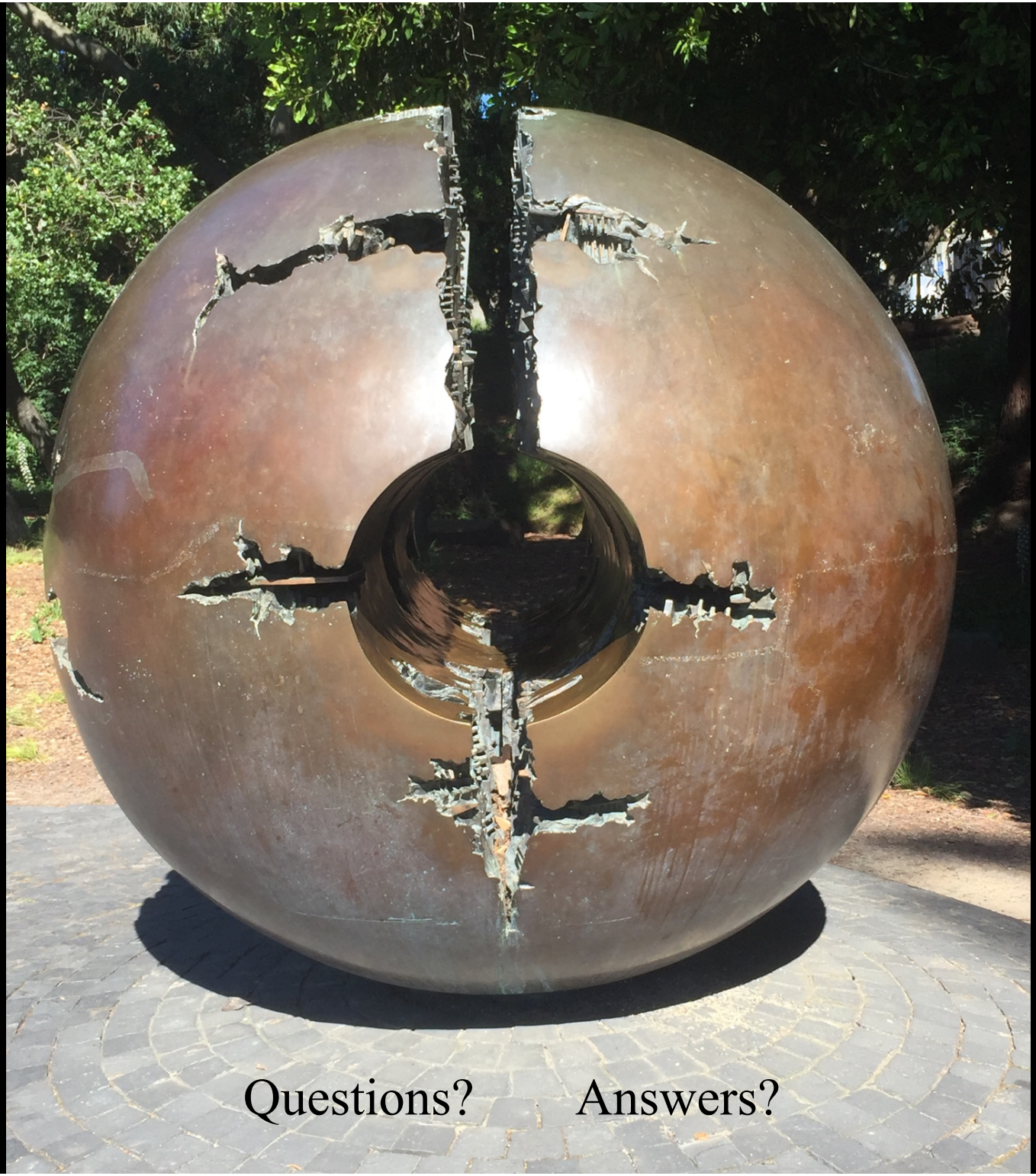
Questions?
Answers?